

# Applications of Acoustic and Electromagnetic Propagation

by

**Elias Bircher**

Thesis Proposal Submitted in Partial Fulfillment of the  
Requirements for the Degree of  
Bachelor of Applied Science

in the  
School of Engineering Science  
Faculty of Applied Science

© **Elias Bircher 2023**  
**SIMON FRASER UNIVERSITY**  
**Fall 2023**

Copyright in this work is held by the author. Please ensure that any reproduction or re-use is done in accordance with the relevant national copyright legislation.

# APPROVAL

**Name:** Elias Bircher

**Degree:** Bachelor of Applied Science Honours

**Title of Thesis:** Applications of Acoustic and Electromagnetic Propagation

---

Dr. Cheng Li, P.Eng  
Director, School of Engineering Science

**Examining Committee:**

---

Dr. Rodney Vaughan, P.Eng.  
Professor, School of Engineering Science

---

Christopher Hynes, PhD Candidate  
School of Engineering Science

---

Dr. Shawn Sederberg, P.Eng.  
Professor, School of Engineering Science

**Date Approved:** 2024-01-11

---

# Declaration of Committee

**Name:** Elias Bircher

**Degree:** Bachelor of Applied Science

**Thesis title:** Applications of Acoustic and Electromagnetic Propagation

**Committee:**

**Dr. Rodney G. Vaughan, P.Eng**  
Academic Supervisor  
Professor, Engineering Science

**Dr. Christopher G. Hynes**  
Supervisor  
Engineering Science

**Dr. Shawn Sederberg, P.Eng**  
Committee Member  
Professor, Engineering Science

# Abstract

A fish tracking model and an acoustic multi-layered structure are presented using the theory of transmission lines to demonstrate propagation through various layered media. The fish tracking model is an electromagnetic propagation model used in conjunction with experimentally collected data to pinpoint the path travelled by spawning salmon, allowing for the study of fine-scale fish migration in remote and challenging landscapes. Although appearing radically different, acoustic propagation shares much the same formalism as electromagnetic propagation; therefore, the second portion of this thesis uses a similar transmission line model to analyze the acoustic loss of a single, double, and triple-pane window – a challenging problem that provides useful information for both architects and researchers alike. Both models provide foundational work and illuminate limitations in applying it directly to real world problems. The electromagnetic propagation yields small deviations in gain across the area of interest resulting in easily accomplished large scale tracking. For finer resolution, more analysis would be required on the data produced. The acoustic transmission line model provides insight into the design of windows, however, current results indicate that only a single layer is modelled accurately.

**Keywords:** Acoustic Propagation; Electromagnetic Propagation; Electromagnetism; Fresnel Equations; Friis Equation; Oblique Incidence

# Acknowledgements

I would like to extend my gratitude to Dr. Rodney Vaughan, my academic supervisor, for the project idea and offering support, addressing queries, and meticulously reviewing the thesis. Furthermore, I thank Dr. Christopher Hynes for his generous provision of a simulation using CST for the fish transmitter, assistance with questions, and contributions to thesis editing. Special thanks to the other lab members for fostering a welcoming environment and their readiness to assist, and to Dr. Shawn Sederberg for serving on the committee. Finally, sincere thanks to my family for their continuous support throughout my degree and this thesis.

# Table of Contents

<b>Declaration of Committee</b>	<b>ii</b>
<b>Abstract</b>	<b>iii</b>
<b>Acknowledgements</b>	<b>iv</b>
<b>Table of Contents</b>	<b>v</b>
<b>List of Figures</b>	<b>viii</b>
<b>List of Acronyms</b>	<b>xi</b>
<b>1 Introduction</b>	<b>1</b>
1.1 Propagation Modelling for Fish Tracking . . . . .	1
1.1.1 Background . . . . .	2
1.1.2 Contribution . . . . .	3
1.2 Acoustic Propagation Model for Multi-layer Structures . . . . .	3
1.2.1 Background . . . . .	3
1.2.2 Contributions . . . . .	5
1.3 Road Map . . . . .	5
<b>2 Fish Tracking</b>	<b>7</b>
2.1 Assumptions . . . . .	7
2.2 Underlying Principles . . . . .	8
2.2.1 Air - Water Interface . . . . .	8
2.2.2 Attenuation . . . . .	11
2.2.3 Transmission Lines . . . . .	11
2.2.4 Transmit and Receive Antennas . . . . .	13
2.2.5 Spherical Spreading . . . . .	15
2.2.6 Total Path Loss . . . . .	15
2.3 Model Implementation and Verification . . . . .	16
2.3.1 Media Interface . . . . .	16
2.3.2 Attenuation and Spherical Loss . . . . .	17

2.3.3	Transmit and Receive Antennas . . . . .	18
2.4	Results . . . . .	23
2.4.1	TE and TM . . . . .	23
2.5	Discussion . . . . .	28
2.5.1	System Improvement . . . . .	29
<b>3</b>	<b>Acoustic Modelling Multi-layer Structures</b>	<b>31</b>
3.1	Assumptions . . . . .	32
3.2	Underlying Principles . . . . .	32
3.2.1	Acoustic Electromagnetic Equivalent . . . . .	32
3.2.2	Power, Intensity and Hearing . . . . .	33
3.2.3	Single-pane and Double-pane . . . . .	34
3.2.4	Transmission Loss and Absorption Coefficient . . . . .	35
3.2.5	Transmission Lines . . . . .	37
3.3	Model Implementation and Verification . . . . .	39
3.3.1	Single-pane Three mm Experimental Result Comparison . . . . .	40
3.3.2	Linear, Polynomial, Spline - Single-pane Comparison . . . . .	40
3.4	Results . . . . .	43
3.4.1	Single-pane . . . . .	43
3.4.2	Double-pane . . . . .	43
3.4.3	Triple Pane . . . . .	45
3.4.4	Double-pane Verification - 4 mm Glass, 6 mm Spacing . . . . .	45
3.5	Discussion . . . . .	46
<b>4</b>	<b>Conclusion and Recommendations</b>	<b>48</b>
4.1	Conclusion . . . . .	48
4.2	Future Work - Fish Tracking . . . . .	49
4.3	Future Work - Acoustic Modelling . . . . .	50
	<b>Bibliography</b>	<b>51</b>
	<b>Appendix A Fish Tracking - Details</b>	<b>54</b>
A.1	Fresnel Equations - Comparison between References . . . . .	54
A.1.1	Perpendicular - TE . . . . .	54
A.1.2	Parallel - TM . . . . .	57
A.1.3	TE and TM Polarisation Plots . . . . .	61
A.2	Overall Power . . . . .	62
A.2.1	TE+TM Gain . . . . .	62
A.2.2	TE Gain . . . . .	76
A.2.3	TM Gain . . . . .	88

<b>Appendix B Code</b>	<b>101</b>
B.1 Fish Propagation . . . . .	101
B.1.1 Fish Propagation Model . . . . .	101
B.1.2 Fresnel Equations . . . . .	118
B.2 Acoustic Propagation . . . . .	128
B.2.1 Fitting to Single-layer . . . . .	128
B.2.2 Multi-layer Transmission Line . . . . .	133



# List of Figures

Figure 1.1	The Big Bar landslide in the Fraser Canyon. . . . .	1
Figure 1.2	Hierarchy of controls . . . . .	4
Figure 1.3	Double, triple and quadruple pane windows . . . . .	5
Figure 2.1	TE and TM polarisation diagram. . . . .	8
Figure 2.2	Semi-infinite transmission line modelling the air-water interface. . .	12
Figure 2.3	Angle of incidence in degrees at the air-water interface across the river site for the Eastside downstream receiver. . . . .	17
Figure 2.4	The calculated transmissivity, $ \tau ^2 \operatorname{Re}\left\{\frac{\eta_T}{\eta_I}\right\}$ (dB), due to the wave crossing the air-water interface. . . . .	18
Figure 2.5	Spherical spreading loss at Eastside downstream site (dB). . . . .	19
Figure 2.6	Spherical spreading loss at iBeam P1 site (dB). . . . .	20
Figure 2.7	Interpolated Yagi-Uda Gain. . . . .	21
Figure 2.8	Yagi-Uda Gain Pattern in situ (dB). . . . .	22
Figure 2.9	Simulation of directivity of a transmitter similar to the Sigma Eight TX-PSC-I-1200 and Lotek MCFT3-3A transmitter. . . . .	22
Figure 2.10	Total system loss 0.5(TE+TM) - Eastside downstream site (dB). . .	25
Figure 2.11	Total system loss 0.5(TE+TM) - iBeam p1 site (dB). . . . .	26
Figure 2.12	Total system loss 0.5(TE+TM) - Razorback upstream site (dB). . .	27
Figure 2.13	Total loss 0.5(TE+TM) - Averaged dB gain over all sites (dB). . .	29
Figure 3.1	Multi-layer transmission and reflection . . . . .	31
Figure 3.2	The theoretical transmission loss based on the mass law theory of a single-panel. . . . .	35
Figure 3.3	The theoretical transmission loss for a double-panel compared to the mass law theory of a single-panel. . . . .	36
Figure 3.4	Multi-Layer transmission line. . . . .	37
Figure 3.5	Two-port network model relating the input voltage and current to the output voltage and current. . . . .	37
Figure 3.6	Experimental transmission loss and reflected power . . . . .	41
Figure 3.7	Real and imaginary components of fitted parameters compared to experimental values. . . . .	42

Figure 3.8	Experimental transmit power for a single-pane Three mm window compared with the interpolated transmission line solution. . . . .	43
Figure 3.9	Polynomial fit used on a double-pane window setup. Three mm glass with varying thickness air spacing between panes. . . . .	44
Figure 3.10	Polynomial fit used on a double-pane window setup. Three mm glass with varying thickness argon spacing between panes. . . . .	44
Figure 3.11	Polynomial fit used on a triple-pane window setup. Three mm glass with varying thickness air spacing between panes. . . . .	45
Figure 3.12	Polynomial fit used on a triple-pane window setup. Three mm glass with varying thickness argon spacing between panes. . . . .	45
Figure 3.13	Measured transmitted power for a double-pane, 4 mm glass and 6 mm spacing, window compared with the transmission line solution that has been interpolated. This is using an argon gap. . . . .	46
Figure A.1	TE and TM Fresnel coefficients. . . . .	61
Figure A.2	TE and TM Fresnel Power. . . . .	62
Figure A.3	Total system Loss 0.5(TE+TM)- Eastside Downstream site (dB). The receiver is located at 10U 559418.2593 km E, 15674469.93 km N.	63
Figure A.4	Total system Loss 0.5(TE+TM)- Eastside Upstream site (dB). The receiver is located at 10U 559418.2593 km E, 15674469.93 km N. .	64
Figure A.5	Total system Loss 0.5(TE+TM)- Eddy Downstream site (dB). The receiver is located at 10U 559218.498 km E, 15674445.6 km N. . . .	65
Figure A.6	Total system Loss 0.5(TE+TM)- Eddy Upstream site (dB). The receiver is located at 10U 559217.0907 km E, 15674446.48 km N. . . .	66
Figure A.7	Total system Loss 0.5(TE+TM)- iBeam p1 site (dB). The receiver is located at 10U 559261.9979 km E, 15674586.02 km N. . . . .	67
Figure A.8	Total system Loss 0.5(TE+TM)- iBeam p2 site (dB). The receiver is located at 10U 559268.0157 km E, 15674572.97 km N. . . . .	68
Figure A.9	Total system Loss 0.5(TE+TM)- iBeam p5 site (dB). The receiver is located at 10U 559268.0248 km E, 15674541.94 km N. . . . .	69
Figure A.10	Total system Loss 0.5(TE+TM)- iBeam p6 site (dB). The receiver is located at 10U 559266.0324 km E, 15674533.02 km N. . . . .	70
Figure A.11	Total system Loss 0.5(TE+TM)- Jenny Downstream site (dB). The receiver is located at 10U 559221.7604 km E, 15674302.06 km N. .	71
Figure A.12	Total system Loss 0.5(TE+TM)- Jenny Upstream site (dB). The receiver is located at 10U 559221.7604 km E, 15674302.06 km N. .	72
Figure A.13	Total system Loss 0.5(TE+TM)- Nose site (dB). The receiver is located at 10U 559245.1976 km E, 15674486.4 km N. . . . .	73

Figure A.14	Total system Loss 0.5(TE+TM)- Razorback Downstream site (dB). The receiver is located at 10U 559185.8782 km E, 15674173.07 km N.	74
Figure A.15	Total system Loss 0.5(TE+TM)- Razorback Upstream site (dB). The receiver is located at 10U 559191.6489 km E, 15674169.36 km N.	75
Figure A.16	Total system loss TE- Eastside Downstream site (dB).	76
Figure A.17	Total system loss TE- Eastside Upstream site (dB).	77
Figure A.18	Total system loss TE- Eddy Downstream site (dB).	78
Figure A.19	Total system loss TE- Eddy Upstream site (dB).	79
Figure A.20	Total system loss TE- iBeam p1 site (dB).	80
Figure A.21	Total system loss TE- iBeam p2 site (dB).	81
Figure A.22	Total system loss TE- iBeam p5 site (dB).	82
Figure A.23	Total system loss TE- iBeam p6 site (dB).	83
Figure A.24	Total system loss TE- Jenny Downstream site (dB).	84
Figure A.25	Total system loss TE- Jenny Upstream site (dB).	85
Figure A.26	Total system loss TE- Nose site (dB).	86
Figure A.27	Total system loss TE- Razorback Downstream site (dB).	87
Figure A.28	Total system Loss TM- Eastside Downstream site (dB).	88
Figure A.29	Total system Loss TM- Eastside Upstream site (dB).	89
Figure A.30	Total system Loss TM- Eddy Downstream site (dB).	90
Figure A.31	Total system Loss TM- Eddy Upstream site (dB).	91
Figure A.32	Total system Loss TM- iBeam p1 site (dB).	92
Figure A.33	Total system Loss TM- iBeam p2 site (dB).	93
Figure A.34	Total system Loss TM- iBeam p5 site (dB).	94
Figure A.35	Total system Loss TM- iBeam p6 site (dB).	95
Figure A.36	Total system Loss TM- Jenny Downstream site (dB).	96
Figure A.37	Total system Loss TM- Jenny Upstream site (dB).	97
Figure A.38	Total system Loss TM- Nose site (dB).	98
Figure A.39	Total system Loss TM- Razorback Downstream site (dB).	99
Figure A.40	Total system Loss TM- Razorback Upstream site (dB).	100

## List of Acronyms

**ANC** Active Noise Cancellation

**EM** electromagnetic

**DFO** Department of Fisheries and Oceans

**RDL** River Dynamics Lab

**RF** Radio Frequency

**TE** Transverse Electric

**TM** Transverse Magnetic

**PPE** Personal Protective Equipment

**MEG** Mean Effective Gain

**SFU** Simon Fraser University

**SPL** Sound Pressure Level

# Chapter 1

## Introduction

### 1.1 Propagation Modelling for Fish Tracking

On June 23, 2019, a landslide was detected 60 km north of Lillooet in a part of the Fraser River canyon known as Big Bar. 110,000 cubic meters of rock fell off a 125-meter cliff into the Fraser River creating a seven-meter waterfall [1, 2]. The hydraulic barrier jeopardized migrating salmon from returning to their spawning locations upstream in the upper Fraser Basin [3]. This in turn impacted the ecology of the river including the current salmon biodiversity [3]. A project is being undertaken by the Simon Fraser University (SFU) School of Environmental Science to radio-track salmon as they encounter the landslide-affected part of the river. This part of the thesis covers the theory and application of propagation analysis at a river system in order to increase the tracking accuracy of the passing salmon.



Figure 1.1: The Big Bar landslide in the Fraser Canyon. The landslide caused a massive hydraulic barrier in the river [4].

### 1.1.1 Background

The landslide obstruction saw a drastic change in the natural spawning with “less than 1% of early Stuart Sockeye and 11% of early Chinook migrating past the slide in 2019” [2] highlighting the devastating impact of the landslide. To preserve the salmon’s natural life cycle, the provincial and federal governments, in conjunction with First Nations, have stepped in to assist with saving the salmon. Many approaches have been used to get past the landslide blockage to the salmon including the usage of a helicopter to transport salmon past the slide site, blasting rock to free the blocked area, building a concrete salmon ladder and pumping salmon past the blocked portion using a pneumatic salmon pump system [5]. These solutions have shown various degrees of success going from a handful of fish being able to pass when the slide occurred, to October 24<sup>th</sup> 2020 when there was a total of "161,000 salmon detected 40 km upstream of slide site to date" [5]. For perspective, in the last decade, this area had seen an estimate in the order of 10 million [6].

Although the multi-pronged response to this natural disaster saved thousands of salmon, there is still a lack of understanding around the intricacies of salmon migration. The Big Bar landslide is not a unique scenario and "the chance of future landslides in the Fraser Canyon is real" [3]. To better understand how the salmon select their migration pathway, Dr. Evan Byrnes, post-doctoral student with the River Dynamics Lab (RDL) at SFU, the Department of Fisheries and Oceans (DFO) and Ms. Sabrina Sixta, a PhD student at the University of Toronto, are analyzing radio tracking data of salmon as they travel through the Big Bar landslide site. This process includes catching and tagging salmon with a radio transmitter downstream of the blockage and using Yagi-Uda antennas along the shoreline to receive the salmon signals. By analyzing the data, the hope is to answer important ecological questions such as [7]:

- How does time spent migrating or the energy used migrating drive the salmon’s migration pathway selection?
- Does the pathway selected depend on flow rate, temperature, or some other environmental factor?

The current setup and analysis can determine if a salmon has passed the area under investigation, however, it is not currently possible to locate the salmon. A position estimate is needed to be able to draw any conclusions regarding the pathway selection of the salmon. To assist the research team in answering their ecological migration pathway questions, the goal of this part of the thesis is to determine the theoretical positioning of the salmon in the river based on the power received at the receiver. This propagation model will be used in conjunction with experimental gain data gathered by the RDL and DFO to create a state-space model in order to provide a final estimation of a fish’s location. By understanding the migratory behaviour of the salmon, the research has the potential to help navigate salmon through landslides and changing environmental conditions in the future.

Many electromagnetic (EM) textbooks [8, 9, 10, 11] cover propagation topics such as the Fresnel equations, oblique incidence, transmission lines etc., however they do not provide detailed analysis of these topics and their application to real world challenges such as propagation through an air-water interface followed by conductive loss.

Propagation into fresh water has been studied [12] however, the study consisted of planar waves and does not include spherical spreading, antenna gains and any physical geometry of the propagation environment. Fine-scale fish tracking has been investigated [13, 14, 15] but it has either involved a machine learning model [13] that predicted locations based solely on experimental results, or involved mobile tracking using either a boat or car to determine the actual location of the fish by maximizing the received signal [14]. These solutions present their own respective problems and would not work at the Big Bar site. The remote and rugged terrain prevents following fish to identify their position. Also, unlike calm lake conditions, the rapids of the Fraser River require a metal hulled boat with a transmitter on a pole, therefore using solely test data would be erroneous as the experimental measurement represents different conditions to the fish travelling naturally.

### **1.1.2 Contribution**

The main contribution of this thesis is a comprehensive analysis of the propagation problem of fish passing through a high flow river section using a deterministic transmission line model to calculate the gain at every point in a raster of the Fraser River landslide site. The model was generalized such that any raster of river locations along with any receiving antenna pattern can be imported and the code will provide the expected gain. Another contribution is a transmission line analysis for acoustic propagation through multiple layers.

## **1.2 Acoustic Propagation Model for Multi-layer Structures**

In lossless propagation, EM and acoustic propagation share similarities from their respective wave equations [16]. This can be leveraged to analyze an acoustic propagation problem of transmission through a multi-layer window, more commonly known as a multi-pane window. Propagation within homes and specifically through windows is a challenge that manufacturers and architects struggle to analyze or optimize [17].

### **1.2.1 Background**

As cities become more crowded and noisier, it is becoming increasingly important to reduce the noise from our surroundings for both our physical health and mental well-being [18]. "Chronic annoyance and sleep disturbance, resulting in severe heart disease and metabolic disorders such as diabetes, and hearing impairment and poorer mental health" [18] are all conditions attributed to noise pollution. Acoustics has had a recent surge in popularity in

academia [19] and in industry where there has been widespread commercialization of Active Noise Cancellation (ANC) devices.

Analyzing the noise pollution problem as a hazard we can use the Hierarchy of Controls in Figure 1.2, a five-step process to reduce risk and a method for ranking a solutions effectiveness against risk created by the National Institute for Occupational Safety and Health [20]. ANC devices would sit at the lowest rung of Personal Protective Equipment (PPE) and offer the least effective protection against the noise pollution. This thesis will investigate the physics behind an "Engineering Solution" of reducing the noise that people are exposed to by altering the construction of windows to provide greater sound isolation.

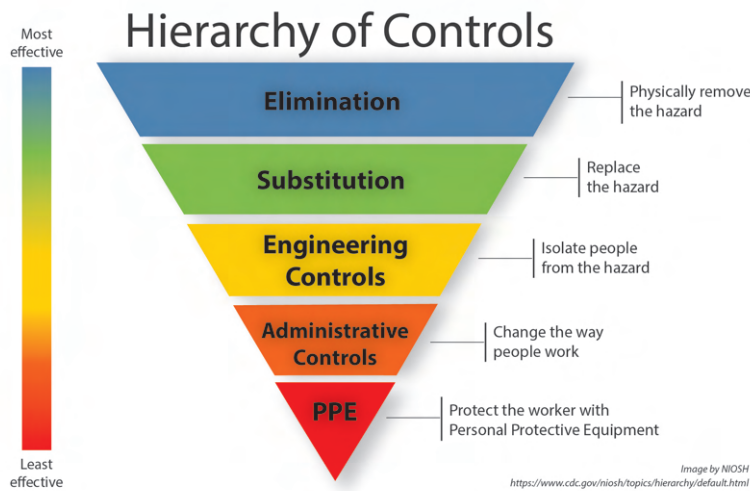


Figure 1.2: Hierarchy of controls. A process to reduce risk and a method to rank a solution’s effectiveness at safeguarding a person from a hazard [20].

It is possible to easily compare various construction layouts, different medium and spacing’s between the panes and different numbers of glass panes by creating a generalized model with acoustic transmission equations to determine the power loss as the sound propagates through a multi-layer window. This model can be used as a learning tool to rationalize experimental acoustic results and provides an understanding of how to design more acoustically isolating windows.

Acoustic propagation is a relatively well researched topic, and there are a variety of theoretical and experimental works in textbooks and research papers about acoustic propagation, specifically propagation through windows [16, 22, 23, 24, 25]. Many of the works provide very thorough theoretical and experimental analysis to model various types of acoustic scenarios that can’t be replicated in an undergraduate thesis.



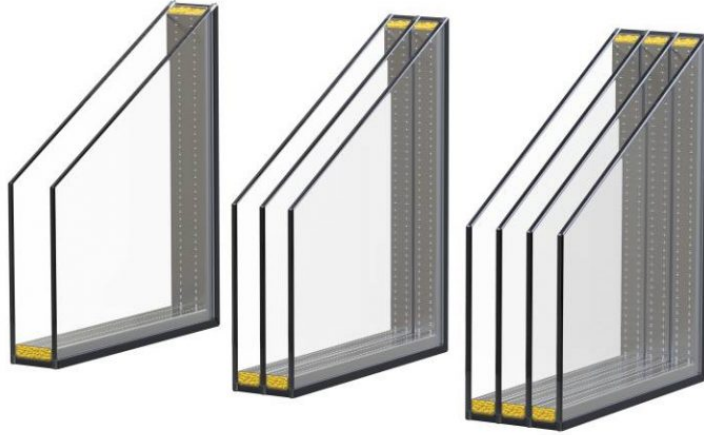


Figure 1.3: Double, triple and quadruple pane windows [21].

### 1.2.2 Contributions

The key contribution is using the experimental results presented for single layered acoustic transmission [24] and using them to complete a transmission line model that can be used to analyze more complex, multi-layered scenarios. The transmission line model is leveraged to compare the exponential loss mechanism of EM with the experimental results for both single and double-pane windows.

## 1.3 Road Map

The thesis has four chapters.

- Chapter 1 provides an introduction and background motivation on the importance and contribution of the thesis to the field of propagation.
- Chapter 2 covers the fish tracking model. It will highlight the underlying principles that the model simulates. The chapter will detail how the model was implemented including any important parameters and assumptions made. The chapter will provide verification of the results and the results for the model. It will then provide discussion points on the results relevant to the scenario.
- Chapter 3 covers the acoustic propagation model for multi-layer structures. It will highlight the underlying principles that the model simulates and delve deeper into the implementation of a multi-layer transmission line. The chapter will detail how the model was implemented including any important parameters and assumptions and it will then provide discussion points on the results.

- Chapter 4 concludes the thesis and provides future work suggestions for both the fish tracking and the acoustic model.

## Chapter 2

# Fish Tracking

The fish-tracking model uses propagation concepts to get an estimate of the signal strength of a fish at a specific spot in the river. Ideally this model would match with experimentally collected data however there are a variety of assumptions that need to be made. The model can be used as a basis providing information on how realistic it is to track spawning salmon using signal strength.

### 2.1 Assumptions

The assumptions to simplify the model include:

- The model does not include line-of-sight blockages like the cliffs present in the area under investigation.
- The transmitting antenna is treated as having an averaged gain in all directions, called Mean Effective Gain (MEG). Since we are unsure of the flow of the river or the direction the fish swims, it is impossible to know what angle the EM wave might be emanating from the transmitter. Using the MEG is a useful statistical approach to simplify the situation. The receiving antenna is stationary with a fixed orientation therefore the gain is taken from its gain pattern.
- No multi-path signals are considered. The only path considered is line-of-sight between the transmitter and receiver. This is an important omission since the model occurs within a canyon potentially creating many multi-path signals.
- All waves are assumed to be plane waves, simplifying the field equations and the relationships between the electric and magnetic fields.
- The pattern averaging means that the model uses half of the Transverse Electric (TE) polarisation and half of the Transverse Magnetic (TM) polarisation to describe how the plane wave travels across the water's surface.

- The plane wave crosses a flat surface, there are no waves or ripples in the model of the river surface.

## 2.2 Underlying Principles

The approach for the salmon tracking propagation follows closely from wireless communications propagation, however a key difference is that this scenario requires transmission between two media, whereas most wireless propagation only involves free space. The key elements that the model include are: the air-water interface, the attenuation due to the water, the antenna gains and the spherical spreading of the EM wave.

### 2.2.1 Air - Water Interface

Two approaches were taken to model the air-water interface: a fields approach using the Poynting vector and using the Fresnel equations. The Fresnel equations result from the boundary conditions imposed on the electric and magnetic fields. Both the Poynting vector and the Fresnel equations result in the same solution.

Due to the geometry of the problem, the EM fields are obliquely incident on the surface and as such the plane wave needs to be decomposed into TE and TM modes [26].

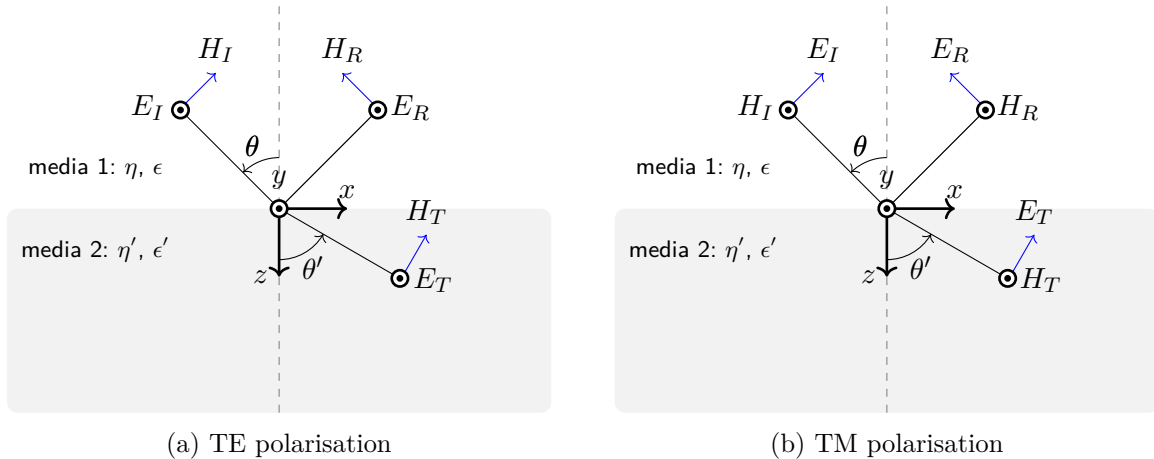


Figure 2.1: TE and TM polarisation diagram.(a) TE polarisation, also commonly referred to as the perpendicular or s-polarisation. The electric field oscillates perpendicular to the plane of the diagram, (b) TM polarisation, also commonly referred to as the parallel or p-polarisation. The electric field oscillates in the plane of the diagram.

### Field Approach

The fields approach uses both E and H fields to calculate the time-averaged power flux density using the Poynting vector of the incident wave in air and the transmitted wave in water. The below derivation follows for the TE scenario. With the fields known at any

location we can calculate the time-averaged power flux density or equivalently the time-averaged Poynting vector:

$$\langle \vec{S} \rangle = \frac{1}{2} \text{Re} \{ \vec{E} \times \vec{H}^* \}. \quad (2.1)$$

To obtain the ratio of the transmitted to incident power flux, we first start with the equation for the electric and magnetic fields in both media [8], where the apostrophe denotes the second medium, water:

$$E(r) = \hat{y} E_0 [e^{-jk(x \sin \theta_i + z \cos \theta_i)} + \Gamma_{TE} e^{-jk(x \sin \theta_r - z \cos \theta_r)}] \quad (2.2)$$

$$E'(r) = \hat{y} \tau_{TE} E_0 e^{-jk'(x \sin \theta' + z \cos \theta')} \quad (2.3)$$

$$H(r) = \frac{E_0}{\eta} \left[ (-\hat{x} \cos \theta_i + \hat{z} \sin \theta_i) e^{-jk(x \sin \theta_i + z \cos \theta_i)} + \Gamma_{TE} (\hat{x} \cos \theta_r + \hat{z} \sin \theta_r) e^{-jk(x \sin \theta_r - z \cos \theta_r)} \right] \quad (2.4)$$

$$H'(r) = \frac{E_0 \tau_{TE}}{\eta'} \left[ (-\hat{x} \cos \theta' + \hat{z} \sin \theta') e^{-jk'(x \sin \theta' + z \cos \theta')} \right]. \quad (2.5)$$

The complex reflection and transmission coefficients,  $\Gamma_{TE}$  and  $\tau_{TE}$ , are given by the following Fresnel equations using the notation of [8] for now:

$$\Gamma_{TM} = \frac{\eta' \cos(\theta') - \eta \cos(\theta)}{\eta' \cos \theta' + \eta \cos \theta}, \quad \Gamma_{TE} = \frac{\eta' \cos \theta - \eta \cos \theta'}{\eta' \cos \theta + \eta \cos \theta'} \quad (2.6)$$

$$\tau_{TM} = \frac{2\eta' \cos \theta'}{\eta' \cos \theta' + \eta \cos \theta} = 1 + \Gamma_{TM}, \quad \tau_{TE} = \frac{2\eta' \cos \theta}{\eta' \cos \theta + \eta \cos \theta'} = 1 + \Gamma_{TE}. \quad (2.7)$$

The remaining variables can be written compactly as:

$$\text{Wave Number} = \begin{cases} k = \omega \sqrt{\mu_0 \epsilon} \\ k_x = k \sin \theta, k_z = k \cos \theta \end{cases} \quad (2.8)$$

$$\text{Permittivity} = \begin{cases} \epsilon = \epsilon_R - j\epsilon_I \\ \epsilon_R = \epsilon_0 \epsilon_r \end{cases} \quad (2.9)$$

$$\text{Wave Impedance: } \eta = \sqrt{\frac{\mu}{\epsilon}} \quad (2.10)$$

The imaginary portion of the permittivity of fresh water complicates the analysis in the water. We can use geometrical properties due to boundary conditions to simplify the analysis. Firstly, the wave number in the  $x$ -direction remains the same no matter what material the wave goes into:

$$k'_x = k_x. \quad (2.11)$$

Secondly, the  $z$ -component of the wave number changes due to the difference in permittivities. When dealing with non-magnetic materials, such as water and air,  $\mu = \mu_0$  is constant across the boundary:

$$k'_z = k' \cos \theta' = \beta'_z - j\alpha'_z.$$

Using the wave numbers we see that the transmitted fields will have a spatial dependence that goes as:

$$e^{-jk'_z z} e^{-jk_x x} = e^{-\alpha'_z z} e^{-j(\beta'_z z + k_x x)}.$$

In the case of a lossy material the attenuation is due to  $e^{-\alpha'_z z}$  and the travelling wave is the remaining parts. It is interesting to note that the attenuation portion is only due to the  $z$ -component of the wave as it travels.

In the case of the TE Mode,  $E_x = 0$ ,  $E_z = 0$ , and  $H_y = 0$ , we can split the overall E and H equations (2.5) into the incident, reflected and transmitted portion. Since the wave is continuous in the  $x$ -direction, (2.11), we only need to look in the  $z$ -direction to find the ratio of incident, reflected and transmitted power flux density. The  $z$ -component of the power flux density above the water, using notation from [10] for now, is:

$$P_{Air_z} = \frac{1}{2} \text{Re}\{\vec{E} \times \vec{H}^*\}_z = \frac{|E_0|^2}{2\omega\mu_0} k_z (1 - |\Gamma_{TE}|^2) \quad (2.12)$$

where the incident and reflected fluxes in the  $z$ -direction are [8]:

$$P_{I_z} = \frac{1}{2} \text{Re}\{\vec{E} \times \vec{H}^*\}_z = \frac{|E_0|^2}{2\omega\mu_0} k_z \quad (2.13)$$

$$P_{R_z} = \frac{1}{2} \text{Re}\{\vec{E} \times \vec{H}^*\}_z = -\frac{|E_0|^2}{2\omega\mu_0} k_z |\Gamma_{TE}|^2 \quad (2.14)$$

$$P_{Air_z} = P_{I_z} + P_{R_z}. \quad (2.15)$$

The  $z$ -directed transmitted power flux density in the water is [8]:

$$P_{T_z} = \frac{|E_0|^2}{2\omega\mu_0} \beta'_z |\tau_{TE}|^2 e^{-2\alpha'_z z}. \quad (2.16)$$

The ratio of received to transmitted power is:

$$\frac{\text{Transmitted Power}}{\text{Initial Power}} = |\tau_{TE}|^2 \frac{\beta'_z}{k_z} e^{-2\alpha'_z z} = |\tau_{TE}|^2 \frac{\eta}{\cos \theta} \text{Re}\left\{\frac{\cos \theta'}{\eta'}\right\} e^{-2\alpha'_z z}. \quad (2.17)$$

This can be generalized to TE and TM polarisations using the following definition for the wave impedance:

$$\eta_T = \begin{cases} \eta_{TE} = \frac{\eta}{\cos \theta} & \text{For the TE case} \\ \eta_{TM} = \eta \cos \theta & \text{For the TM case} \end{cases} \quad (2.18)$$

$$\frac{\text{Transmitted Power}}{\text{Initial Power}} = |\tau|^2 \eta_T \operatorname{Re} \left\{ \frac{1}{\eta_T'} \right\} e^{-2\alpha'_z z}. \quad (2.19)$$

### 2.2.2 Attenuation

When using the Fresnel equations directly, the attenuation needs to be taken separately into account and added since the Fresnel equations only provide the boundary conditions for the fields and for the power at the air-water interface. Although the Fraser River is fresh water, at the site of the land slide there is an associated conductivity of the water. The attenuation due to the conductivity is given by the following variables adapted from [10]:

$$e^{-2\alpha'_z z} = e^{-2\operatorname{Re}\{jk'_z z\}} = e^{2\operatorname{Im} k'_z z} \quad (2.20)$$

$$\operatorname{Im}\{k'_z\} = \operatorname{Im} \left\{ \sqrt{\omega^2 \mu_0 \epsilon' - k_x^2} \right\} \quad (2.21)$$

$$\alpha'_z = \left[ \frac{\sqrt{(\omega^2 \mu_0 \epsilon'_R - k_x^2)^2 + (\omega^2 \mu_0 \epsilon'_I)^2} - (\omega^2 \mu_0 \epsilon'_R - k_x^2)}{2} \right]^{\frac{1}{2}} \quad (2.22)$$

with the permittivity as defined by (2.9). The attenuation due to the conductive losses contains an angular dependence with the  $k_x$  term, however, due to the small conductivity value, the difference in attenuation between normal incidence and  $90^\circ$  incidence is only 0.08 dB at a depth of five meters. For the depths of interest, the incident angle does not impact the attenuation.

### 2.2.3 Transmission Lines

Using a two-layer semi-infinite transmission line model, see Figure 2.2, it is possible to obtain the same values as either the fields approach or the combined Fresnel equations and attenuation term.

It is important to recast the EM variables, wave impedance and wave number, into transmission line equation variables, characteristic impedance, and propagation constant. The transmission line explicitly works for one dimension of propagation, yet still models oblique incidence, since the lossy propagation parameters are derived solely from the terms perpendicular to the interface, as shown in (2.16) and (2.15). The characteristic impedance of the transmission line is equal to the transverse wave impedance that is used when analyzing

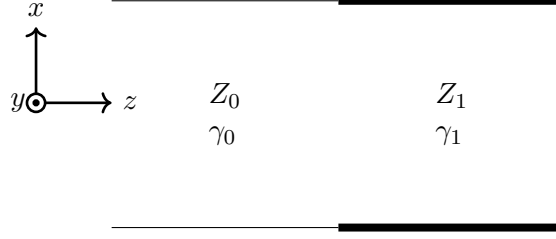


Figure 2.2: Semi-infinite transmission line modelling the air-water interface and attenuation within the water. In our model the water is viewed as infinitely deep therefore there are no reflections at the bottom of the river.

the problem from a fields perspective:

$$Z = \begin{cases} \eta_{TE} = \frac{\eta}{\cos \theta} & \text{TE polarisation} \\ \eta_{TM} = \eta \cos \theta & \text{TM polarisation} \end{cases} \quad (2.23)$$

The complex propagation constant is related to the wave number, here expressed as:

$$\gamma = jk_z = \alpha_z + j\beta_z. \quad (2.24)$$

Whereas with EM fields we are dealing with E and H fields, with the transmission line we use voltages and currents. The general solutions to the transmission line follow from a wave equation:

$$V(z) = V_0 (e^{-\gamma_0 z} + \Gamma_T e^{\gamma_0 z}) \quad , \quad I(z) = \frac{V_0}{Z_0} (e^{-\gamma_0 z} - \Gamma_T e^{\gamma_0 z}). \quad (2.25)$$

The  $\gamma_0$  refers to  $\gamma$  in free space. The reflection and transmission coefficient given in terms of impedance are:

$$\Gamma_T = \frac{Z_1 - Z_0}{Z_1 + Z_0} \quad , \quad \tau = \frac{2Z_1}{Z_1 + Z_0}. \quad (2.26)$$

The specific solution for the semi-infinite transmission line is known:

$$V(z), I(z) = \begin{cases} V(z) = V_0 e (e^{-\gamma_0 z} + \Gamma_T e^{\gamma_0 z}) & z \leq 0 \\ I(z) = \frac{V_0}{Z_0} (e^{-\gamma_0 z} - \Gamma_T e^{\gamma_0 z}) & z \leq 0 \\ V(z) = V_1 e^{-\gamma_1 z} & z \geq 0 \\ I(z) = \frac{V_1}{Z_1} e^{-\gamma_1 z} & z \geq 0 \end{cases}$$



The voltage and current must be continuous across the boundary. Placing the boundary at  $z = 0$ , we obtain that  $V(0^-) = V(0^+)$  and  $I(0^-) = I(0^+)$ , reducing our solutions to:

$$V(0) = V_0(1 + \Gamma_T) = V_1 \quad (2.27)$$

$$I(0) = \frac{V_0}{Z_0}(1 - \Gamma_T) = \frac{V_1}{Z_1} \quad (2.28)$$

$$V_1 = V_0(1 + \Gamma_T) \quad (2.29)$$

$$V_1 = \frac{V_0 Z_1}{Z_0}(1 - \Gamma_T) \quad (2.30)$$

The power, here in watts rather than power density in watts/m<sup>2</sup>, at any point can be calculated using:

$$P = \frac{1}{2} \operatorname{Re}\{V(z)I(z)^*\} \quad (2.31)$$

with  $V_0$  and  $I_0$  being the maximum amplitude values. The power input to the transmission line is given by:

$$P_{in} = \frac{|V_0|^2}{2Z_0}. \quad (2.32)$$

The power at any point  $l$  in the water can be given as:

$$P(l) = \frac{1}{2} \operatorname{Re}\left\{\frac{1}{Z_1^*}\right\} |V_1|^2 e^{-2\alpha l} = \frac{|V_0|^2}{2Z_0} (1 - |\Gamma_T|^2) e^{-2\alpha l}. \quad (2.33)$$

Taking the ratio of received to transmitted power:

$$\frac{P(l)}{P_{in}} = \frac{\frac{1}{2} \operatorname{Re}\left\{\frac{1}{Z_1^*}\right\} |V_0|^2 (1 - |\Gamma_T|^2) e^{-2\alpha l}}{\frac{1}{2} \operatorname{Re}\left\{\frac{1}{Z_0^*}\right\} |V_0|^2} = (1 - |\Gamma_T|^2) e^{-2\alpha l} = |\tau|^2 \operatorname{Re}\left\{\frac{\eta_T}{\eta_T'}\right\} e^{-2\alpha l}, \quad (2.34)$$

we observe the transmission line model yields accurate results for oblique incidence into a lossy medium, and these results align with the previous two sections (2.19).

## 2.2.4 Transmit and Receive Antennas

The implementation of the antennas into the propagation model follows two steps: the directional gain of the antenna and the polarisation mismatch due to the alignment of the antennas.

### Gain of the Antenna

The directivity of the antenna provides information on the ratio of radiation intensity in a given direction from the antenna to the total radiation density in all directions. It requires

both information on the co-polar power and cross-polar power patterns. The directivity is calculated as follows:

$$D(\theta_0, \phi_0) = \frac{|\mathbf{g}(\theta_0, \phi_0)|^2}{\frac{1}{4\pi} \int_0^{2\pi} \int_0^\pi |\mathbf{g}(\theta, \phi)|^2 \sin \theta d\theta d\phi}, \quad (2.35)$$

where  $\mathbf{g}(\theta, \phi)$  is the electric field pattern:

$$\mathbf{g}(\theta, \phi) = g_\theta(\theta, \phi)\hat{\theta} + g_\phi(\theta, \phi)\hat{\phi}. \quad (2.36)$$

The gain of the antenna is given by the directivity of the antenna and the antenna efficiency [27] and can be expressed as:

$$G(\theta, \phi) = \eta_{ant} D(\theta, \phi) \quad (2.37)$$

The antenna efficiency includes the ohmic losses but not any feed mismatch loss, the *realized* gain includes both [28].

### Mean Effective Gain

In a mobile setting, oftentimes used for mobile communications, a MEG will be used instead of a directive gain to describe the behaviour of an antenna under a statistical distribution of incoming waves. This technique can be leveraged in the fish transmitter scenario as the MEG can be used to statistically account for the motion of the fish and its transmitter.

$$MEG = \int \left( \frac{XPD}{1 + XPD} P_\theta(\Omega) G_\theta(\Omega) + \frac{1}{1 + XPD} P_\phi(\Omega) G_\phi(\Omega) \right) d\Omega \quad (2.38)$$

$$= \eta \int \left( \frac{XPD}{1 + XPD} P_\theta(\Omega) D_\theta(\Omega) + \frac{1}{1 + XPD} P_\phi(\Omega) D_\phi(\Omega) \right) d\Omega \quad (2.39)$$

$$XPD = \frac{P_\theta}{P_\phi} \quad (2.40)$$

with  $P_\theta$  the total power in  $\theta$ -polarisation and  $P_\phi$  the total in the  $\phi$ -polarisation [27].  $XPD$  is defined as "the ratio between two average polarisation powers" [27].

The power quantities and directivity are normalised such that:

$$\int P_\theta(\Omega) d\Omega = 1 \quad (2.41)$$

$$\int P_\phi(\Omega) d\Omega = 1. \quad (2.42)$$

In a completely random environment with the incoming wave being uniform in three dimensions, we can take  $XPD = 1$  and the power in each polarisation to be  $P_\theta = P_\phi = \frac{1}{4\pi}$ .

The MEG will then evaluate to be half of the efficiency of the radiating antenna [29, 27].

$$MEG_{\text{random}} = \eta \int \left( \frac{1}{1+1} \frac{1}{4\pi} D_{\theta}(\Omega) + \frac{1}{1+1} \frac{1}{4\pi} D_{\phi}(\Omega) \right) d\Omega = \frac{\eta}{2} \quad (2.43)$$

### 2.2.5 Spherical Spreading

Plane waves do not have any spherical spreading, therefore a term is added in free space calculations to account for the geometric spreading. The model has the added complication that the source continues to spread as it crosses the air-water interface. Instead of calculating the path loss for each portion, we add the distance-to-wavelength ratios of both the air and water component.

$$\text{Path gain due to spherical spreading} = \left( \frac{1}{4\pi \left( \frac{d_1}{\lambda_1} + \frac{d_2}{\lambda_2} \right)} \right)^2 \quad (2.44)$$

In this scenario  $d_1$ , and  $\lambda_1$  are the distance the ray travels and the wavelength in air.  $d_2$  and  $\lambda_2$  are similarly defined for water. Since we are calculating a point-to-point gain, the (2.44) term accounts for the spherical radiation that occurs in all directions and not just in two-dimensional space. At 150 MHz,  $\lambda_1 = 1.9986$  m and  $\lambda_2 = 0.2221$  m.

### 2.2.6 Total Path Loss

The total path loss, inverse of path gain, can be best expressed using the Friis path loss equation with some modification. The Friis equation is derived solely for free space [30] therefore we have to add meaningful additions to account for the air-water interface and the subsequent attenuation. The original Friis equation can be written as:

$$\frac{P_r}{P_t} = G_t G_r \left( \frac{\lambda}{4\pi d} \right)^2 \quad (2.45)$$

where  $G_t$  and  $G_r$  are the gains of the transmitting and receiving antenna respectively. Using the modified spherical spreading, the conductive attenuation, the polarisation mismatch and the reflected power at the air-water interface, we can adapt the Friis free space equation to the following form:

$$\frac{P_r}{P_t} = G_t G_r \left( \frac{1}{4\pi \left( \frac{d_1}{\lambda_1} + \frac{d_2}{\lambda_2} \right)} \right)^2 |\tau|^2 \text{Re} \left\{ \frac{\eta_T}{\eta'_T} \right\} e^{-2\alpha'_z z} \eta_{pol} \quad (2.46)$$

where  $\tau$ ,  $\eta_T$  and  $\eta'_T$  are selected as either their TE or TM values depending on the scenario. The spherical spreading term is (2.44). The conductive attenuation is (2.20). The polarisation mismatch is  $\eta_{pol}$ . Here, it is assumed that  $\eta_{pol}$  represents an averaged polarisation

mismatch between the transmit and receive antennas. The reflected power at the air-water interface is given by equation(2.19).

## 2.3 Model Implementation and Verification

The fish tracking model was implemented using Matlab. Dr. Evan Byrnes and the RDL provided csv rasters for each of the 13 receivers set up along the Big Bar Fraser River site. These rasters included the following data: height of the antenna, distances from the antenna to the 20,814 latitude and longitudes of the rivers surface, the bearing and the pitch of the antenna and a variety of other data. The model output is a csv file including the site name, the longitude and latitude of a spot on the river surface, depth in the river ranging from -0.1 m to -1.6 m, the gain value of TE and TM polarisations and an equally weighted combination of the two,  $0.5(\text{TE}+\text{TM})$ , antenna latitude and longitude and the height of the antenna.

In order to provide a meaningful comparison for the river conditions during the experimental data collection, low tide, and when the fish will pass through the river site, each antenna site was run ranging the offset height from -1 m to +15 m. A 15 m offset means that the river is 15 m closer to the Yagi-Uda receiving antenna than at the time of measurement. The rasters of predicted gain data provided by this thesis alongside experimental data collected by the DFO and the RDL will then be fed into a machine learning model developed to determine the final prediction location of the fish based on the received signal strength.

For our model we used the following values and constants. The conductivity was the only value that was measured and provided by the DFO:

$$\epsilon_0 = 8.854 \times 10^{-12} \text{ F/m}$$

$$\epsilon'_r = 81$$

$$\mu_0 = 4\pi \times 10^{-7} \text{ H/m}$$

$$\sigma = 0.014 \text{ S/m}$$

$$f = 150 \text{ MHz.}$$

$$\epsilon' = \epsilon_0 \epsilon'_r - j \frac{\sigma}{\omega}$$

### 2.3.1 Media Interface

The first step is to calculate the loss due to the Fresnel equations, (2.6) and (2.7), on the raster. In reality the salmon is the transmitter and the Yagi-Uda is the receiver, however due to the nature of the Fresnel equations it is possible that a point source emanating from the salmon would not necessarily meet the Yagi-Uda as a point-to-point ray. Using either the Yagi-Uda as the transmitter or the salmon tag as the transmitter results in the same

total path gain. At this stage, a basic model is made that considers the propagation across the river surface depending on the angle of incidence. A shortened raster of the river site for one of the locations is shown in Figure 2.3 with the angles of incidence from the Yagi-Uda. Based on the angles of incidence, the Fresnel TE and TM polarisation transmissivity values are shown in the following two plots, Figure 2.4. This represents the amount of power that gets transmitted at the surface of the river.

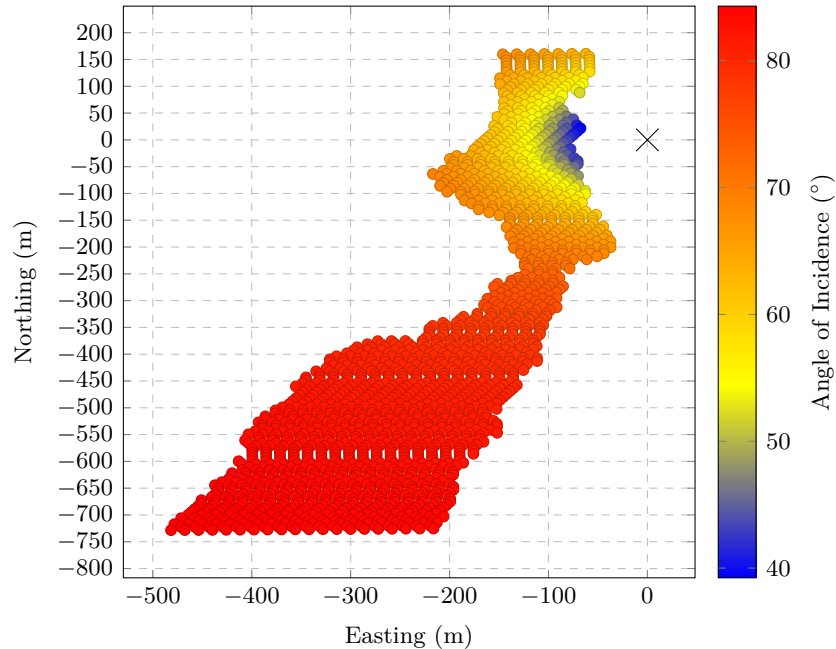


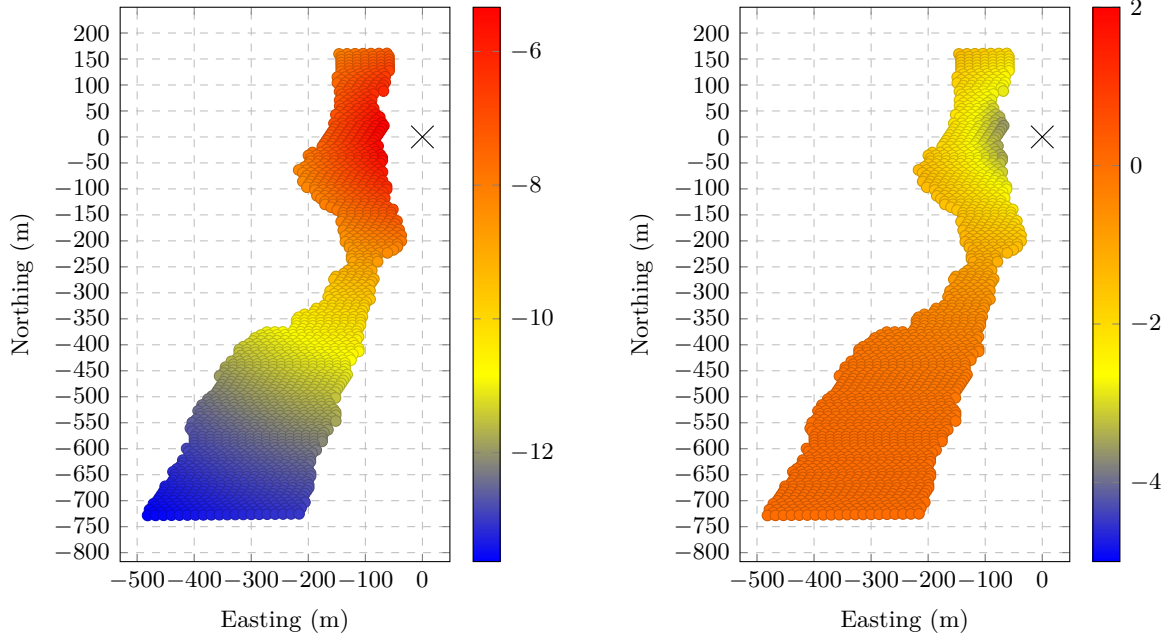
Figure 2.3: Angle of incidence in degrees at the air-water interface across the river site for the Eastside downstream receiver. The angle is defined as the angle from the normal to the surface of the river. The Eastside downstream receiver is located at 10U 559418.259 km E, 15674469.934 km N.

### 2.3.2 Attenuation and Spherical Loss

The two remaining propagation losses are added. The first propagation loss is due to spherical spreading of the EM wave, (2.44), and the second is due to the attenuation within the water (2.20). The impact of the spherical spreading of the EM wave is presented in Figure 2.5 and Figure 2.6.

Although the antennas are situated in different locations, the iBeam antenna is 36 m to the water and the Eastside antenna is 240 m, the spherical spreading relationship, (2.44) means that most of the power loss occurs in the first few meters after the transmission.

The attenuation in water exhibits a linear loss in dB relative to the depth of water that is independent of the incoming angle. This is because the conductivity was measured to be very small. Therefore, the conductive attenuation does not differentiate between antenna sites.



(a) Eastside downstream TE

(b) Eastside downstream TM

Figure 2.4: The calculated transmissivity,  $|\tau|^2 \text{Re}\left\{\frac{\eta_T}{\eta_T}\right\}$  (dB), due to the wave crossing the air-water interface. a) Fresnel TE - Transmissivity (dB). b) Fresnel TM - Transmissivity (dB).

### 2.3.3 Transmit and Receive Antennas

Following the loss terms, the antenna gains are added to complete the Friis equation (2.47). The radiation patterns of both transmitting and receiving antenna couldn't be verified experimentally since our pattern measurement chambers do not go to a low enough frequency.

#### Gain of the Antennas

The receive antenna was a three element Yagi-Uda antenna. Photos of the experimental gain profile of the Yagi-Uda antennas were received from the manufacturer. The azimuthal and elevation plots that were received indicated there was an error in the analysis of the radiation pattern. The peak gain in the azimuthal plot did not correspond to the peak gain in the elevation plot. However, the difference was marginal, approximately one dB between the cuts. The elevation plot was selected, and it was assumed that the radiation pattern was symmetrical around the boom of the Yagi-Uda antenna. Yagi-Uda antennas do contain a high level of symmetry. The data points were extrapolated visually from the photo into a csv file. With these points, an interpolation was done in Matlab to calculate the gain of the antenna at any point. The final Matlab model of the Yagi-Uda gain pattern can be seen in Figure 2.7.

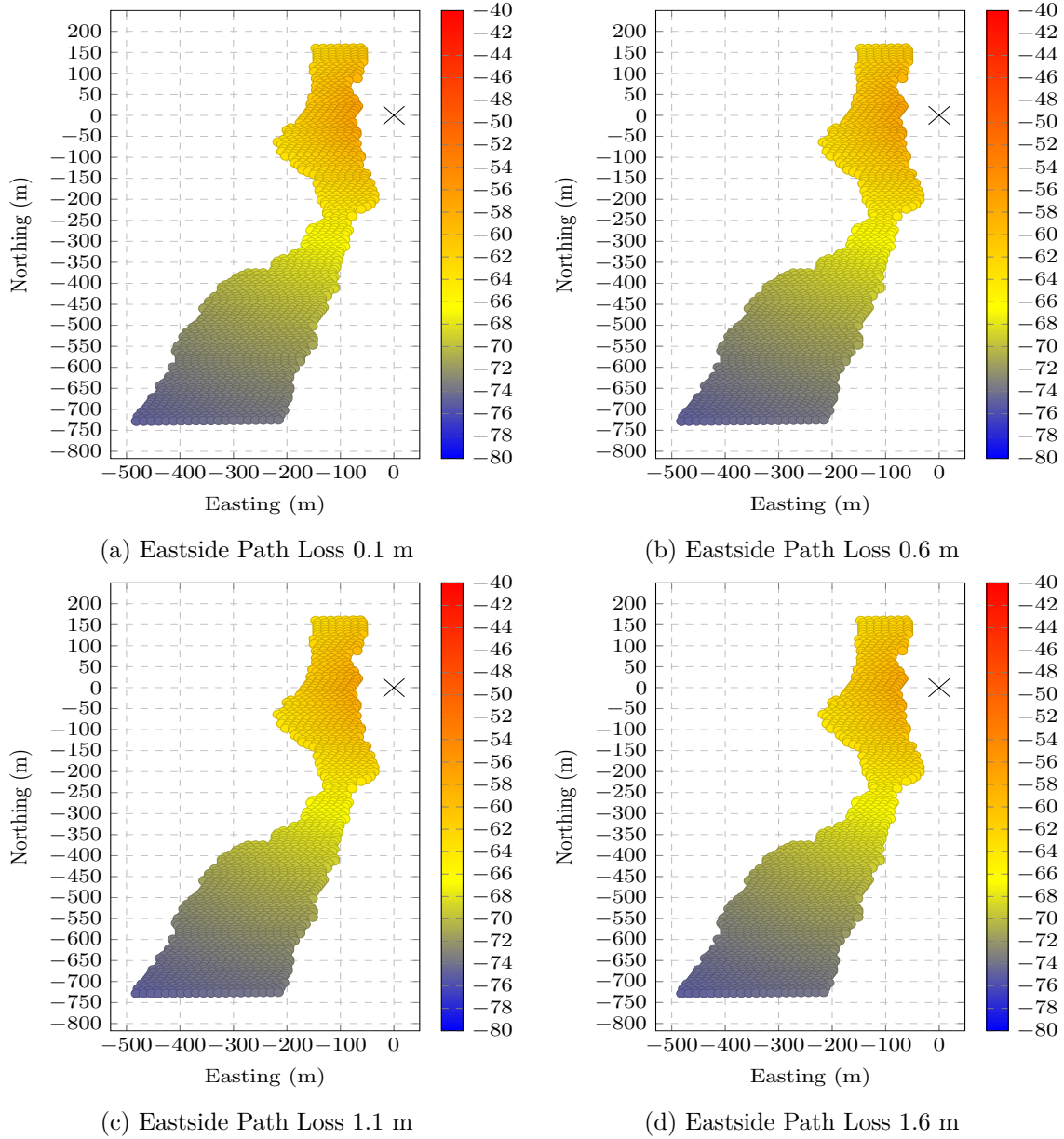


Figure 2.5: Spherical spreading loss at Eastside downstream site (dB).

For each coordinate point on the surface of the river, the model calculated the angle in both elevation and azimuthal planes between the boom of the antenna and the location of the water's surface. The symmetry of the radiation pattern around the boom allowed the maximum of these two angles to be used to provide the final gain value, this value was  $G_R$ . The gain in-situ for two sites is presented in Figure 2.8 showcasing the spherical nature of the main lobe.

There are two different transmit antennas used by the DFO, the Sigma Eight TX-PSC-I-1200 and a Lotek MCFT3-3A tag. These tags consist of a small electronics capsule

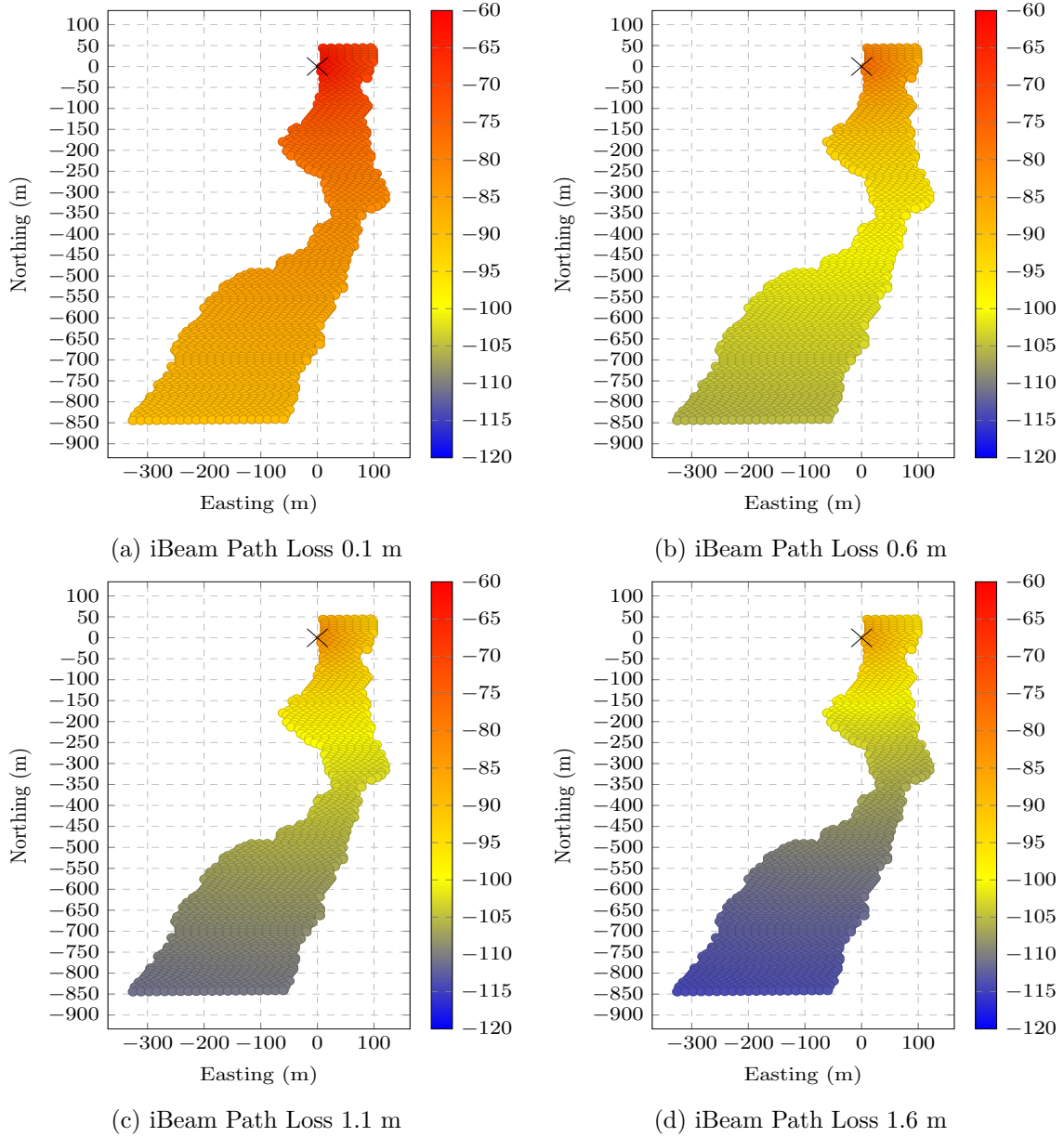


Figure 2.6: Spherical spreading loss at iBeam P1 site (dB). The iBeam P1 site is located at 10U 559261.998 km E, 15674586.021 km N.

attached to a dipole that is anywhere from 27.6 - 31.5 cm. In use, the capsule gets inserted into the fish's mouth and the dipole is left trailing out of the mouth and along the length of the fish. No data was provided for the operation of these devices therefore a simulation was carried out. The simulation included a 30 cm dipole, electrically short in free space, that was aligned with the electronics capsule, see Figure 2.9. The resultant directivity pattern was that of an electrically *long* dipole with multiple lobes, see Figure 2.9. Due to the complexity of the physical implementation of this antenna, the dipole being able to bend and rotate



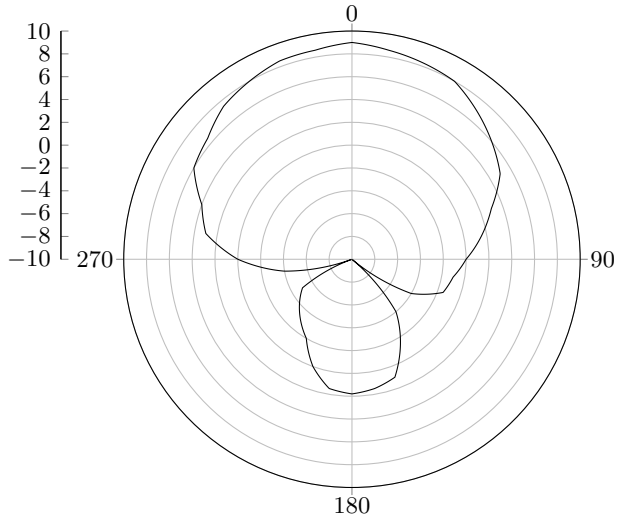


Figure 2.7: Interpolated Yagi-Uda Gain.

around the fish, the fish changing orientation, and the currents impacting both the fish and the antenna, an MEG was taken instead of a directive gain. Assuming the incoming wave distribution is omni-directional and equally-polarized, the MEG is evaluated to be half of the efficiency, (2.43). Under the model of a perfect electric conductor, the efficiency of the antenna is 0 dB i.e. 100%. If we include an approximation that the transmitting antenna is impedance matched but has a radiation efficiency of  $\eta = -1$  dB and we then factor half of the power (2.43), resulting in -3 dB, the overall mean effective realized gain is -4 dB, this value was taken for  $G_T$  in the simplified Friis equation below.

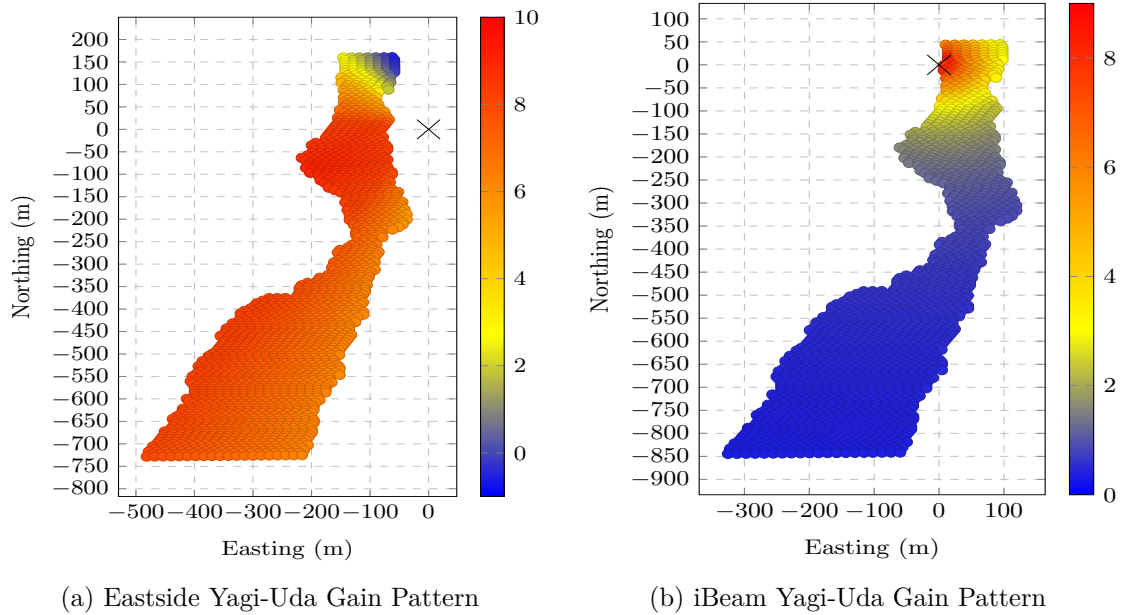


Figure 2.8: Yagi-Uda Gain Pattern in situ (dB). a) Eastside downstream receiver location. b) iBeam p1 receiver location.

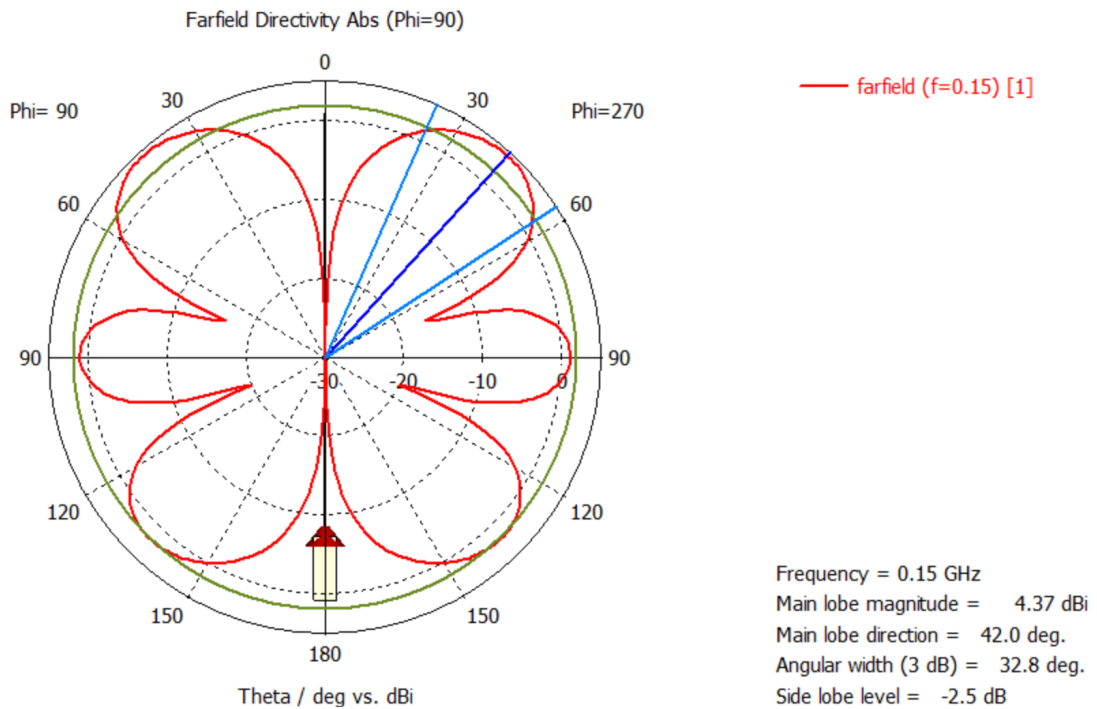


Figure 2.9: Simulation of directivity of a transmitter similar to the Sigma Eight TX-PSC-I-1200 and Lotek MCFT3-3A transmitter. Plot generated by, and used with permission from Dr. Christopher Hynes.

## Polarisation Mismatch of Air-Water Interface

An option for future work is to implement a more complex and potentially accurate polarisation matching system. A correct polarisation mismatch could not be implemented in this thesis due to the lack of data on the position and orientation of the fish transmitter. Instead of using the exact polarisation mismatch, a statistical approximation was taken where the plane wave was decomposed equally with half of the signal being TE polarisation and the other half TM polarisation. The two antennas were also assumed to have a polarisation mismatch of  $\eta_{pol} = -3$  dB in the model. The total path loss equation then becomes:

$$\frac{P_r}{P_t} = G_t G_r \left( \frac{1}{4\pi \left( \frac{d_1}{\lambda_1} + \frac{d_2}{\lambda_2} \right)} \right)^2 e^{-2\alpha'_z z} \quad (2.47)$$

$$\times \frac{1}{2} \left( |\tau_{TE}|^2 \operatorname{Re} \left\{ \frac{\eta_{TE}}{\eta'_{TE}} \right\} + |\tau_{TM}|^2 \operatorname{Re} \left\{ \frac{\eta_{TM}}{\eta'_{TM}} \right\} \right) \eta_{pol}. \quad (2.48)$$

Note that it has been assumed here that there is a single polarisation mismatch efficiency term,  $\eta_{pol}$ , and the total power is equal in each polarisation.

## 2.4 Results

As previously mentioned, the polarisation that was selected was half of the TE and half of the TM polarisation. Although this is the final result, the TE and the TM polarisation are presented individually in Appendix A.2 to highlight the differences and the impact that these differing polarisations have on the overall system. Individually the TE and the TM polarisations share similarities with the combined polarisation plots in terms of the spatial gain resolution trends. If a receiver location demonstrates high spatial resolution with the combined polarisation plots, the TE and TM polarisations will individually show similar resolution. The key difference however between combined polarisation and single polarisation occurs for locations in the river that are far from the receiver, in these limits the TE polarisation plots show the signal strength decreasing faster compared to the TM. The combined polarisation plot does not show this difference.

### 2.4.1 TE and TM

Setting the scene for the figures below,

- The Eastside downstream receiver is pointed at a bearing of  $245^\circ$  angled at  $20^\circ$  below horizontal. Its closest point to the water is 112 m away.
- The iBeam p1 receiver is angled at  $45^\circ$  below horizontal. Its closest point to the water is 36 m away.

- The Razorback upstream receiver is pointed at a bearing of  $113^\circ$  angled at  $18.8^\circ$  below horizontal. Its closest point to the water is 76 m away.

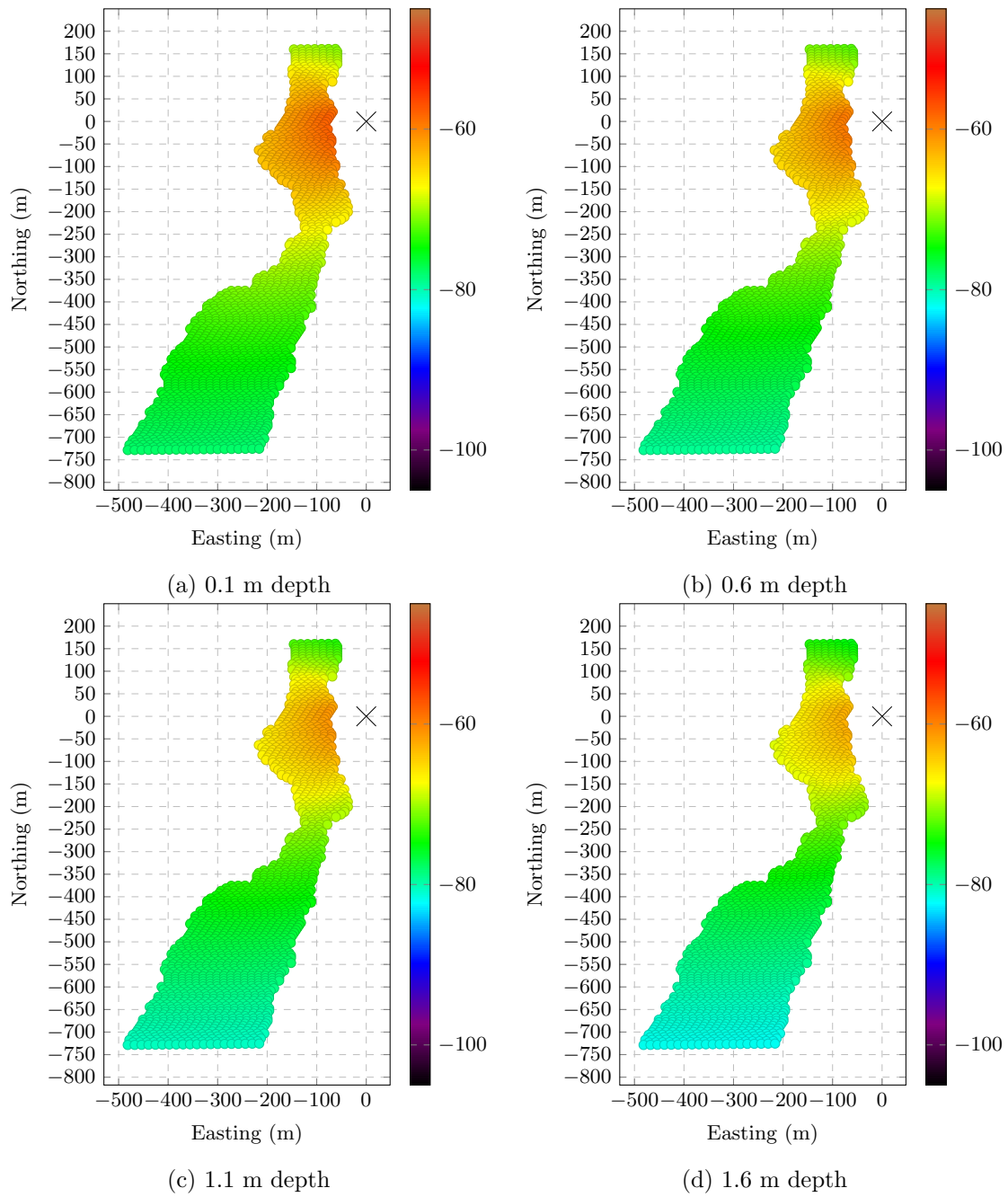


Figure 2.10: Total system loss  $0.5(\text{TE}+\text{TM})$  - Eastside downstream site (dB).

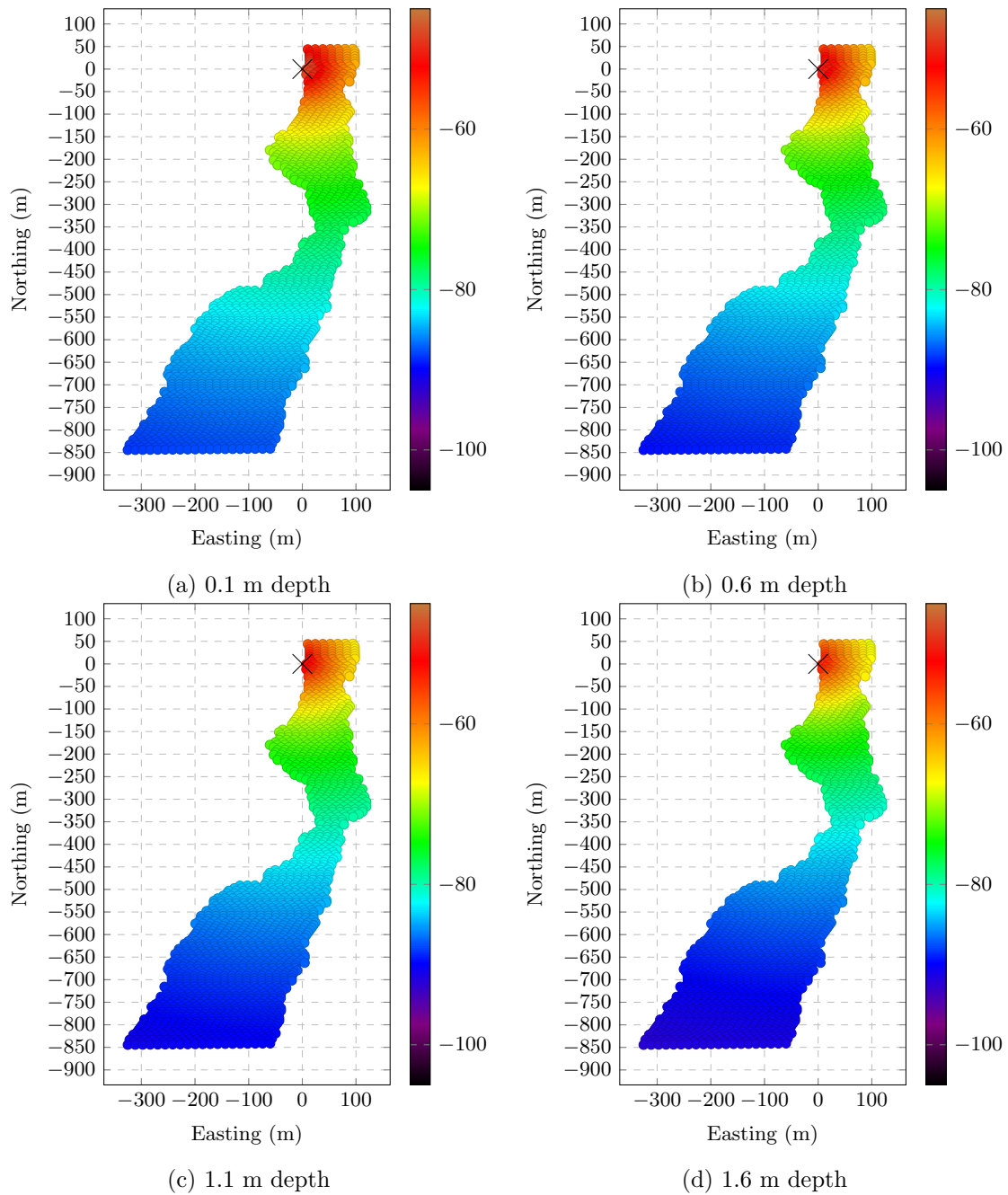


Figure 2.11: Total system loss  $0.5(\text{TE}+\text{TM})$  - iBeam p1 site (dB).

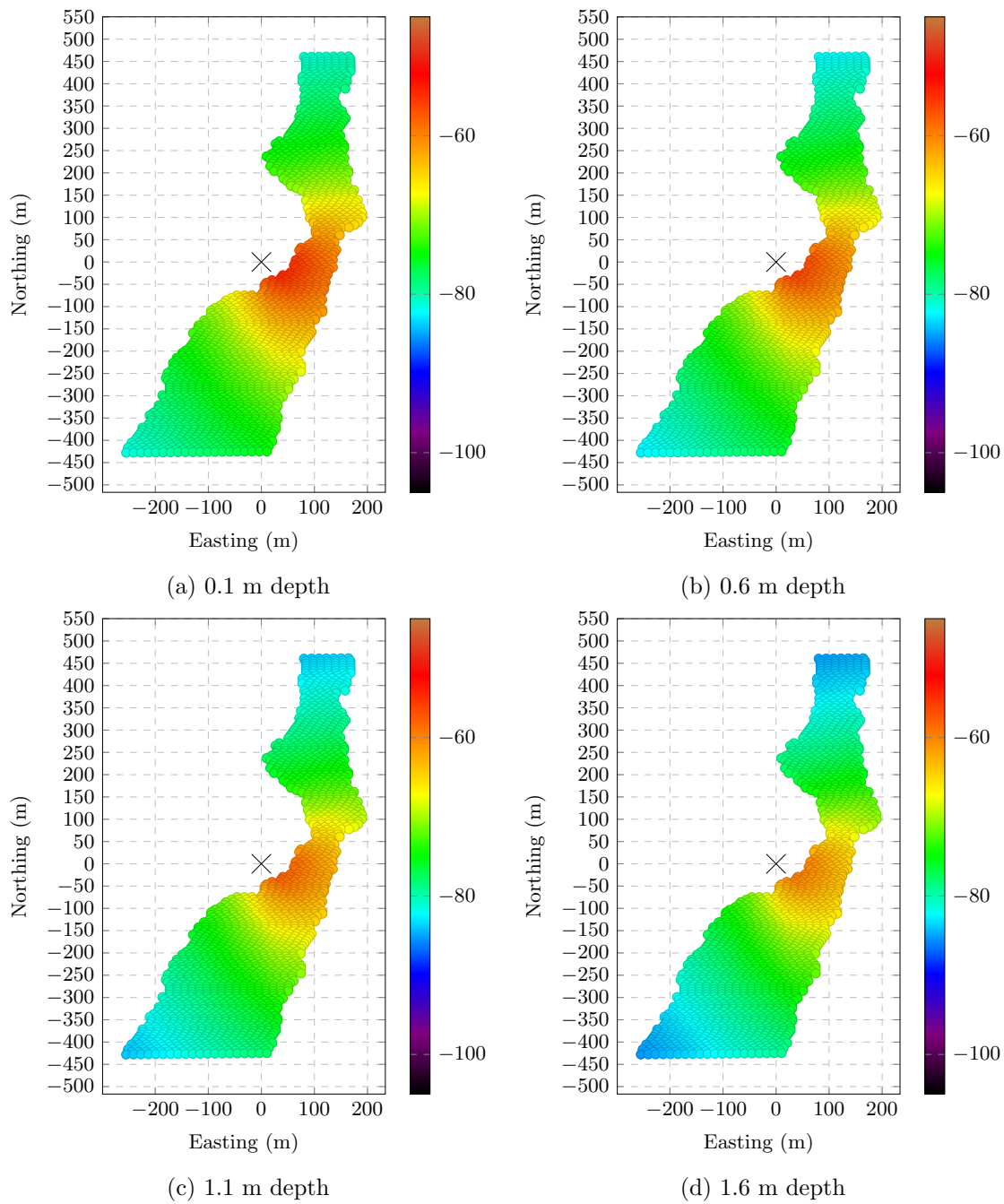


Figure 2.12: Total system loss  $0.5(\text{TE}+\text{TM})$  - Razorback upstream site (dB). Razorback upstream is located at 10U 559191.649 km E, 15674169.357 km N.

## 2.5 Discussion

The results show that some of the antenna locations don't provide high spatial resolution compared to other locations. At a latitude of 51.21852, the largest spatial resolution across the 92 m span of the river is 8.5 dB difference for the "Eddy" upstream receiver while the Razorback upstream receiver has the worst resolution with a difference of 0.77 dB across the river span. In order for the detection location to be useful, the total received power would be high, and there would be large fluctuations of received values across the river, at various depths within the river, and along the length of the river.

Of the three receiver locations presented, the iBeam receiver provides the greatest discrepancy along the width, length, and depth of the river. This receiver was unique in that it was pointing almost directly down into the water. The antennas that are further from the water and pointing closer to the horizon, Eastside and Razorback, show no differences across the width of the river however they do provide sensitivity for where a fish might be along the length of the river. The Eastside and Razorback positions also receive greater signal strength from the entire river whereas the iBeam receiver has a simulated received power of less than -90 dB for the spots on the river furthest from its position.

Irrespective of antenna location and the angle that the antenna is facing, the TM gain shows lower loss overall compared to TE. The overall power is an important consideration as it is better to have a stronger signal than a weaker signal that could be close to the noise floor. The difference between polarisation gains agrees with the Fresnel equation theory, see Figures A.1, A.2 and 2.4, where we see that the larger the incident angle is from normal, the less power we have transmitted in the TE polarisation however we have more power transmitted in the TM polarisation.

These results are three from thirteen of the receiver locations, see Appendix A.2 for all sites. Individually each placement has a strength, whether it is greater received power overall or greater discrepancy in power along the river, however tracking a fish will be challenging using only one of the receiver locations. The biggest opportunity in tracking will be to use some combination of these locations together to minimize the regions that the fish can be located in, see Figure 2.13. Averaging over all of the locations provides a bleak outlook. Based on the current receiver locations the gain pattern does not give a high resolution in terms of the spatial gain variation. It is also clear that there are a lot of antenna locations all within a nearby proximity. The average gain leads to a pattern that is similar to the iBeam p1 site, see Figure 2.11. The current averaging of all locations creates a distribution that is similar to if there was only one receiver located near the large cluster of receivers. Although it would be beneficial to space the antennas out and place them in a configuration close to the rivers surface the topography of the river canyon does not make this an easy task.



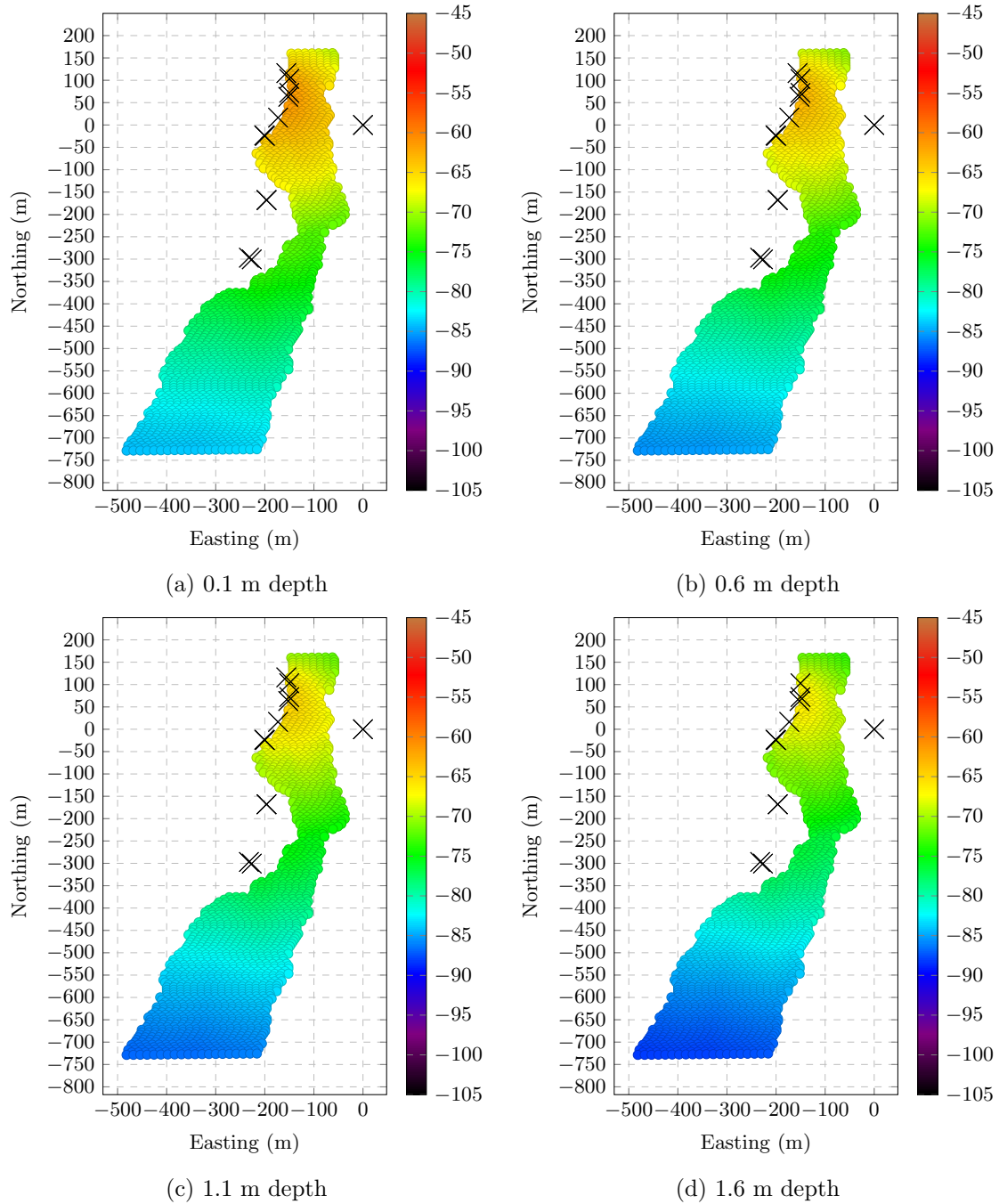


Figure 2.13: Total loss  $0.5(\text{TE}+\text{TM})$  - Averaged dB gain over all sites (dB). All distances referenced to Eastside downstream, 10U 559418.2593 km E, 15674469.93 km N.

### 2.5.1 System Improvement

There are a variety of possible improvements that can be made to improve the radio tracking. Although there are diverse theoretical ways to improve the system, there are many limitations. The limitations primarily revolve around the physical environment in which

the tracking is taking place. The rugged terrain limits the possible locations where antennas can be placed and the rushing river with debris eliminates the possibility of placing any equipment inside the river, whether it be acoustic or radiofrequency. There are some elements that are within our control and could be implemented with relative ease.

- Use antennas orthogonal to one another; the ability to use both polarisations would be beneficial in order to get more data.
- Position the antennas as close as possible to the river's surface. Minimizing the distance between the receiver and the water will eliminate most of the path loss leading to an overall higher received strength.
- Orient the antennas with the boom towards the river. The more the antenna points towards the river the greater differentiation along the surface of the river. This approach has lower received strength further from the receiver location but that can be overcome by spacing out the remaining antennas.
- Obtain more directional antennas. The beam width of the current antennas is approximately  $110^\circ$  and as such when these antennas are positioned a large distance from the rivers surface, the gain of the antennas is seen as very uniform over large areas of interest.
- Try and leverage the advantages of TM polarisation to obtain a larger received signal compared to using the TE polarisation.

## Chapter 3

# Acoustic Modelling Multi-layer Structures

The acoustic modelling uses multi-layer transmission lines to model the transmission and reflection mimicking windowpanes and spacings between panes. The following figure represents a window model schematically:

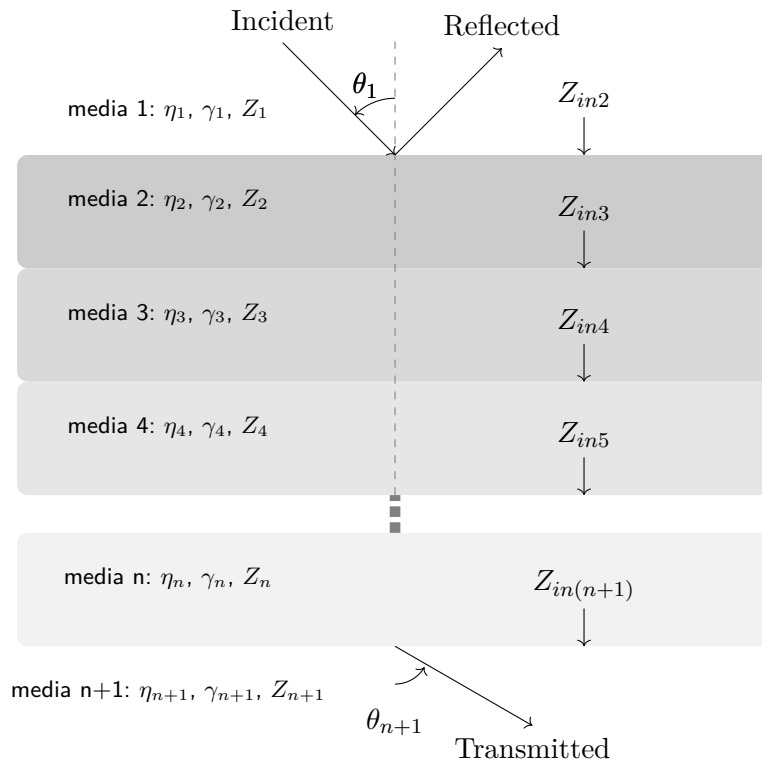


Figure 3.1: Multi-layer transmission and reflection

## 3.1 Assumptions

Like the EM model there are a few assumptions:

- The attenuation follows the same exponential decay used in EM propagation (2.20). When a wave enters a medium, the signal decays exponentially, this allows the acoustic propagation to be modelled with a transmission line.
- The model uses random incidence, modelled here by having no oblique incidence. This is a commonly used technique in acoustics for propagation between rooms [24].
- Gasses such as air and argon, commonly used gasses between panes, are lossless materials and there is no dissipation as the sound wave propagates.
- There is no spherical spreading of the acoustic wave. The spreading would have to be considered for a more realistic dataset however this model considers only a plane wave with no spreading.

## 3.2 Underlying Principles

### 3.2.1 Acoustic Electromagnetic Equivalent

In liquids the lossless acoustic propagation model and the lossless EM propagation scenarios share similarities due to their respective wave equation [31, 32]. The fundamental element comparisons are:

Acoustic Terminology	Electromagnetic Equivalent
Pressure: $p$	E
Velocity: $v$	H
Density: $\rho$	Permeability: $\mu$
Compressibility: $K = \frac{1}{B}$	Permittivity: $\epsilon$

Table 3.1: EM acoustic analogy. Some texts prefer an interchange of E and H here depending on if it is using TE or TM polarisation [31].

In liquids, the acoustic model contains a relationship to the conductivity in EM propagation:

$$\sigma = \frac{1}{\text{Viscosity}} = \frac{1}{\eta}$$

[31, 32]. The only qualifier is that this only holds for visco-elastic fluids [31, 32]. An important relationship that relates material parameters is that the compressibility  $K = \frac{1}{B}$  is equal to the inverse of B, the Bulk modulus. Bulk modulus is the stiffness of the material. Putting these fundamental variables together means that many of the useful parameters such as the wave impedance and wave number can be re-written in terms of the acoustic parameters.

Acoustic Terminology	Electromagnetic Equivalent
$Z = \sqrt{\rho B} = \sqrt{\frac{\rho}{K}} = \frac{\rho \omega}{k} \text{ (3.1)}$	$\eta = \sqrt{\frac{\mu}{\epsilon}} = \frac{\mu \omega}{k}$
$k = \omega \sqrt{\frac{\rho}{B}} = \omega \sqrt{K \rho} = \frac{\omega}{c} \text{ (3.2)}$	$k = \omega \sqrt{\mu \epsilon} = \frac{\omega}{c}$
$c = \sqrt{\frac{B}{\rho}} = \frac{1}{\sqrt{K \rho}}$	$c = \frac{1}{\sqrt{\mu \epsilon}}$

Table 3.2: EM acoustic analogy for composite variables.

### 3.2.2 Power, Intensity and Hearing

Unlike EM where the power flux density (2.1) is the key metric, acoustics has multiple measurements of importance since human hearing does not explicitly recognize the power or intensity of an acoustic wave. The important quantities in acoustics are:

- Sound Pressure Level (SPL):

$$SPL = 10 \log_{10} \left( \frac{p^2}{p_{ref}^2} \right) \quad (3.3)$$

where  $p_{ref}$  is the dynamic pressure of the smallest sound that a human can hear. Its value is 20  $\mu\text{Pa}$  or  $20 \cdot 10^{-6} \text{ N/m}^2$  [16, 33]. The human ear can hear a range of 1 dB SPL, the quietest sound, to over 120 dB SPL, the point at which noise can cause immediate damage to the ear [34]. The SPL is the metric commonly attributed to any measurement of how "noisy" an object is.

- Intensity level (IL):

$$IL = 10 \log_{10} \left( \frac{I}{I_{ref}} \right) \quad (3.4)$$

with the reference intensity,  $I_{ref} = 10^{-12} \text{ W/m}^2$ , corresponds to the intensity of the reference dynamic pressure. Intensity in a plane wave is defined using [33] as:

$$I = \frac{p^2}{\rho_0 c}$$

with  $p$  the pressure. The relationship between intensity level and sound pressure level is:

$$IL = SPL + 10 \log_{10} \left( \frac{p_{ref}^2}{\rho_0 c I_{ref}} \right) \quad (3.5)$$

### 3.2.3 Single-pane and Double-pane

Although the lossless model offers a direct relationship between EM and acoustic parameters, the different mechanical implementations, whether it is single-pane or double-pane transmission, require separate considerations. Acoustic propagation is complicated due to different propagation phenomena based on the surrounding mechanical setup of the problem, how the windowpanes are attached to one another, how they are held within the frame impact the results [24].

#### Single-pane - Mass Law

The transmission loss and absorption coefficient of single layers, or single-pane construction, follows the theoretical mass law [24, 33]. The absorption coefficient is defined as [24]:

$$\alpha = 1 - |R|^2 = \frac{1}{1 + \left(\frac{\omega m_s}{2Z_0}\right)^2} \quad (3.6)$$

with  $Z_0$  the specific impedance of air, units of rayl: kg/m<sup>2</sup>s, and  $m_s$  is the surface mass density. The transmission loss, or sound reduction is defined as [24]:

$$R_{Tloss} = -10 \log_{10} \tau = 10 \log_{10} \frac{I_0}{I_t} = 10 \log_{10} \left[ 1 + \left( \frac{\omega m_s \cos \theta}{2\rho_0 c} \right)^2 \right] \quad (3.7)$$

with  $I_0$  the incident sound intensity and  $I_t$  the transmitted intensity. This results in a theoretical transmission loss that follows the trend of Figure 3.2.

#### Double-pane - Mass Law

For constructions with more than one layer, there are added acoustic complications. The primary reason is the gap between the panes, whether it be air, argon, or some other gas, acts like a spring. For various frequency regions, the mass elements and the spring behave differently complicating the issue. This frequency dependence has a large impact on the overall performance of the system [24]. The theoretical transmission loss of a double layer

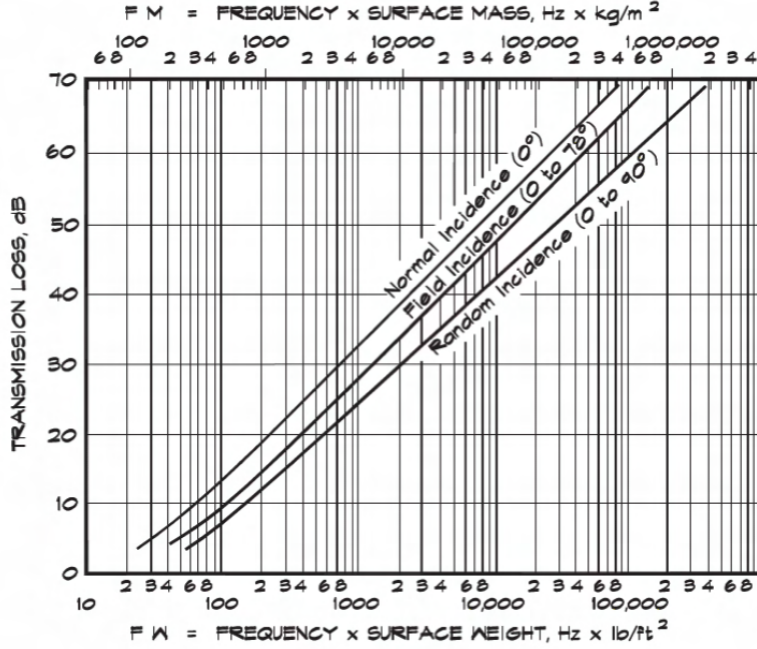


Figure 3.2: The theoretical transmission loss based on the mass law theory of a single-panel. Image copied from [35].

configuration is:

$$\begin{aligned}
 R_{Tloss} &= -10 \log_{10} \tau = 10 \log_{10} \frac{I_0}{I_t} \\
 &= 10 \log_{10} \left( 1 + \left[ \frac{\omega M}{3.6 \rho_0 c_0} - \frac{\omega^2 m_1 m_2}{(3.6 \rho_0 c_0)^2} (1 - e^{-2jkd}) \right]^2 \right) \quad (3.8)
 \end{aligned}$$

$$M = m_1 + m_2 \quad (3.9)$$

$$k = \frac{2\pi f}{c_0} \quad (3.10)$$

$$d = \text{Panel spacing} \quad (3.11)$$

$$m_1, m_2 = \text{Surface mass density of the layers.} \quad (3.12)$$

This results in a theoretical transmission loss that follows the trend of Figure 3.3.

### 3.2.4 Transmission Loss and Absorption Coefficient

In EM the two important parameters that dictate the propagation of the wave are the wave impedance,  $\eta$  (2.10) and the propagation constant,  $\gamma$  (2.24). Since the permittivity can be a complex function, for lossy materials the wave impedance and propagation constant become complex functions resulting in a model that covers both lossless and lossy propagation. The theoretical derivation of complex acoustic impedance and propagation constant are not well

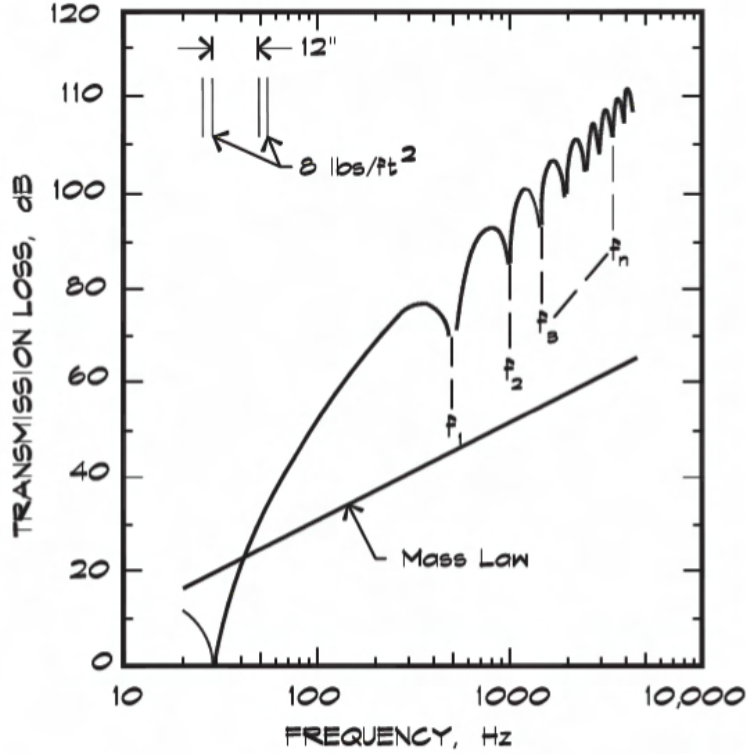


Figure 3.3: The theoretical transmission loss for a double-panel compared to the mass law theory of a single-panel. Image copied from [35].

defined, therefore experimental results can be used to calculate these values. Propagation between rooms is a commonly researched topic that provides information to researchers, architects, and companies alike on the acoustic qualities of their products [24, 36, 35, 37, 23, 33]. The most common measurements often provide two pieces of data: the absorption coefficient and the sound reduction index, otherwise known as the transmission loss.

- Random incidence absorption coefficient is defined as :

$$\alpha = 1 - |R|^2. \quad (3.13)$$

This is the portion of the incident wave power that enters the layer. From an EM point of view, this is the Fresnel transmissivity power, the power that is immediately available at the surface of the interface.

- The sound reduction or transmission loss is defined as:

$$R_{Tloss} = -10 \log_{10} \tau = 10 \log \frac{I_0}{I_T}. \quad (3.14)$$



This corresponds to the power lost travelling through a layer. In the case of a single-pane of glass, the sound reduction is the ratio of intensity incident on the glass to the intensity directly after the pane of glass.

The absorption coefficient and transmission loss measurements are done using international standards: ISO 354 for the absorption coefficient and ISO 16283, ISO 140 for the sound reduction index. Both the absorption coefficient and the sound reduction index values are for random incidence therefore allowing our model to use normal incidence. Knowing the intensity at the incident interface and at the interface leaving the structure, the absorbed intensity can be calculated, and the entire layer can be characterized with a transmission line.

### 3.2.5 Transmission Lines

The acoustic transmission line model requires adapting the transmission line model presented in the fish tracking model see Section 2.2.3, to encompass multiple layers, more than two. One of the key tools in analyzing multi-layer transmission line models is the ABCD matrix from two-port modelling. It is possible to solve wave equations using boundary conditions and arrive at the correct solution however this approach is cumbersome when dealing with a three-pane window design, or equivalently, a seven-layer transmission line.

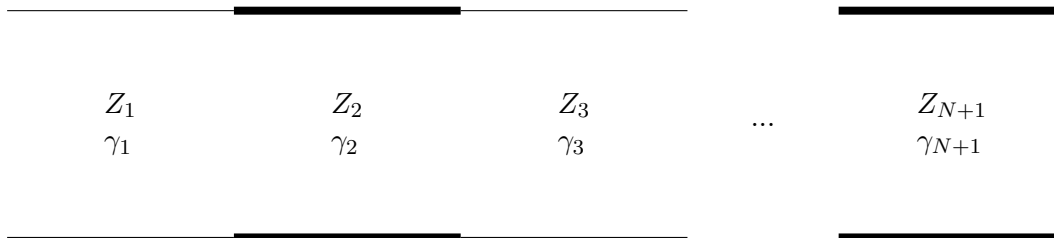


Figure 3.4: Multi-Layer transmission line.

The ABCD matrix relates the voltage and current at the input of the two-port network to the voltage and current at the output of the network. Cascading these systems allows for modelling of multiple layers of a transmission line by relating the input and output voltage and currents of the system. Each two-port network is its own transmission line with a characteristic impedance and wave propagation constant. The values of a transmission line

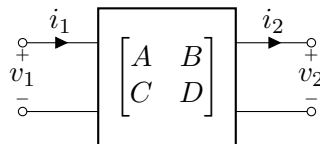


Figure 3.5: Two-port network model relating the input voltage and current to the output voltage and current.

ABCD matrix are covered thoroughly in many texts, eg. [8], and the result will be given:

$$\begin{bmatrix} V_1 \\ I_1 \end{bmatrix} = \begin{bmatrix} A & B \\ C & D \end{bmatrix} \begin{bmatrix} V_2 \\ I_2 \end{bmatrix} \quad (3.15)$$

For transmission lines the ABCD matrix is given by:

$$\begin{bmatrix} A & B \\ C & D \end{bmatrix} = \begin{bmatrix} \cosh(\gamma l) & Z \sinh(\gamma l) \\ Y \sinh(\gamma l) & \cosh(\gamma l) \end{bmatrix} \quad (3.16)$$

Plugging this into an inverted ABCD matrix we can calculate the voltage and current at the outlet, or port two, compared to the inlet, or port 1. This is given by:

$$\begin{aligned} \begin{bmatrix} V_2 \\ I_2 \end{bmatrix} &= \frac{1}{\cosh^2(\gamma l) + \sinh^2(\gamma l)} \begin{bmatrix} \cosh(\gamma l) & -Z \sinh(\gamma l) \\ -Y \sinh(\gamma l) & \cosh(\gamma l) \end{bmatrix} \begin{bmatrix} V_1 \\ I_1 \end{bmatrix} \\ &= \begin{bmatrix} \cosh(\gamma l) & -Z \sinh(\gamma l) \\ -Y \sinh(\gamma l) & \cosh(\gamma l) \end{bmatrix} \begin{bmatrix} V_1 \\ I_1 \end{bmatrix} \end{aligned} \quad (3.17)$$

Cascaded matrices can easily be implemented into a recursive relation making it easier for the computer to solve. To initialize the values, we collapse the multi-layer transmission line down to a single interface to calculate the overall reflection coefficient. This determines the voltage and current at the first interface relative to the incoming signal. This can be accomplished by transforming the impedance of the transmission lines or by analyzing the small signal reflections and transmissions to determine an equation for the overall reflection of the system. For a multi-layered system with more than three layers, it is easier to calculate the reflection by transforming the impedances:

$$Z_{in} = Z_0 \frac{Z_L + Z_0 \tanh(\gamma l)}{Z_0 + Z_L \tanh(\gamma l)}. \quad (3.18)$$

This can be re-written recursively:

$$Z_{in(i)} = Z_i \frac{Z_{in(i+1)} + Z_n \tanh(\gamma_i l_i)}{Z_i + Z_{in(i+1)} \tanh(\gamma_i l_i)} \quad i = n, n-1, n-2, \dots, 2. \quad (3.19)$$

Using the notation from Figure 3.4 we first initialize  $Z_{in(i+1)}$  to be  $Z_{n+1}$ . Then the equation can be solved recursively to find the input impedance at layer 1. With the input impedance, the reflection coefficient can be calculated:

$$\Gamma = \frac{Z_{in2} - Z_1}{Z_{in2} + Z_1}. \quad (3.20)$$

This method immediately takes into account all of the various reflections between layers. The voltage and current can now be initialized at the first interface as:

$$V_1 = V_{1+}(1 + \Gamma) \quad (3.21)$$

$$I_1 = \frac{V_{1+}}{Z_1}(1 - \Gamma) \quad (3.22)$$

where  $V_{1+}$  is the input voltage. Both  $V_1$  and  $I_1$  can then be input into (3.17) and recursively calculated to find the output voltage and current.

### 3.3 Model Implementation and Verification

Although there are theoretical models, see Figures 3.3 and 3.2, the complications arise from modelling real lossy media as a transmission line. One of the challenges of acoustic modelling for real materials is represented by the thirteen different equations needed to estimate the speed of sound in different materials depending on the type of vibrational wave [35]. Instead of calculating the acoustic parameters for materials, the following values were used for the speed of sound and the densities of the materials:

Variable	Air	Glass	Argon
c [m/s]	343	4540	319
$\rho$ [kg/m <sup>3</sup> ]	1.293	2500	1.603

Table 3.3: Material acoustic properties used throughout

To fit the reality of the acoustic transmission to a transmission line model, we had to make a simplification in terms of the analysis and use experimental data to obtain the impedance and propagation constants. Viewing this problem in terms of a transmission line problem, we can model the single-pane window problem as a three-layer transmission line with air, glass, and lastly, another air layer. Using the transmission line techniques covered in Section 3.2.5 it is possible to solve the transmission line equation using the absorption coefficient and the transmission loss values to obtain unknown parameters in the transmission line model. The transmission loss is defined as (3.14) however for the sake of this thesis all results presented will be taken as the negative of this value to follow the same convention as the EM scenario. Using the absorption coefficient and the transmission loss value in the transmission line model, the lossy impedance and wave propagation constant of glass were taken to be an unknown. The gasses before and after a pane of glass were considered to be lossless and were taken as a given value using the impedance of a lossless fluid, (3.1), and the wave number, (3.2).

For the system to converge to a solution for the impedance and wave propagation constant of glass, a few assumptions were made on the variables based on theory from the EM scenario. The wave impedance should be a complex value that is positive. Therefore,

the real impedance portion was set to (3.1). The imaginary portion was constrained to be positive but was left to be fitted. The wave propagation factor was fitted similarly with the imaginary portion of the term being to be equal to (3.2). The real part of the propagation constant was constrained to be positive to ensure that the material attenuated correctly. Once the terms were fit for the six test frequencies given in [24, 33, 35, 23, 38, 39, 40], a linear, polynomial and spline fit in MATLAB were applied to obtain the total impedance and propagation constant over the whole range of frequencies: 125 Hz to 4 kHz. Implementing these values into the propagation model allowed for certain elements such as: the number of layers, the spacing of the layers, the thickness of the glass and the chemical compositions of the media in between the panes of windows to be changed.

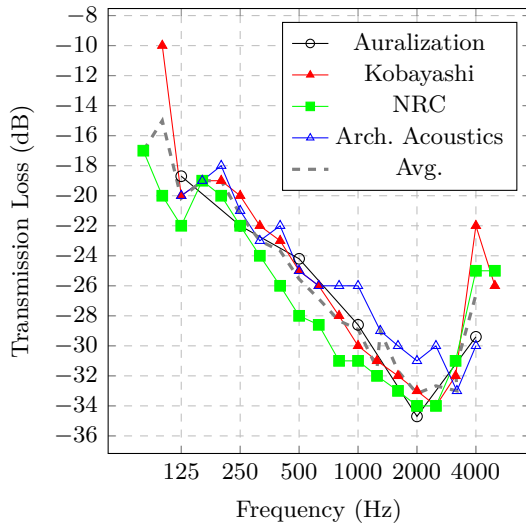
Three different configurations were simulated, single-pane, double-pane and triple-pane with both air and argon as the medium between panes. The transmission line model values were also compared against experimental results found in Auralization [24] for a three mm single-pane window as well for a double-pane system with 4 mm thick glass and a 6 mm spacing.

### **3.3.1 Single-pane Three mm Experimental Result Comparison**

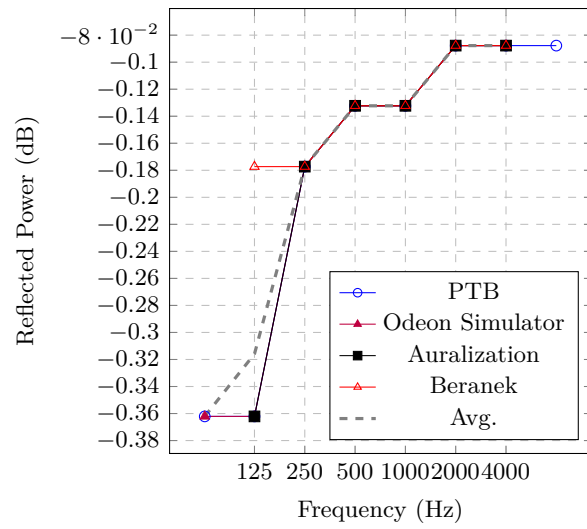
There are a variety of sources providing experimental data on three mm single-pane glass [24, 33, 35, 23, 38, 39, 40], these datasets include the sound transmission loss, and in some instances, the absorption coefficient. There are fewer sources providing the absorption coefficient of glass since it is commonly used as a barrier between two rooms and not to absorb noise within a room. The different experimental results are tabulated and averaged in Figure 3.8. There are some experimental differences specifically with the transmission loss values at high frequencies. Although these experiments do follow standards, there is a high variability owing to the challenging nature of acoustic experiments [23].

### **3.3.2 Linear, Polynomial, Spline - Single-pane Comparison**

Using data from the single-pane of glass, it is possible to compare the experimental values from the textbook to the final extrapolated impedance values that were obtained. To do this, three different interpolations were used, a linear, polynomial and spline interpolation. Since the values are interpolated, the results of the single-pane transmission window won't match exactly the averaged experimental measurements that were used. We can analyze the differences between the interpolation results and the experimental results in two ways, by comparing the results from the solved impedance and wave propagation constant and by comparing the final transmission model to the experimental data. The comparison of interpolated versus non interpolated data for the impedance and propagation constant is shown in Figure 3.8.



(a) Negative value of transmission loss



(b) Reflected power

Figure 3.6: Experimental transmission loss and reflected power. a) Transmission loss through the Three mm single-pane of glass from various studies and an average value of the studies. These values are the negative of the experimental value for consistency with the way loss is defined in the fish tracking b) Using the absorption coefficients to calculate the reflected power. Beranek data provides an averaged data set of two different experiments.

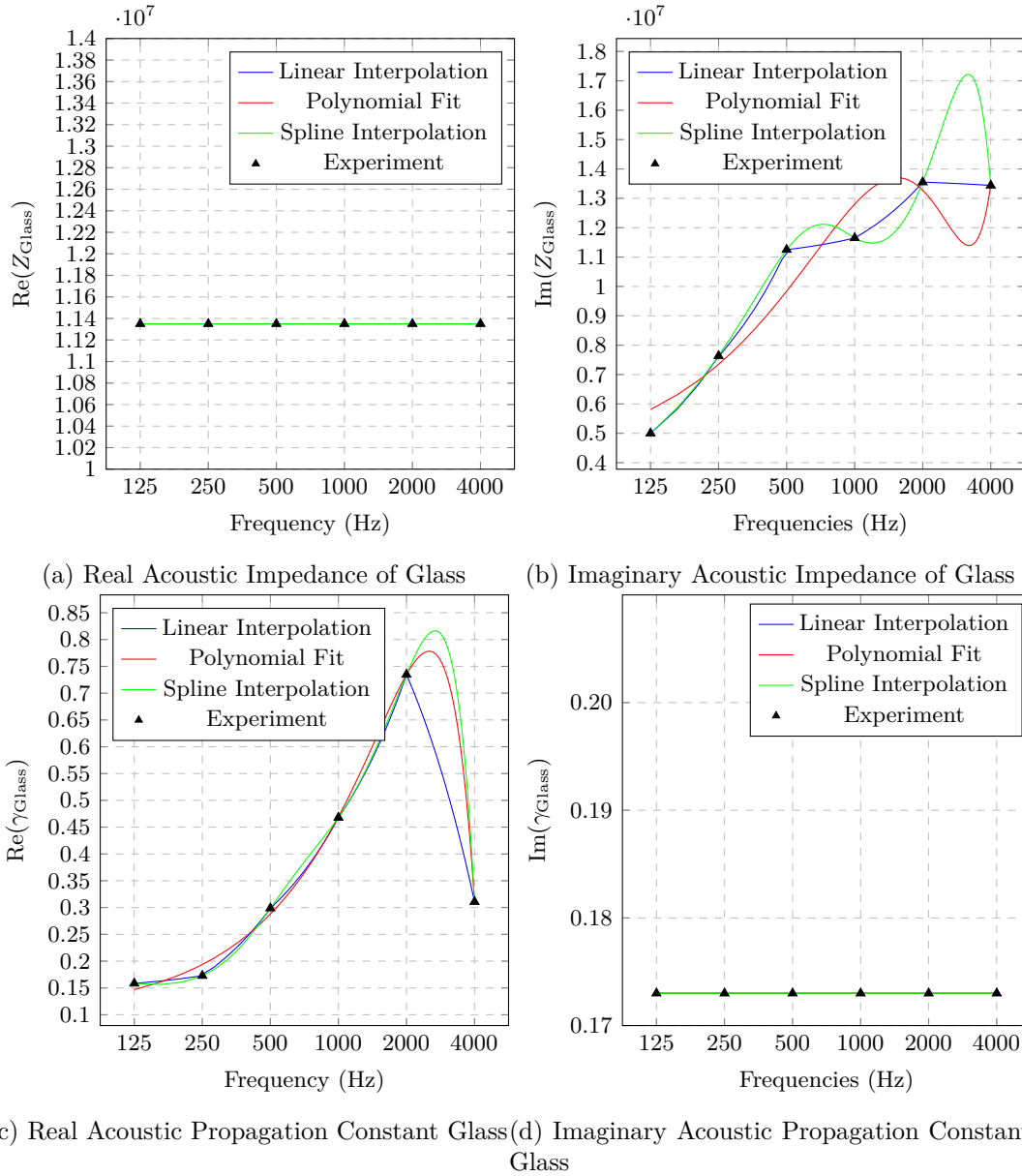


Figure 3.7: Real and imaginary components of fitted parameters compared to experimental values. a) Real portion of  $Z_{\text{glass}}$ , b) Imaginary portion of  $Z_{\text{glass}}$ , c) Real portion of  $\gamma_{\text{glass}}$ , d) Imaginary portion of  $\gamma_{\text{glass}}$

## 3.4 Results

### 3.4.1 Single-pane

Using the linear, polynomial and spline data, we can get the following single-pane theoretical versus experimental comparison: There are small discrepancies due to the fitting of the

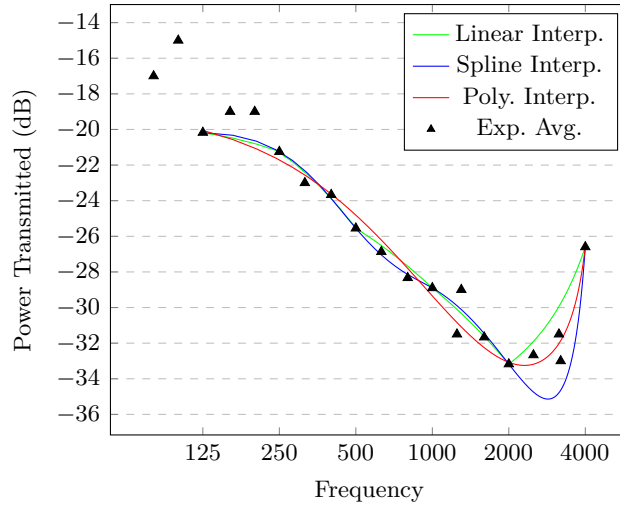
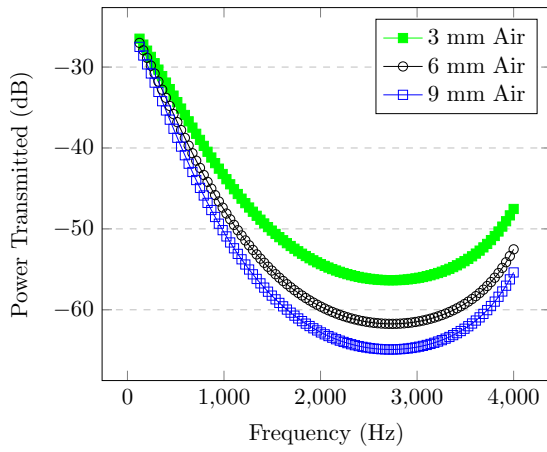


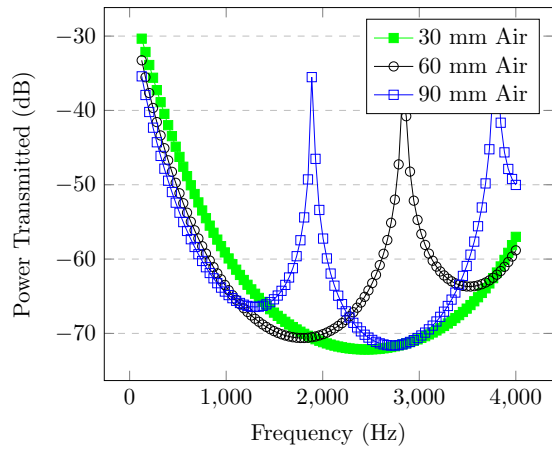
Figure 3.8: Experimental transmit power for a single-pane Three mm window compared with the interpolated transmission line solution. There is extra transmission loss data that was not considered in the interpolations since the corresponding absorption coefficients did not exist. The only data points that were fitted were 125, 250, 500, 1000, 2000, 4000 Hz.

parameters between the experimental results and interpolated results with the polynomial fit providing the closest interpolation to the experimental data.

### 3.4.2 Double-pane

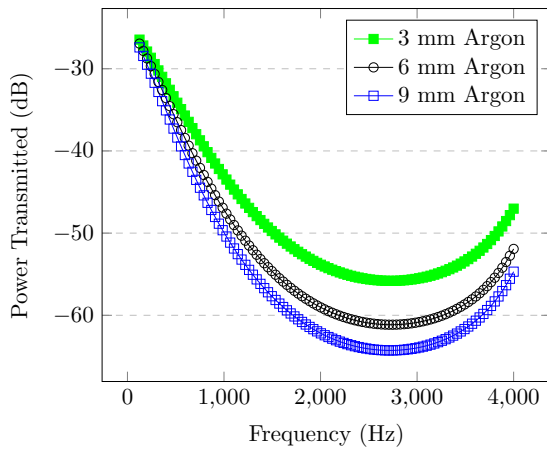


(a) Thin Spacing

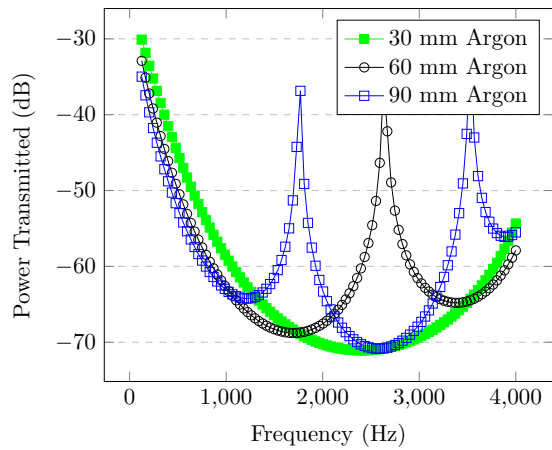


(b) Medium Spacing

Figure 3.9: Polynomial fit used on a double-pane window setup. Three mm glass with varying thickness air spacing between panes.



(a) Thin Spacing



(b) Medium Spacing

Figure 3.10: Polynomial fit used on a double-pane window setup. Three mm glass with varying thickness argon spacing between panes.



### 3.4.3 Triple Pane

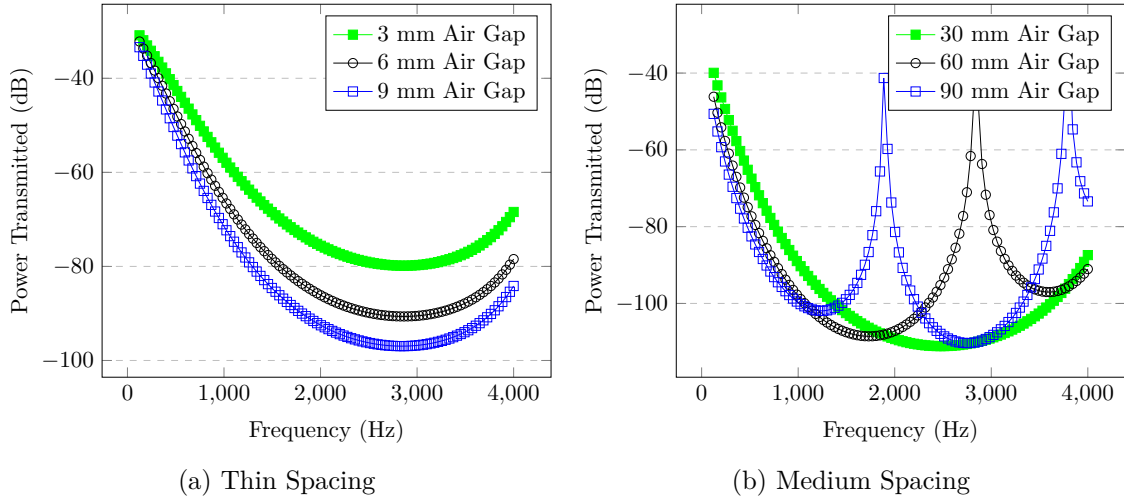


Figure 3.11: Polynomial fit used on a triple-pane window setup. Three mm glass with varying thickness air spacing between panes.

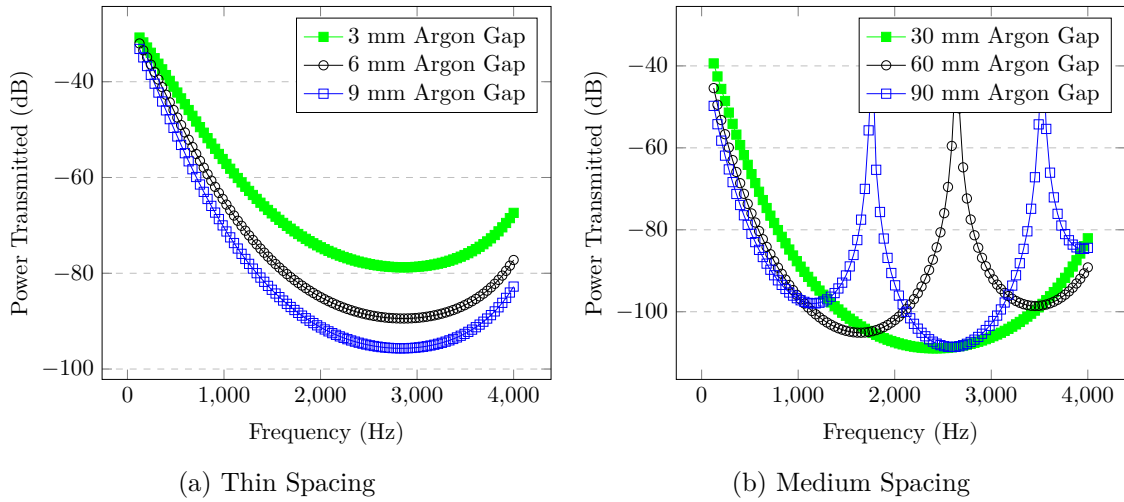


Figure 3.12: Polynomial fit used on a triple-pane window setup. Three mm glass with varying thickness argon spacing between panes.

### 3.4.4 Double-pane Verification - 4 mm Glass, 6 mm Spacing

Using the same interpolated impedance values obtained from the single-pane measurements, it is possible to change the thickness of the glass. As a comparison and as a form of verification for the transmission line, a double-pane configuration that was measured in [24] was reconstructed with the transmission line. This configuration uses a pane of glass that is 4 mm thick followed by a spacing of 6 mm. Below are the results and comparison between

the experimental and 4 mm thick double-pane window model. There are large discrepancies between the two models with differences greater than 20 dB. The experimental values result in much more power being transmitted compared to the transmission line model.

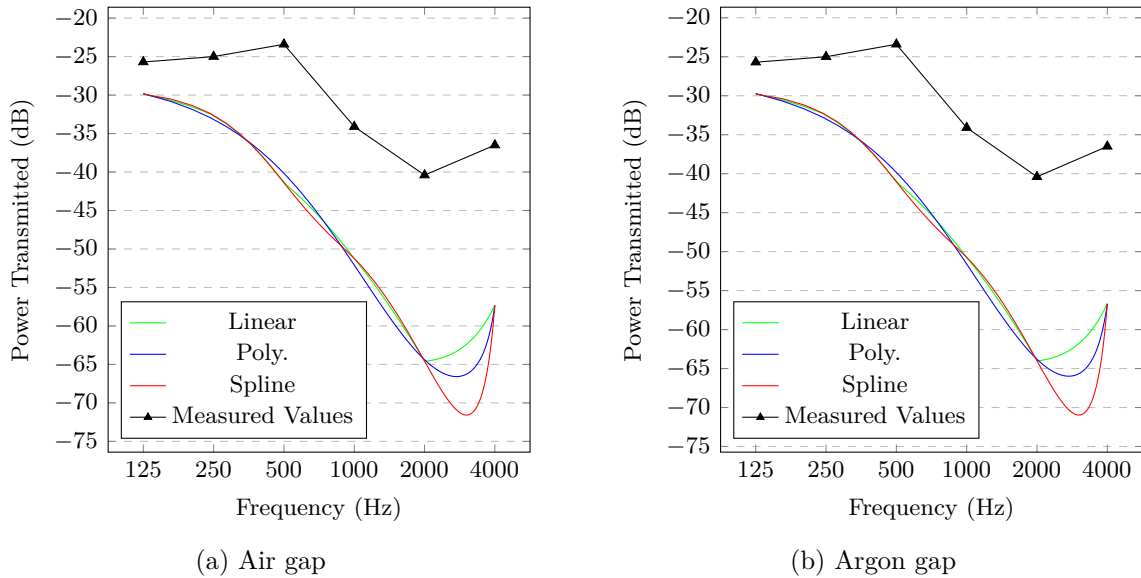


Figure 3.13: Measured transmitted power for a double-pane, 4 mm glass and 6 mm spacing, window compared with the transmission line solution that has been interpolated. This is using an argon gap.

### 3.5 Discussion

Although the transmission line model provides ease of understanding and implementation, there are clear shortcomings in reconciling its results with known experimental results. The results using the transmission line technique for a double-pane window led to less power transmitted through the window compared to the experimental data. This is possibly due to the resonance frequency of the double-pane window causing the window to perform worse than what would be theoretically expected or due to error in experimental measurement.

Even though the transmission line model does not provide great agreement there are a variety of other interesting results obtained through its use. Depending on the spacings between the panes of glass, there are resonances that occur wherein the window has worse acoustic blocking. These resonances are the large peaks in the graphs where the window transmits most of the incident power. At the lowest frequency that is tested, 125 Hz, sound in air has a wavelength of 2.7 m and at the largest frequency, 4000 Hz, sound has a wavelength of 8.58 cm. For the double-pane window with an air gap of 9 cm there are two resonant frequencies, 1886.36 Hz and 3804.26 Hz which correspond to a wavelength of 0.1818 m and 0.0902 m. Therefore, it makes sense that a 9 cm window spacing would result in a large

amount of the sound transmitted at these frequencies as the gap is equal to both  $\lambda$  and  $1/2\lambda$  of those frequencies. In this scenario, the transmission line is acting like a quarter wave transformer, or more specifically, an integer multiple of a quarter wave transformer. In the application of windows in a building scenario, we would want to minimize any of these resonances as they lead to a large portion of the sound transmitting through the system.

Argon, an excellent heat insulator, does not make a noticeable impact for small spacings between panes. When analyzing the acoustic parameters, table 3.3 there is a discrepancy between the values for air and argon. There is a difference of 24 m/s in the speed of sound and a difference of 0.31 kg/m<sup>3</sup> however this does not translate to a visible difference in transmitted power at small spacings between panes. At larger spacing, however, there is a noticeable difference with air gaps creating a larger spread in transmitted powers compared to argon, especially at resonant frequencies.

The real-life experimental measurements showcase the flaws with using the mass law for single layer acoustic transmission. The mass law predicts a trend of -6db/octave [25]. Using Figure 3.8 between 125 Hz and 1000 Hz there are 3 octaves which corresponds to a theoretical decrease of 18 dB. Both the experimental and fitted transmission line data models have a drop of only 10 dB over the same octaves. The mass law also suggests that this roll-off continues, see Figure 3.2 however the experimental results clearly demonstrate that after 2000 Hz, the trend is reversed, and more power begins making its way through the window.

## Chapter 4

# Conclusion and Recommendations

### 4.1 Conclusion

A physics-based approach has been implemented to model the received signal strength of a fish as it swims upstream. This model can be used moving forward in conjunction with experimental data gathered by the RDL and the DFO to create a state space model that can pinpoint the location of a salmon. The results of the physics-based approach show that there are current drawbacks and setbacks to the current arrangement of receiving antennas and limitations due to the underlying phenomena.

The existing system suffers from low received signal strength, due to the large distances that the antennas are positioned from the rivers surface. This path loss in air works against us with the majority of the loss occurring in the first few meters as it propagates through air. The physical geography of the canyon limits how close the antennas can be placed to the water. The system also suffers from a low resolution in terms of spatial positioning based on the received gain. The low spatial resolution is compounded as the attenuation in water is exponential decay that shows no variance based on incoming angle. Therefore, if there is no spatial resolution obtained near the surface of the water, there won't be more spatial resolution at lower depths. The attenuation does however provide reasonable differentiation within depths of the river with a 5 dB difference for every 2 meters in depth. This is an improvement over the roughly 8.5 dB change we see over 92 meters at the surface of the river.

Acoustic propagation was evaluated using both experimental data and using the concepts of transmission line models. The transmission line model provides good agreement for the results for single-pane transmission, this is to be expected as the data was fitted using this data. The double-pane transmission line model no longer shows close agreement with differences in excess of 20 dB. This difference is due to the transmission line theory not adequately modelling the impact of the spring-like gap between the panes or errors with the experimental results. Instead, the transmission line models only the reflections, refractions, and attenuations within the material and while this works for EM propagation, the me-

chanical impacts of acoustic propagation mean that there needs to be further research into the attenuation model. Although the theory currently does not explain these phenomena well, the single-pane transmission model provides a fresh perspective on acoustic propagation and a new way to think about the concept, opening the doors to many possibilities currently employed in the electromagnetic world such as designing filters.

Propagation is an important field of research and underpins many of the key fundamentals behind Radio Frequency (RF) communication and auditory communication. This thesis allowed for a comprehensive analysis into the underlying principles of propagation for both acoustics and electromagnetics. The work that was done offered a wide variety of research opportunities from mathematical derivations and EM principles to going through specification sheets for various receivers and transmitters. As well, this project demonstrated my technical abilities from the usage of software tools such as Matlab to the implementation of both the salmon and the acoustic model. This project provided invaluable foundational theoretical knowledge while also creating useful models that can have a real-world impact in the ongoing research fields of ecological salmon studies and acoustic modelling. Although the project provided important results, it also revealed further questions laying the groundwork for many future projects and areas of research.

## 4.2 Future Work - Fish Tracking

- A more advanced attenuation model could be implemented using experimentally measured permittivity of the Fraser River water at the frequency of operation, 150 MHz. The  $\epsilon_I$  may not follow the known conductivity loss using the guessed conductivity in  $\sigma/\omega$ .
- Use flow simulation to estimate the position and orientation of the fish transmitter to implement a more accurate quantification of the polarisation mismatch. The transmitting antenna could be simulated in its actual position allowing for the fields to be calculated and the polarisation mismatch calculation could be carried out.
- Use the current model to simulate a variety of locations and orientations to get greater received power and larger variations in received signal across the river.
- A more statistical model could be beneficial whereby the exact details of the propagation scenario become less important, but the statistical significance of an occurrence becomes more important. This could allow for a rough layer of a specific distribution to be used to model waves on the surface of the river.
- The RDL has recently completed a LiDAR measurement campaign whereby they measured the details of the elevation of the canyon alongside a secondary dataset where the riverbed was also scanned and measured. This was recently completed and

there is current work being undertaken to stitch these two models together to create one dataset with both the canyon wall elevation and riverbed data together. This data could be a platform to complete a ray tracing scenario.

- The current experimental dataset that has been collected shows a high degree of variability certain downfalls primarily with the method that it was collected. Using a metal boat has impacts the results that were obtained changing any possible values that were collected.
- Redesign the fish transmitter to either use a completely different system, or to optimize the current system.

### 4.3 Future Work - Acoustic Modelling

- Include the temperature dependence of a material's properties to analyze how changing environmental conditions impact the acoustic insulating qualities of windows.
- Use an acoustic impedance tube to find values for the absorption coefficient and for the transmission loss values to compare with existing experimental results.
- Research the loss mechanism that occurs in double-pane and triple-pane setups. Unlike the electromagnetic attenuation given by an exponential decay, it is not currently clear if acoustic attenuation can be modelled using an exponential decay or if an alternative formalism is needed.
- When the double-pane transmission line model aligns closer with experimental data, various tasks can be performed using EM techniques, such as filters. This allows for the design of a window with specific characteristics, such as improved frequency response within a particular range of interest.
- Include spherical spreading of the acoustic wave. This would have an impact even over the small distances of a window frame and the impact should be studied accordingly.

# Bibliography

- [1] Government of Canada, Fisheries and Oceans Canada, “Big bar landslide response summary.” pac.dfo-mpo.gc.ca  
<https://www.pac.dfo-mpo.gc.ca/pacific-smon-pacifique/big-bar-landslide-eboulement/response-reponse-eng.html>(accessed September 7,2023).
- [2] E. Seagren, J. Venditti, E. Byrnes, J. Larimer, M. Hurson, K. Menounos, K. Robinson, M. Saletti, A. Steelquist, C. Williams, M. Wright, and S. Wuitchik, “Landslide impact on flow dynamics, fish migration and genetics of fraser river salmon,” 2022.
- [3] J. Venditti, “Landslide Impact on Flow Dynamics, Fish Migration and Genetics of Fraser River Salmon,” proposal, Simon Fraser University, Jan. 2021.
- [4] CTV News, “Photos of big bar landslide.” bc.ctvnews.ca  
<https://bc.ctvnews.ca/photos-show-big-bar-area-before-and-after-landslide-1.4510958>(accessed September 10,2023).
- [5] Government of Canada, Fisheries and Oceans Canada, “Infographic: Big bar landslide response - 2020 timeline of key events.” pac.dfo-mpo.gc.ca  
<https://www.pac.dfo-mpo.gc.ca/pacific-smon-pacifique/big-bar-landslide-eboulement/docs/timeline-chronologie-2020-eng.html>(accessed September 7,2023).
- [6] Karin Larsen, “Work at big bar slide site means fraser river salmon should have better chance this year.” cbc.ca  
<https://www.cbc.ca/news/canada/british-columbia/work-at-big-bar-slide-site-means-fraser-river-salmon-should-have-better-chance-this-year-1.6076838>.
- [7] E. Byrnes, K. Robinson, M. Saletti, R. Vaughan, S. Sixta, V. Leos, J. Venditti, and D. Patterson, “Drivers of migration pathway selection of Pacific salmon: time vs energy,” 2023.
- [8] D. M. Pozar, *Microwave engineering*. Addison-Wesley series in electrical and computer engineering, Reading, Mass: Addison-Wesley, 1990.
- [9] S. Ramo, J. R. Whinnery, and T. Van Duzer, *Fields and waves in communication electronics*. New York: Wiley, 1965.
- [10] S. J. Orfanidis, *Electromagnetic Waves and Antennas*. Piscataway, NJ, USA: Rutgers, 2016.

- [11] J. R. Wait, *Electromagnetic wave theory*. New York: Harper & Row, 1985.
- [12] S. Jiang and S. Georgakopoulos, “Electromagnetic Wave Propagation into Fresh Water,” *Journal of Electromagnetic Analysis and Applications*, vol. 2011, July 2011. Publisher: Scientific Research Publishing.
- [13] A. B. Harbicht, T. Castro-Santos, W. R. Ardren, D. Gorsky, and D. J. Fraser, “Novel, continuous monitoring of fine-scale movement using fixed-position radiotelemetry arrays and random forest location fingerprinting,” *Methods in Ecology and Evolution*, vol. 8, pp. 850–859, July 2017.
- [14] J. Koehn, Eiler, M. J.A., and O. W.G, “An improved method for obtaining fine-scale location of radio tags when tracking by boat.,” pp. 379–384, Jan. 2012.
- [15] K. C. Heim, W. R. Ardren, and T. Castro-Santos, “Using recovered radio transmitters to estimate positioning error and a generalized Monte Carlo simulation to incorporate error into animal telemetry analysis,” *Animal Biotelemetry*, vol. 11, p. 26, June 2023.
- [16] Y.-H. Kim, *Sound propagation: an impedance based approach*. Singapore ; Hoboken, NJ: Wiley, 2010. OCLC: ocn586123126.
- [17] N. Granzotto, F. Bettarello, A. Ferluga, L. Marsich, C. Schmid, P. Fausti, and M. Caniato, “Energy and acoustic performances of windows and their correlation,” *Energy and Buildings*, vol. 136, pp. 189–198, Feb. 2017.
- [18] Inger Andersen, “The world’s cities must take on the cacophony of noise pollution.” unep.org  
<https://www.unep.org/news-and-stories/opinion/worlds-cities-must-take-cacophony-noise-pollution>(accessed September 12,2023).
- [19] Google Scholar, “Signal processing top publications?.” scholar.google.ca  
[https://scholar.google.ca/citations?view\\_op=top\\_venues&hl=en&vq=eng\\_signalprocessing](https://scholar.google.ca/citations?view_op=top_venues&hl=en&vq=eng_signalprocessing)(accessed September 15,2023).
- [20] OSHA, “Identifying hazard control options: The hierarchy of controls.” osha.gov  
[https://www.osha.gov/sites/default/files/Hierarchy\\_of\\_Controls\\_02.01.23\\_form\\_508\\_2.pdf](https://www.osha.gov/sites/default/files/Hierarchy_of_Controls_02.01.23_form_508_2.pdf)(accessed September 16,2023).
- [21] Walker Peek, “Soundproof windows - how effective are they?.” residential-acoustics.com  
<https://residential-acoustics.com/soundproof-windows-how-effective-are-they/>(accessed September 13,2023).
- [22] F. Brinkmann, L. Aspöck, D. Ackermann, S. Lepa, M. Vorländer, and S. Weinzierl, “A round robin on room acoustical simulation and auralization,” *The Journal of the Acoustical Society of America*, vol. 145, pp. 2746–2760, Apr. 2019.
- [23] J. D. Quirt, “Sound transmission through windows I. Single and double glazing,” *The Journal of the Acoustical Society of America*, vol. 72, pp. 834–844, Sept. 1982.
- [24] M. Vorländer, *Auralization: fundamentals of acoustics, modelling, simulation, algorithms and acoustic virtual reality*. RWTHedition / RWTH Aachen, England Wales: ASA Press, second edition ed., 2020.



- [25] A. D. Pierce, *Acoustics: an introduction to its physical principles and applications*. Cham: ASA Press, Springer, third edition ed., 2019.
- [26] S. W. Ellingson, *Electromagnetics, Volume 2*. VT Publishing, Jan. 2020.
- [27] R. Vaughan and J. Bach Andersen, *Channels, propagation and antennas for mobile communications*. No. 50 in IEE electromagnetic waves series, London: Institution of Electrical Engineers, 2003. OCLC: ocm49691547.
- [28] C. A. Balanis, *Antenna theory: analysis and design*. New York: Wiley, 2nd ed ed., 1997.
- [29] C. Hynes, P. Hui, J. van Wousterghem, and D. Michelson, “Cross-correlation and total efficiencies of two closely spaced sleeve dipole antennas,” in *2005 IEEE Antennas and Propagation Society International Symposium*, vol. 1B, pp. 799–802 vol. 1B, July 2005. ISSN: 1947-1491.
- [30] J. A. Shaw, “Radiometry and the Friis transmission equation,” *American Journal of Physics*, vol. 81, pp. 33–37, Jan. 2013.
- [31] J. M. Carcione, *Wave fields in real media: wave propagation in anisotropic, anelastic, porous and electromagnetic media*. No. 38 in Handbook of geophysical exploration. Seismic exploration, Amsterdam Boston [etc.]: Elsevier, 2015.
- [32] L. T. Ikelle, “On elastic-electromagnetic mathematical equivalences,” *Geophysical Journal International*, vol. 189, pp. 1771–1780, June 2012.
- [33] L. L. Beranek, *Acoustics*. New York, N.Y: Published by the American Institute of Physics for the Acoustical Society of America, 1986 ed ed., 1986.
- [34] CDC, “What noises cause hearing loss?” [www.cdc.gov](https://www.cdc.gov/ncch/ncsr/ncshs/ncshs.html)  
[https://www.cdc.gov/ncch/hearing\\_loss/what\\_noises\\_cause\\_hearing\\_loss.html](https://www.cdc.gov/ncch/hearing_loss/what_noises_cause_hearing_loss.html) (accessed November 1,2023).
- [35] M. Long, *Architectural Acoustics*. San Diego, United States: Elsevier Science & Technology, 2014.
- [36] P. Lord and D. Templeton, *Detailing for Acoustics*. Taylor & Francis, 3 ed., Oct. 2019.
- [37] Ignacio Fernández Solla, “Acoustic properties of glass: not so simple.” [www.glassonweb.com](http://www.glassonweb.com)  
<http://www.glassonweb.com/article/acoustic-properties-glass-not-so-simple> (accessed October 21,2023).
- [38] Physikalisch-Technische Bundesanstalt, “Absorption coefficient database.” [www.ptb.de](http://www.ptb.de)  
<https://www.ptb.de/cms/ptb/fachabteilungen/abt1/fb-16/ag-163/absorption-coefficient-database.html> (accessed October 25,2023).
- [39] “Odeon Room Acoustics Software.”
- [40] Kien Safety Glass Sdn Bhd, “Sound insulation of glass.” [irp-cdn.multiscreensite.com](http://irp-cdn.multiscreensite.com)  
<https://irp-cdn.multiscreensite.com/05d76747/files/uploaded/Sound%20Insulation%20of%20Glass%20%281396%20KB%29.pdf> (accessed October 23,2023).

# Appendix A

## Fish Tracking - Details

### A.1 Fresnel Equations - Comparison between References

#### A.1.1 Perpendicular - TE

Pozar

Reflection Coefficient:

$$\Gamma = \frac{\eta' \cos(\theta) - \eta \cos(\theta')}{\eta' \cos(\theta) + \eta \cos(\theta')} \quad (\text{A.1})$$

$$\eta = \sqrt{\frac{\mu_0}{\epsilon}} \quad \eta' = \sqrt{\frac{\mu_0}{\epsilon'}} \quad (\text{A.2})$$

Transmission Coefficient:

$$\tau = 1 + \Gamma = \frac{2\eta' \cos \theta}{\eta' \cos \theta + \eta \cos \theta'} \quad (\text{A.3})$$

Power Reflection:

$$|\Gamma|^2 \quad (\text{A.4})$$

Power Transmission:

$$|\tau|^2 \frac{\text{Re}\{\eta \cos \theta'\}}{\text{Re}\{\eta' \cos \theta\}} = 1 - |\Gamma|^2 \quad (\text{A.5})$$

## MIT

Reflection Coefficient:

$$\Gamma = \frac{N_i - N_t}{N_i + N_t} \quad (\text{A.6})$$

$$N_i = \frac{\cos \theta}{\eta} \quad (\text{A.7})$$

$$N_t = \frac{\cos \theta'}{\eta'} \quad (\text{A.8})$$

$\eta$  and  $\eta'$  being the same definition as Pozar. Note that  $N$  is *not* the refractive index.

*Proof.*

$$\Gamma = \frac{\frac{\cos \theta}{\eta} - \frac{\cos \theta'}{\eta'}}{\frac{\cos \theta}{\eta} + \frac{\cos \theta'}{\eta'}} = \frac{\frac{\cos \theta \eta' - \cos \theta' \eta}{\eta \eta'}}{\frac{\cos \theta \eta' + \cos \theta' \eta}{\eta \eta'}} = \frac{\eta' \cos(\theta) - \eta \cos(\theta')}{\eta' \cos(\theta) + \eta \cos(\theta')}$$

□

Transmission Coefficient:

$$\tau = 1 + \Gamma = \frac{2N_i}{N_i + N_t} \quad (\text{A.9})$$

Power Reflection:

$$|\Gamma|^2 \quad (\text{A.10})$$

Power Transmission:

$$|\tau|^2 \frac{\text{Re}\{N_t\}}{\text{Re}\{N_i\}} = 1 - |\Gamma|^2 \quad (\text{A.11})$$

## James Wait

Reflection Coefficient:

$$\begin{aligned} \Gamma &= \frac{N - N'}{N + N'} \\ N &= \frac{u}{j\mu_0\omega}, \quad N' = \frac{u'}{j\mu_0\omega} \\ u &= \gamma \cos \theta, \quad u' = \gamma' \cos \theta' \\ \gamma &= \sqrt{j\mu\omega(\sigma + j\epsilon_{Re}\omega)} \end{aligned} \quad (\text{A.12})$$

*Proof.*

$$\begin{aligned}
\Gamma &= \frac{\frac{\sqrt{j\mu\omega(\sigma+j\epsilon_{Re}\omega)} \cos \theta}{j\mu_0\omega} - \frac{(\sqrt{j\mu\omega(\sigma+j\epsilon_{Re}\omega)})' \cos \theta'}{j\mu_0\omega}}{\frac{\sqrt{j\mu\omega(\sigma+j\epsilon_{Re}\omega)} \cos \theta}{j\mu_0\omega} + \frac{(\sqrt{j\mu\omega(\sigma+j\epsilon_{Re}\omega)})' \cos \theta'}{j\mu_0\omega}} = \frac{\sqrt{j\mu\omega(\sigma+j\epsilon_{Re}\omega)} \cos \theta - (\sqrt{j\mu\omega(\sigma+j\epsilon_{Re}\omega)})' \cos \theta'}{\sqrt{j\mu\omega(\sigma+j\epsilon_{Re}\omega)} \cos \theta + (\sqrt{j\mu\omega(\sigma+j\epsilon_{Re}\omega)})' \cos \theta'} \\
\sigma &= 0 \\
&= \frac{\sqrt{j\mu\omega(j\epsilon_{Re}\omega)} \cos \theta - (\sqrt{j\mu\omega(\sigma+j\epsilon_{Re}\omega)})' \cos \theta'}{\sqrt{j\mu\omega(j\epsilon_{Re}\omega)} \cos \theta + (\sqrt{j\mu\omega(\sigma+j\epsilon_{Re}\omega)})' \cos \theta'} = \frac{j\omega\sqrt{\mu\epsilon_{Re}} \cos \theta - (\sqrt{j\mu\omega(\sigma+j\epsilon_{Re}\omega)})' \cos \theta'}{j\omega\sqrt{\mu\epsilon_{Re}} \cos \theta + (\sqrt{j\mu\omega(\sigma+j\epsilon_{Re}\omega)})' \cos \theta'} \\
&= \frac{j\sqrt{\mu}\sqrt{\epsilon_{Re}} \cos \theta - j\sqrt{\mu'}\sqrt{\epsilon'_{Re} - j\frac{\sigma'}{\omega}} \cos \theta'}{j\sqrt{\mu}\sqrt{\epsilon_{Re}} \cos \theta + j\sqrt{\mu'}\sqrt{\epsilon'_{Re} - j\frac{\sigma'}{\omega}} \cos \theta'} \\
&= \frac{\sqrt{\mu}\sqrt{\epsilon_{Re}} \cos \theta - \sqrt{\mu'}\sqrt{\epsilon'_{Re} - j\frac{\sigma'}{\omega}} \cos \theta'}{\sqrt{\mu}\sqrt{\epsilon_{Re}} \cos \theta + \sqrt{\mu'}\sqrt{\epsilon'_{Re} - j\frac{\sigma'}{\omega}} \cos \theta'} \\
&= \frac{\frac{\sqrt{\mu}}{\sqrt{\epsilon'_{Re} - j\frac{\sigma'}{\omega}}} \cos \theta - \frac{\sqrt{\mu'}}{\sqrt{\epsilon_{Re}}} \cos \theta'}{\frac{\sqrt{\mu}}{\sqrt{\epsilon'_{Re} - j\frac{\sigma'}{\omega}}} \cos \theta + \frac{\sqrt{\mu'}}{\sqrt{\epsilon_{Re}}} \cos \theta'} \\
&= \frac{\frac{\sqrt{\mu}}{\sqrt{\epsilon'_{Re} - j\frac{\sigma'}{\omega}}} \cos \theta - \frac{\sqrt{\mu'}}{\sqrt{\epsilon_{Re}}} \cos \theta'}{\frac{\sqrt{\mu}}{\sqrt{\epsilon'_{Re} - j\frac{\sigma'}{\omega}}} \cos \theta + \frac{\sqrt{\mu'}}{\sqrt{\epsilon_{Re}}} \cos \theta'}
\end{aligned}$$

Note that  $\mu = \mu'$

$$\begin{aligned}
&= \frac{-\frac{\sqrt{\mu'}}{\sqrt{\epsilon'_{Re} - j\frac{\sigma'}{\omega}}} \cos \theta - \frac{\sqrt{\mu}}{\sqrt{\epsilon_{Re}}} \cos \theta'}{\frac{\sqrt{\mu'}}{\sqrt{\epsilon'_{Re} - j\frac{\sigma'}{\omega}}} \cos \theta + \frac{\sqrt{\mu}}{\sqrt{\epsilon_{Re}}} \cos \theta'} = \frac{\eta' \cos(\theta) - \eta \cos(\theta')}{\eta' \cos(\theta) + \eta \cos(\theta')}
\end{aligned}$$

□

Transmission Coefficient:

$$\tau = \frac{2N}{N + N'} = 1 + \Gamma \quad (\text{A.13})$$

Power Reflection:

$$|\Gamma|^2 \quad (\text{A.14})$$

Power Transmission:

$$|\tau|^2 \frac{\text{Re}\{N'\}}{\text{Re}\{N\}} = 1 - |\Gamma|^2 \quad (\text{A.15})$$

## Rutgers

Reflection Coefficient:

$$\Gamma_{TE} = \frac{k_z - k'_z}{k_z + k'_z} \quad (\text{A.16})$$

With  $k_z$  and  $k'_z$  given by 2.8

*Proof.*

$$\begin{aligned} \Gamma &= \frac{\omega\sqrt{\mu\epsilon}\cos\theta - \omega\sqrt{\mu\epsilon'}\cos\theta'}{\omega\sqrt{\mu\epsilon}\cos\theta + \omega\sqrt{\mu\epsilon'}\cos\theta'} \\ &= \frac{\frac{\omega\sqrt{\mu\epsilon}\cos\theta - \omega\sqrt{\mu\epsilon'}\cos\theta'}{\sqrt{\epsilon\epsilon'}}}{\frac{\omega\sqrt{\mu\epsilon}\cos\theta + \omega\sqrt{\mu\epsilon'}\cos\theta'}{\sqrt{\epsilon\epsilon'}}} = \frac{\omega\sqrt{\frac{\mu}{\epsilon'}}\cos\theta - \omega\sqrt{\frac{\mu}{\epsilon}}\cos\theta'}{\omega\sqrt{\frac{\mu}{\epsilon'}}\cos\theta + \omega\sqrt{\frac{\mu}{\epsilon}}\cos\theta'} \\ &= \frac{\eta'\cos(\theta) - \eta\cos(\theta')}{\eta'\cos(\theta) + \eta\cos(\theta')} \end{aligned}$$

□

Transmission Coefficient:

$$\tau_{TE} = 1 + \Gamma_{TE} = \frac{2k_z}{k_z + k'_z} \quad (\text{A.17})$$

Power Reflection:

$$|\Gamma|^2 \quad (\text{A.18})$$

Power Transmission:

$$|\tau|^2 \frac{\text{Re}\{k'_z\}}{\text{Re}\{k_z\}} = 1 - |\Gamma|^2 \quad (\text{A.19})$$

## A.1.2 Parallel - TM

### Pozar

Reflection Coefficient:

$$\Gamma = \frac{\eta'\cos(\theta') - \eta\cos(\theta)}{\eta'\cos(\theta') + \eta\cos(\theta)} \quad (\text{A.20})$$

With  $\eta$  defined the same way as (A.2)

Transmission Coefficient:

$$\tau = \frac{2\eta'\cos\theta'}{\eta'\cos(\theta') + \eta\cos(\theta)} = 1 + \Gamma \quad (\text{A.21})$$

Power Reflection:

$$|\Gamma|^2 \quad (\text{A.22})$$

Power Transmission:

$$|\tau|^2 \operatorname{Re} \left\{ \frac{\eta \cos \theta}{\eta' \cos \theta'} \right\} \quad (\text{A.23})$$

## MIT

Reflection Coefficient:

$$\Gamma = \frac{M_i - M_t}{M_i + M_t} \quad (\text{A.24})$$

$$M_i = \eta \cos \theta \quad (\text{A.25})$$

$$M_t = \eta' \cos \theta' \quad (\text{A.26})$$

$\eta$  and  $\eta'$  being the same definition as Pozar (A.2).

$$\Gamma = \frac{\eta \cos \theta - \eta' \cos \theta'}{\eta \cos \theta + \eta' \cos \theta'}$$

This results in a value that is the negative of the Pozar textbook.

Transmission Coefficient:

$$\tau = 1 + \Gamma = \frac{2M_i}{M_i + M_t} = \frac{2\eta \cos \theta}{\eta \cos \theta + \eta' \cos \theta'} \quad (\text{A.27})$$

Power Reflection:

$$|\Gamma|^2 \quad (\text{A.28})$$

Power Transmission:

$$|\tau|^2 \operatorname{Re} \left\{ \frac{\eta' \cos \theta'}{\eta \cos \theta} \right\} = 1 - |\Gamma|^2 \quad (\text{A.29})$$

Although this form is different as compared to Pozar the resultant power is correct.

## Rutgers

Reflection Coefficient

$$\Gamma = \frac{k'_z \epsilon - k_z \epsilon'}{k'_z \epsilon + k_z \epsilon'} \quad (\text{A.30})$$

With  $k_z$  and  $k'_z$  the same as (2.8)

*Proof.*

$$\begin{aligned}
\Gamma &= \frac{\omega\sqrt{\mu\epsilon'} \cos \theta' \epsilon - \omega\sqrt{\mu\epsilon} \cos \theta \epsilon'}{\omega\sqrt{\mu\epsilon'} \cos \theta' \epsilon + \omega\sqrt{\mu\epsilon} \cos \theta \epsilon'} \\
&= \frac{\omega\sqrt{\mu\epsilon'} \cos \theta' \epsilon - \omega\sqrt{\mu\epsilon} \cos \theta \epsilon'}{\epsilon \epsilon'} \\
&= \frac{\omega\sqrt{\frac{\mu}{\epsilon'}} \cos \theta' - \omega\sqrt{\frac{\mu}{\epsilon}} \cos \theta}{\omega\sqrt{\frac{\mu}{\epsilon'}} \cos \theta' + \omega\sqrt{\frac{\mu}{\epsilon}} \cos \theta} \\
&= \frac{\eta' \cos(\theta') - \eta \cos(\theta)}{\eta' \cos(\theta') + \eta \cos(\theta)}
\end{aligned}$$

□

Transmission Coefficient

$$\tau = \frac{2k'_z \epsilon}{k'_z \epsilon + k_z \epsilon'} = 1 + \Gamma \quad (\text{A.31})$$

Power Reflection

$$|\Gamma|^2 \quad (\text{A.32})$$

Power Transmission:

$$|\tau|^2 \frac{\text{Re}\{k_z \epsilon'\}}{\text{Re}\{k'_z \epsilon\}} = 1 - |\Gamma|^2 \quad (\text{A.33})$$

## James Wait

Reflection Coefficient

$$\Gamma = -\frac{K_{water} - K_{air}}{K_{water} + K_{air}} \quad (\text{A.34})$$

$$K = \frac{u}{\sigma + j\epsilon_d \omega} \quad (\text{A.35})$$

$K$  is James Wait's notation for  $\eta$  the wave impedance.

$$u = \gamma \cos(\theta) = \sqrt{j\mu\omega(\sigma + j\epsilon_d \omega)} \cos(\theta) \quad (\text{A.36})$$

*Proof.*

$$\begin{aligned}
\Gamma &= -\frac{\frac{\sqrt{j\mu\omega(\sigma'+j\epsilon'_{Re}\omega)}\cos(\theta')}{\sigma'+j\epsilon'_{Re}\omega} - \frac{\sqrt{j\mu\omega(\sigma+j\epsilon_{Re}\omega)}\cos(\theta)}{\sigma+j\epsilon_{Re}\omega}}{\frac{\sqrt{j\mu\omega(\sigma'+j\epsilon'_{Re}\omega)}\cos(\theta')}{\sigma'+j\epsilon'_{Re}\omega} + \frac{\sqrt{j\mu\omega(\sigma+j\epsilon_{Re}\omega)}\cos(\theta)}{\sigma+j\epsilon_{Re}\omega}} \\
\sigma &= 0 \\
\Gamma &= -\frac{\frac{\sqrt{j\mu\omega(\sigma'+j\epsilon'_{Re}\omega)}\cos(\theta')}{\sigma'+j\epsilon'_{Re}\omega} - \frac{\sqrt{\mu\omega(\epsilon_{Re}\omega)}\cos(\theta)}{\epsilon_{Re}\omega}}{\frac{\sqrt{j\mu\omega(\sigma'+j\epsilon'_{Re}\omega)}\cos(\theta')}{\sigma'+j\epsilon'_{Re}\omega} + \frac{\sqrt{\mu\omega(\epsilon_{Re}\omega)}\cos(\theta)}{\epsilon_{Re}\omega}} \\
&= -\frac{\frac{j\omega\sqrt{\mu}\sqrt{\epsilon'_{Re}-j\frac{\sigma'}{\omega}}\cos(\theta')}{\sigma'+j\epsilon'_{Re}\omega} - \frac{\sqrt{\mu\omega(\epsilon_{Re}\omega)}\cos(\theta)}{\epsilon_{Re}\omega}}{\frac{j\omega\sqrt{\mu}\sqrt{\epsilon'_{Re}-j\frac{\sigma'}{\omega}}\cos(\theta')}{\sigma'+j\epsilon'_{Re}\omega} + \frac{\sqrt{\mu\omega(\epsilon_{Re}\omega)}\cos(\theta)}{\epsilon_{Re}\omega}} \\
&= -\frac{\frac{j\omega\sqrt{\mu\epsilon'}\cos(\theta')}{j\omega(\epsilon'_{Re}-j\frac{\sigma'}{\omega})} - \frac{\omega\sqrt{\mu\epsilon}\cos(\theta)}{\epsilon_{Re}\omega}}{\frac{j\omega\sqrt{\mu\epsilon'}\cos(\theta')}{j\omega(\epsilon'_{Re}-j\frac{\sigma'}{\omega})} + \frac{\omega\sqrt{\mu\epsilon}\cos(\theta)}{\epsilon_{Re}\omega}} \\
&= -\frac{\frac{j\omega\sqrt{\mu\epsilon'}\cos(\theta')}{j\omega\epsilon'} - \frac{\omega\sqrt{\mu\epsilon}\cos(\theta)}{\epsilon\omega}}{\frac{j\omega\sqrt{\mu\epsilon'}\cos(\theta')}{j\omega\epsilon'} + \frac{\omega\sqrt{\mu\epsilon}\cos(\theta)}{\epsilon\omega}} \\
&= -\frac{\frac{\sqrt{\mu\epsilon'}\cos(\theta')}{\epsilon'} - \frac{\sqrt{\mu\epsilon}\cos(\theta)}{\epsilon}}{\frac{\sqrt{\mu\epsilon'}\cos(\theta')}{\epsilon'} + \frac{\sqrt{\mu\epsilon}\cos(\theta)}{\epsilon}} \\
\Gamma &= -\frac{\eta'\cos(\theta') - \eta\cos(\theta)}{\eta'\cos(\theta') + \eta\cos(\theta)}
\end{aligned}$$

□

This results in a value that is the negative of the Pozar textbook. It results in the same value as calculated with MIT approach.

Transmission Coefficient

$$\tau = \frac{2K_{air}}{K_{water} + K_{air}} \quad (\text{A.37})$$

Power Reflection

$$|\Gamma|^2 \quad (\text{A.38})$$

Power Transmission:

$$|\tau|^2 \text{Re}\left\{\frac{K_{water}}{K_{air}}\right\} = 1 - |\Gamma|^2 \quad (\text{A.39})$$



### A.1.3 TE and TM Polarisation Plots

Coefficients for TE and TM modes:

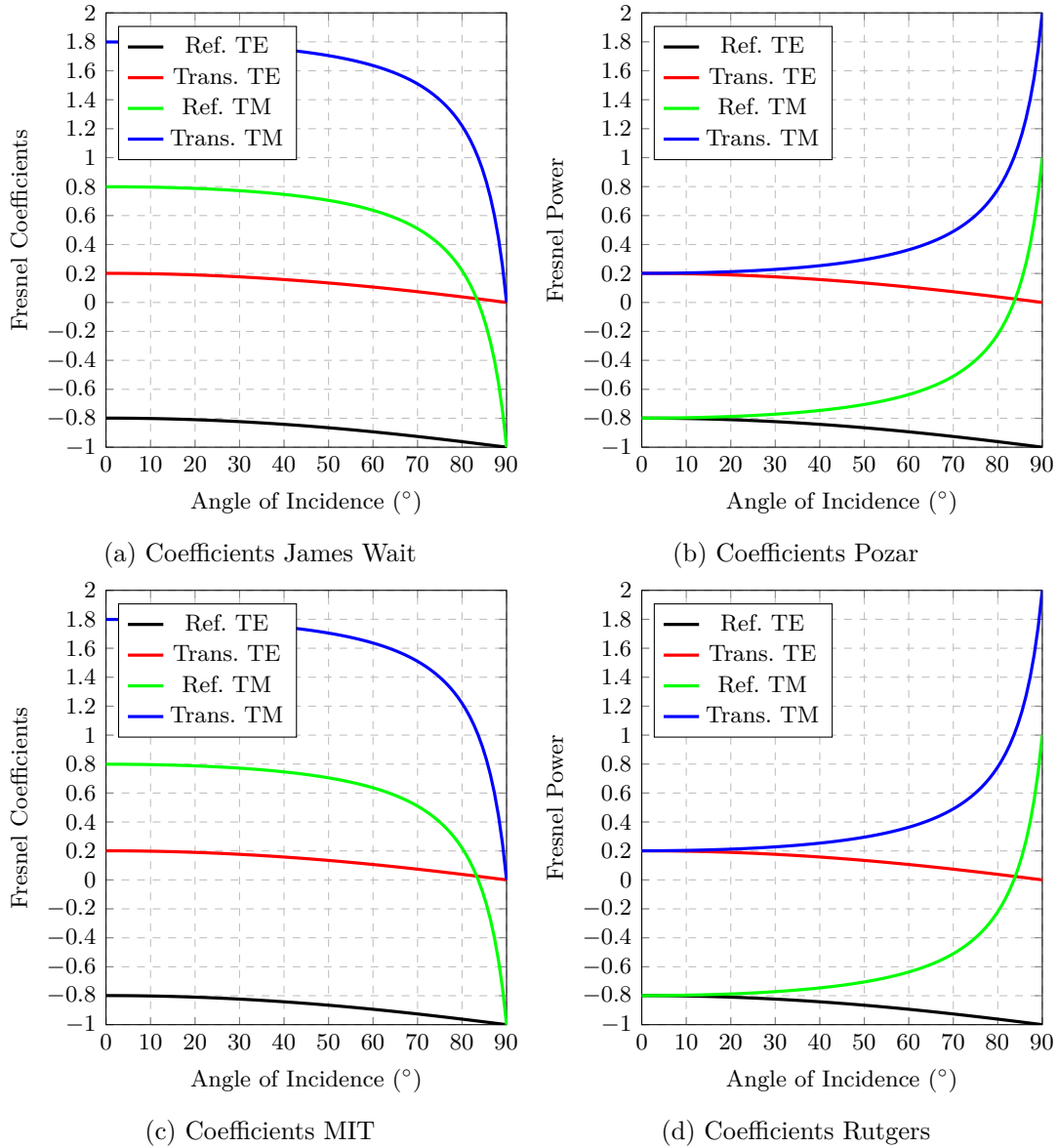


Figure A.1: TE and TM Fresnel coefficients.

This highlights that the coefficients for the TM polarisation are not in agreement with two textbooks containing a difference of a multiplication of negative one.

The power values however agree for both TE and TM polarisations for all 4 derivations. The magnitude squared element removes any of the issues of the negative sign of the coefficients.

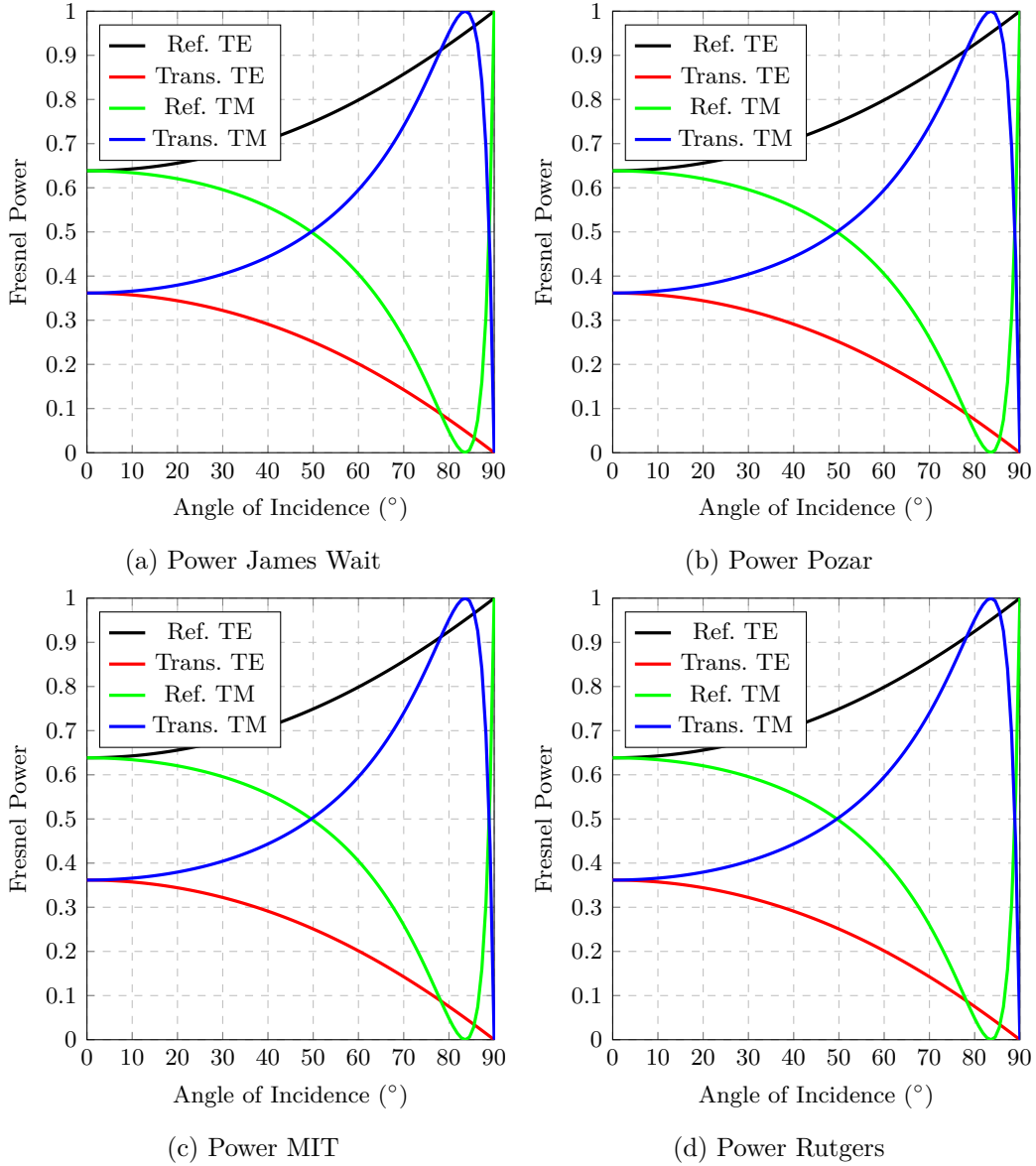


Figure A.2: TE and TM Fresnel Power.

## A.2 Overall Power

### A.2.1 TE+TM Gain

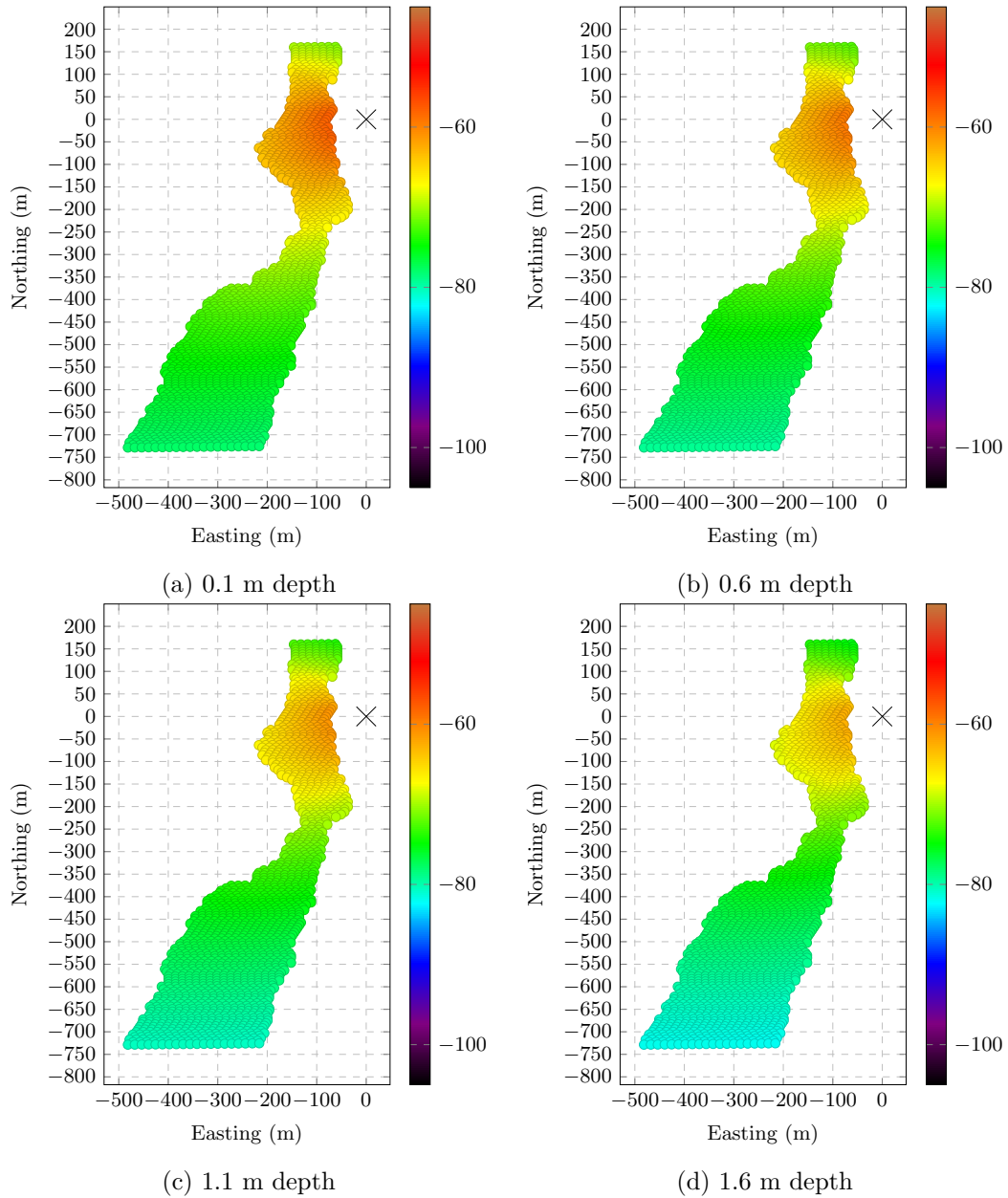


Figure A.3: Total system Loss 0.5(TE+TM)- Eastside Downstream site (dB). The receiver is located at 10U 559418.2593 km E, 15674469.93 km N.

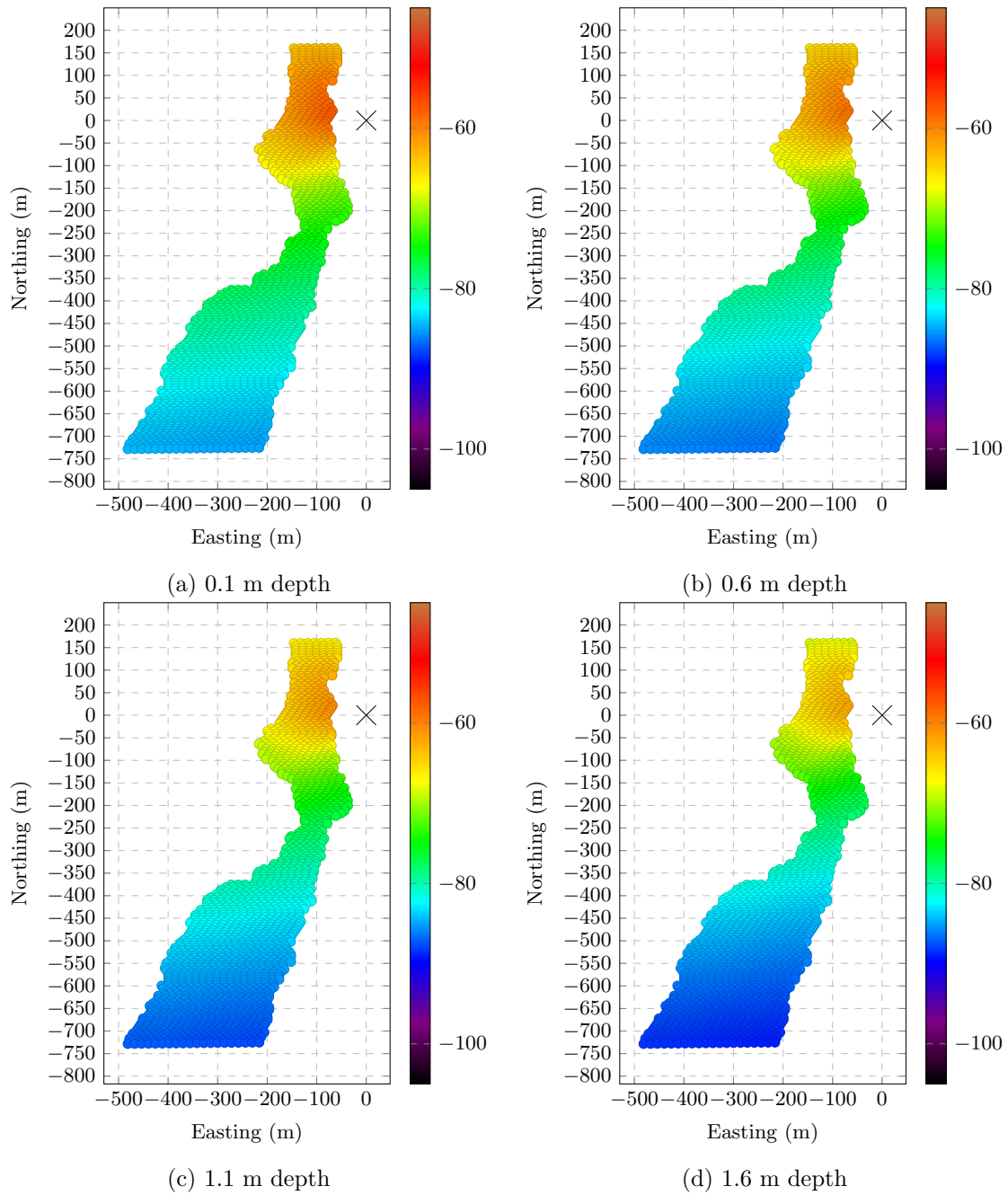


Figure A.4: Total system Loss  $0.5(Te+Tm)$ - Eastside Upstream site (dB). The receiver is located at 10U 559418.2593 km E, 15674469.93 km N.

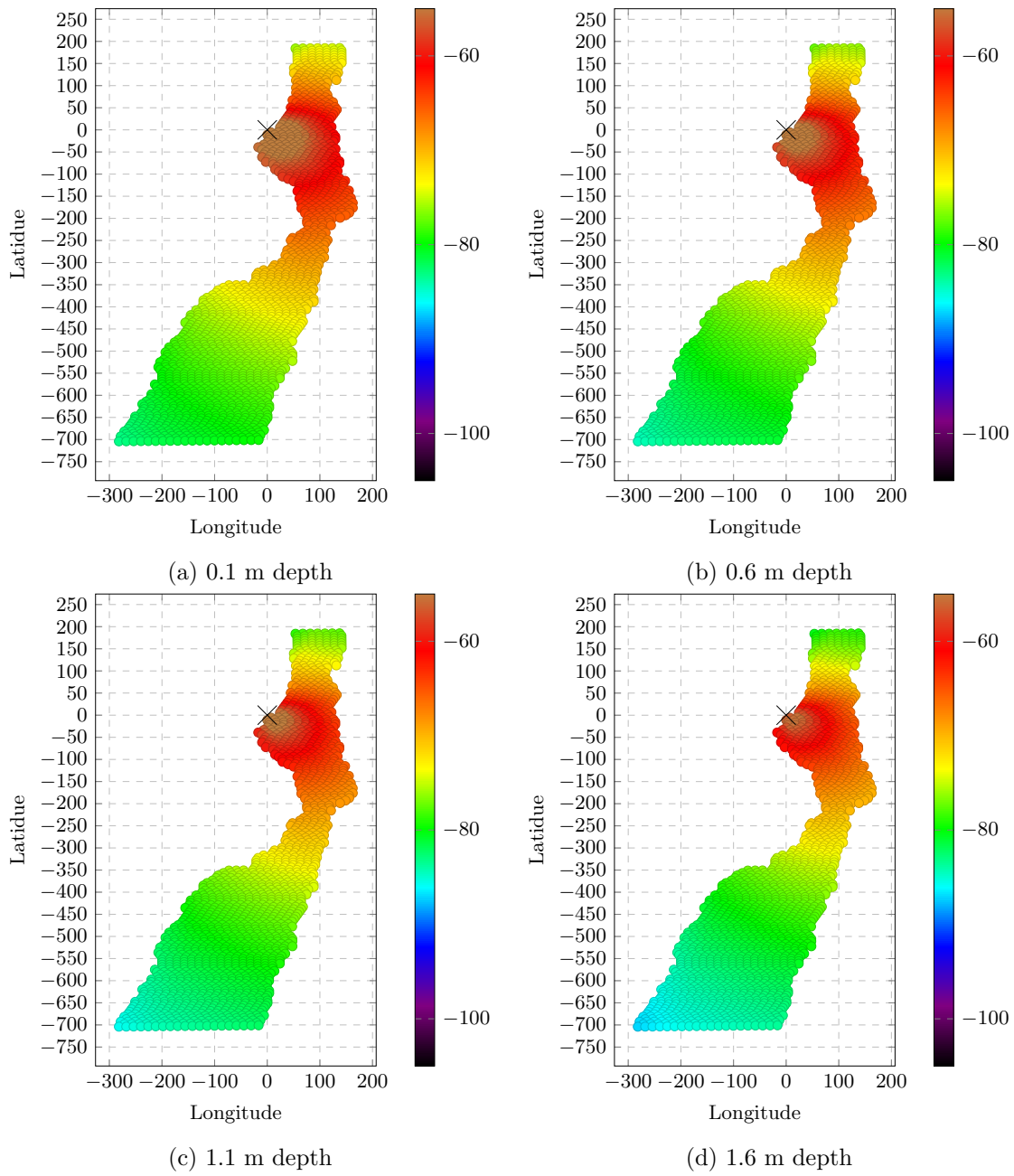


Figure A.5: Total system Loss  $0.5(Te+Tm)$ - Eddy Downstream site (dB). The receiver is located at 10U 559218.498 km E, 15674445.6 km N.

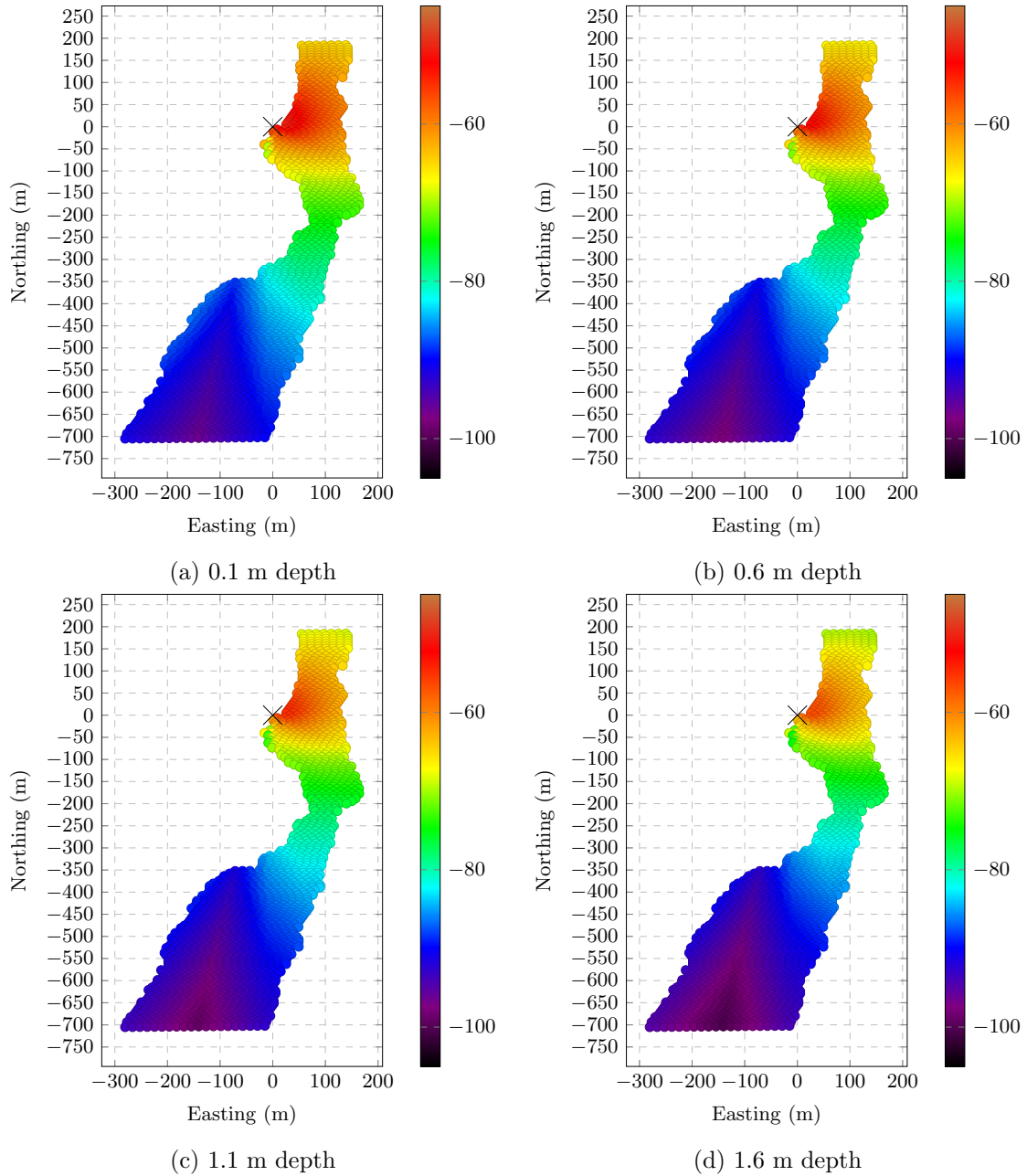


Figure A.6: Total system Loss 0.5(TE+TM)- Eddy Upstream site (dB). The receiver is located at 10U 559217.0907 km E, 15674446.48 km N.

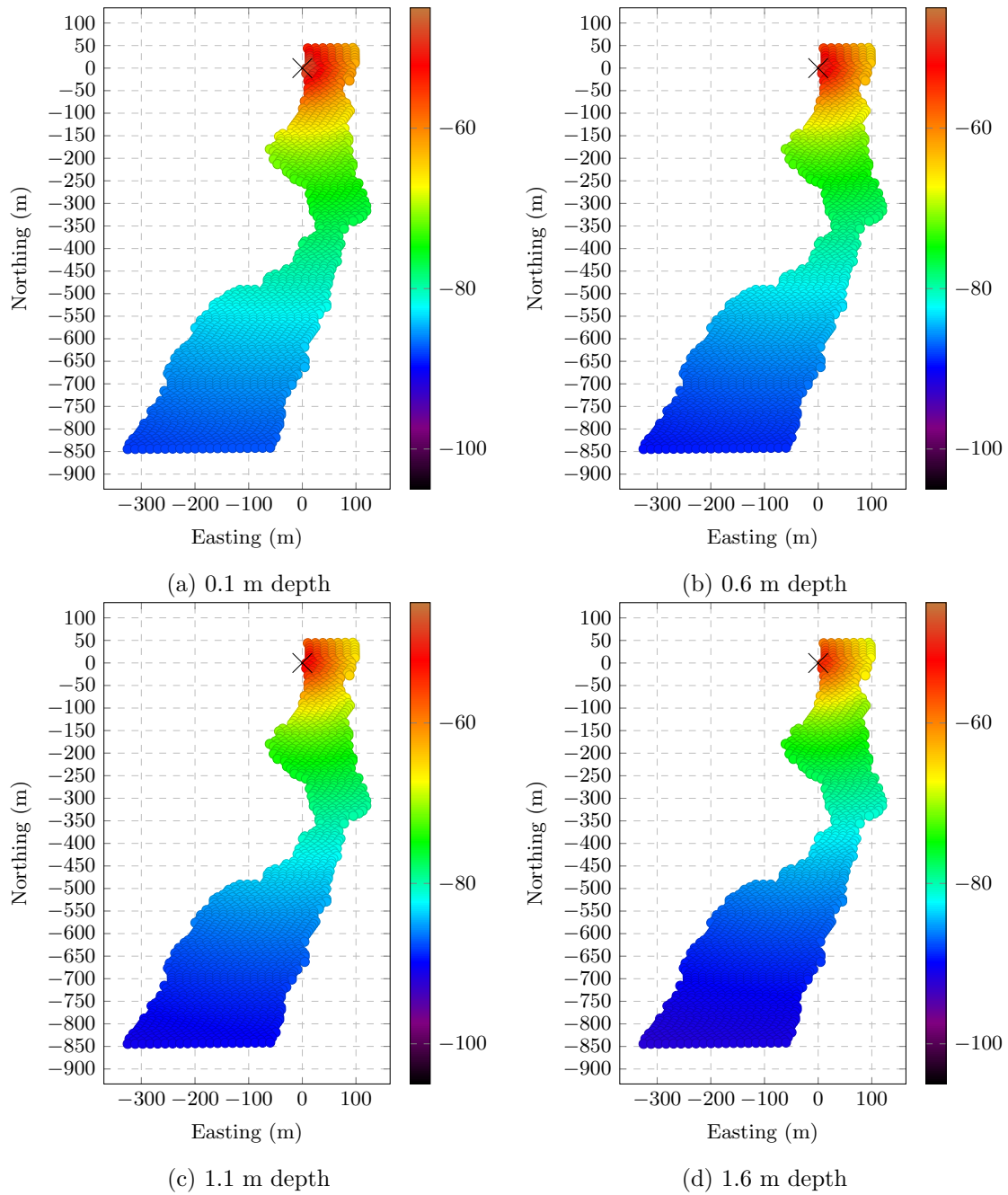


Figure A.7: Total system Loss  $0.5(TE+TM)$ - iBeam p1 site (dB). The receiver is located at 10U 559261.9979 km E, 15674586.02 km N.

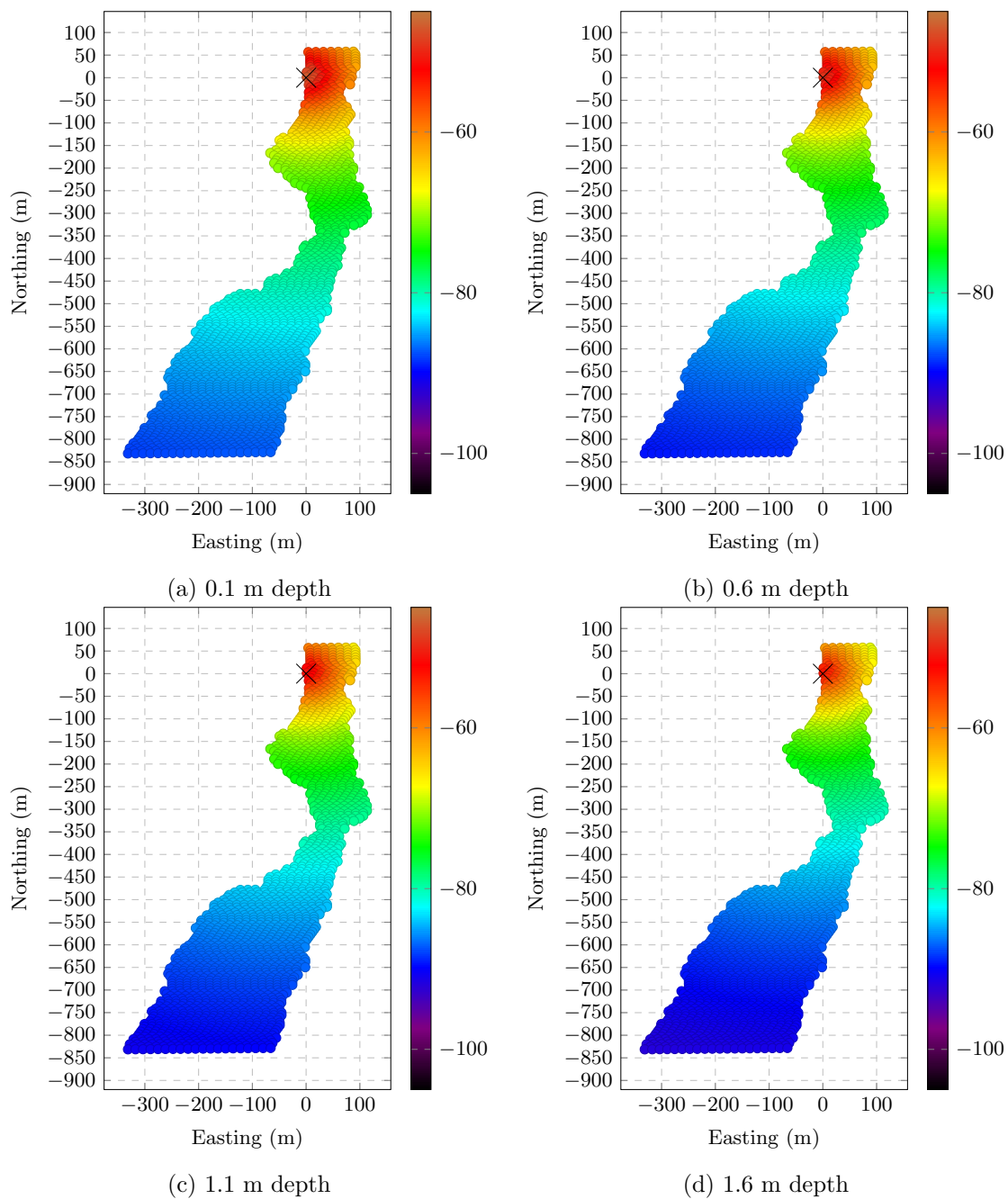


Figure A.8: Total system Loss  $0.5(TE+TM)$ - iBeam p2 site (dB). The receiver is located at 10U 559268.0157 km E, 15674572.97 km N.



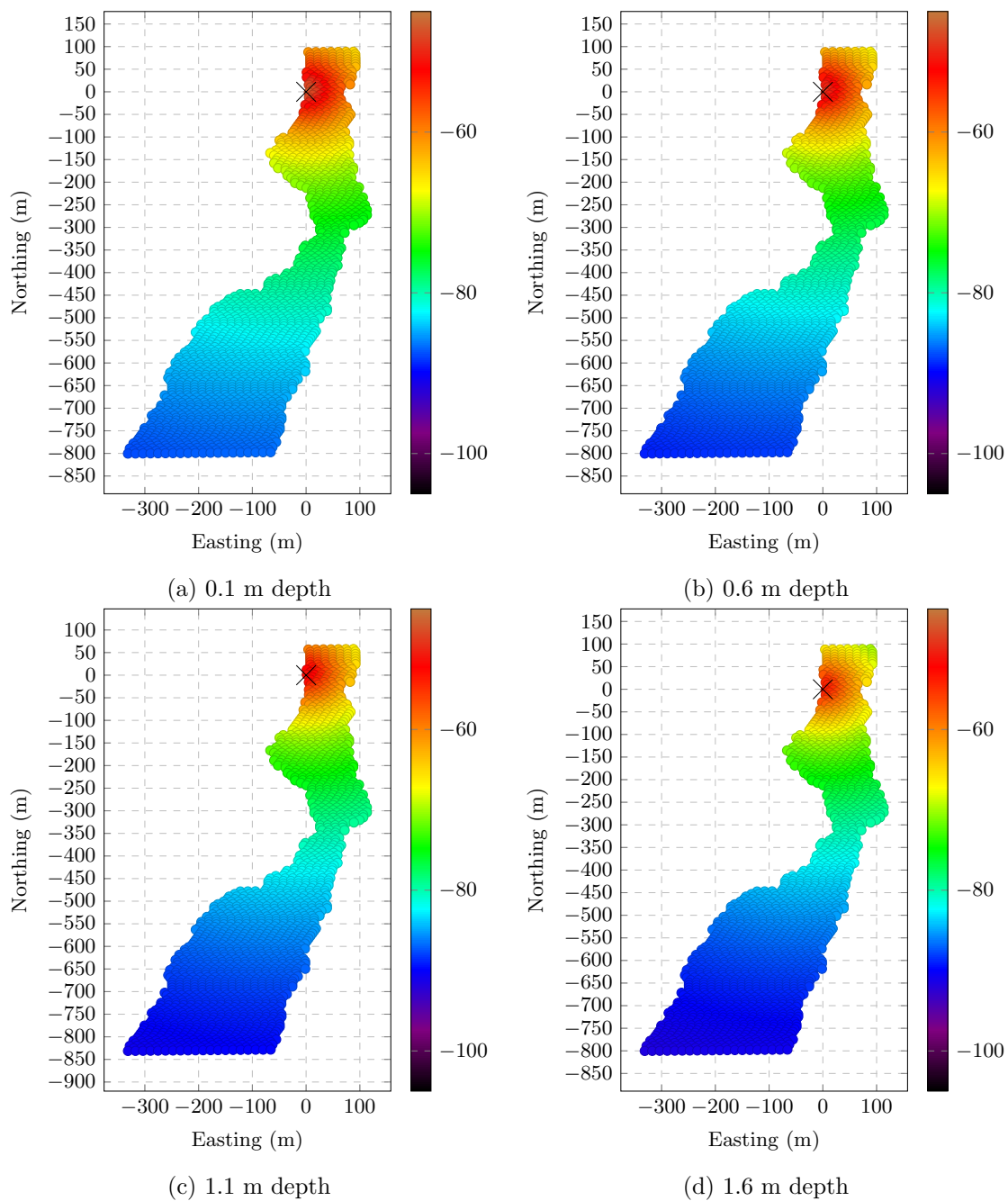


Figure A.9: Total system Loss  $0.5(TE+TM)$ - iBeam p5 site (dB). The receiver is located at 10U 559268.0248 km E, 15674541.94 km N.

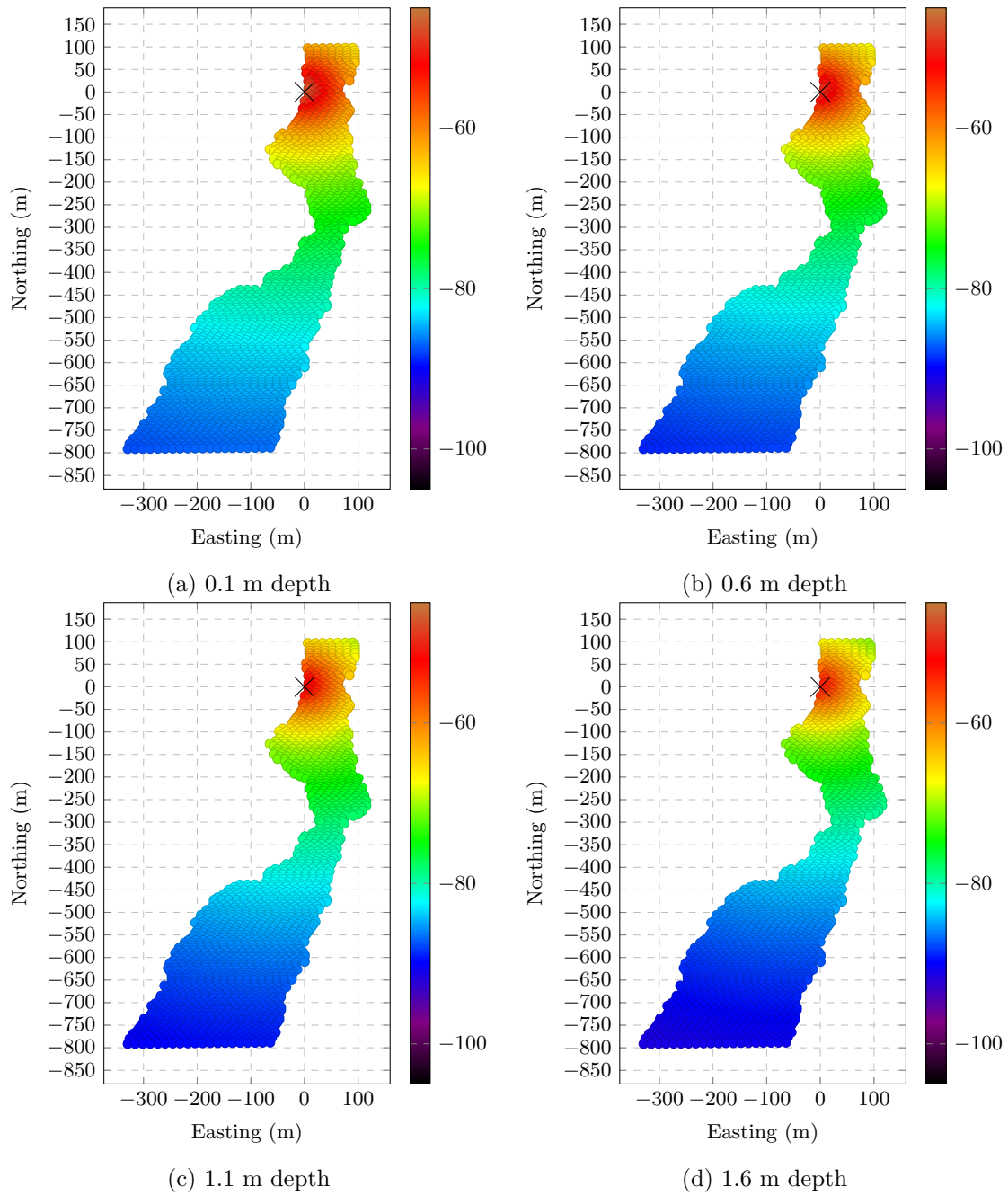


Figure A.10: Total system Loss  $0.5(TE+TM)$ - iBeam p6 site (dB). The receiver is located at 10U 559266.0324 km E, 15674533.02 km N.

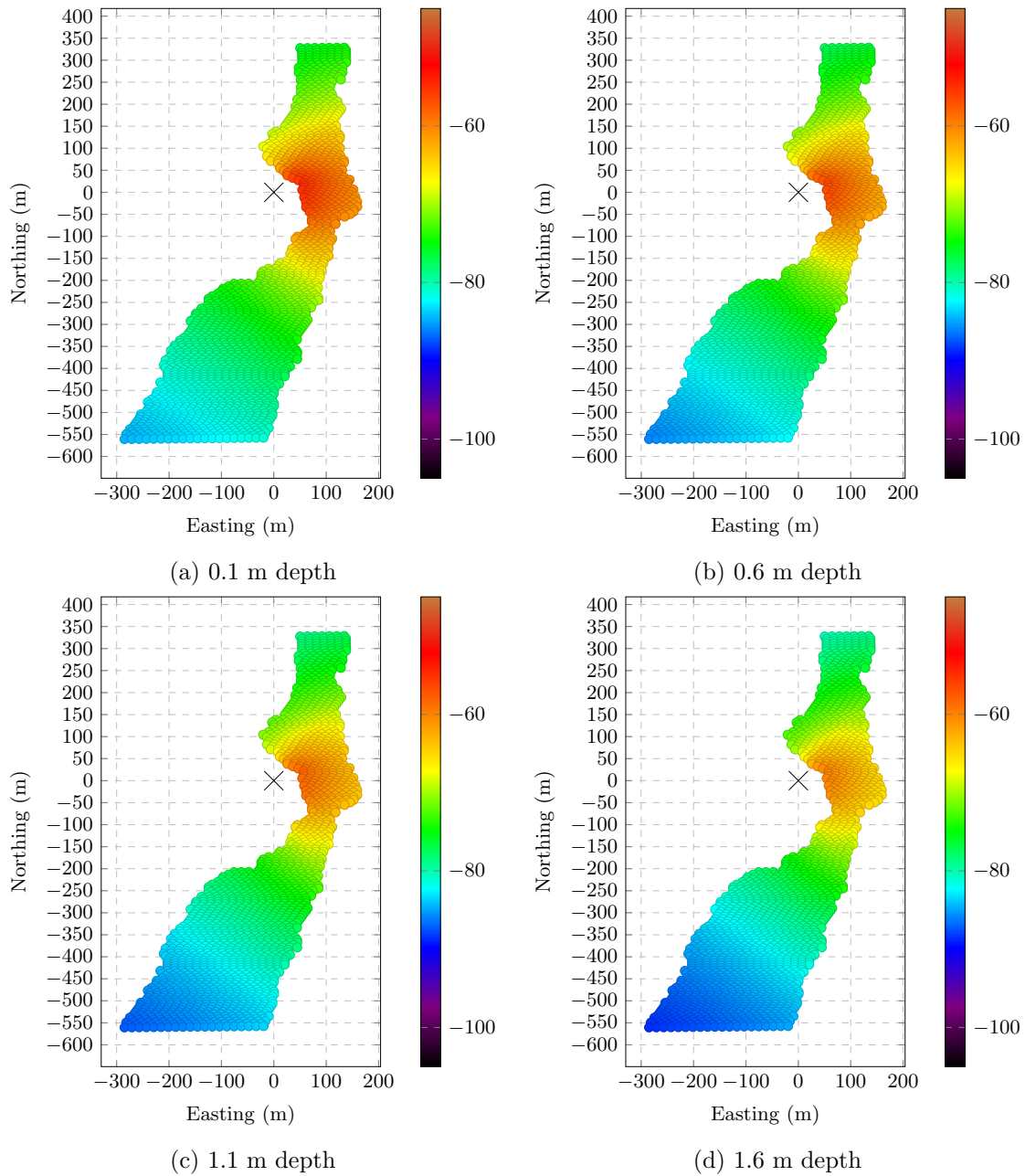


Figure A.11: Total system Loss  $0.5(TE+TM)$ - Jenny Downstream site (dB). The receiver is located at 10U 559221.7604 km E, 15674302.06 km N.

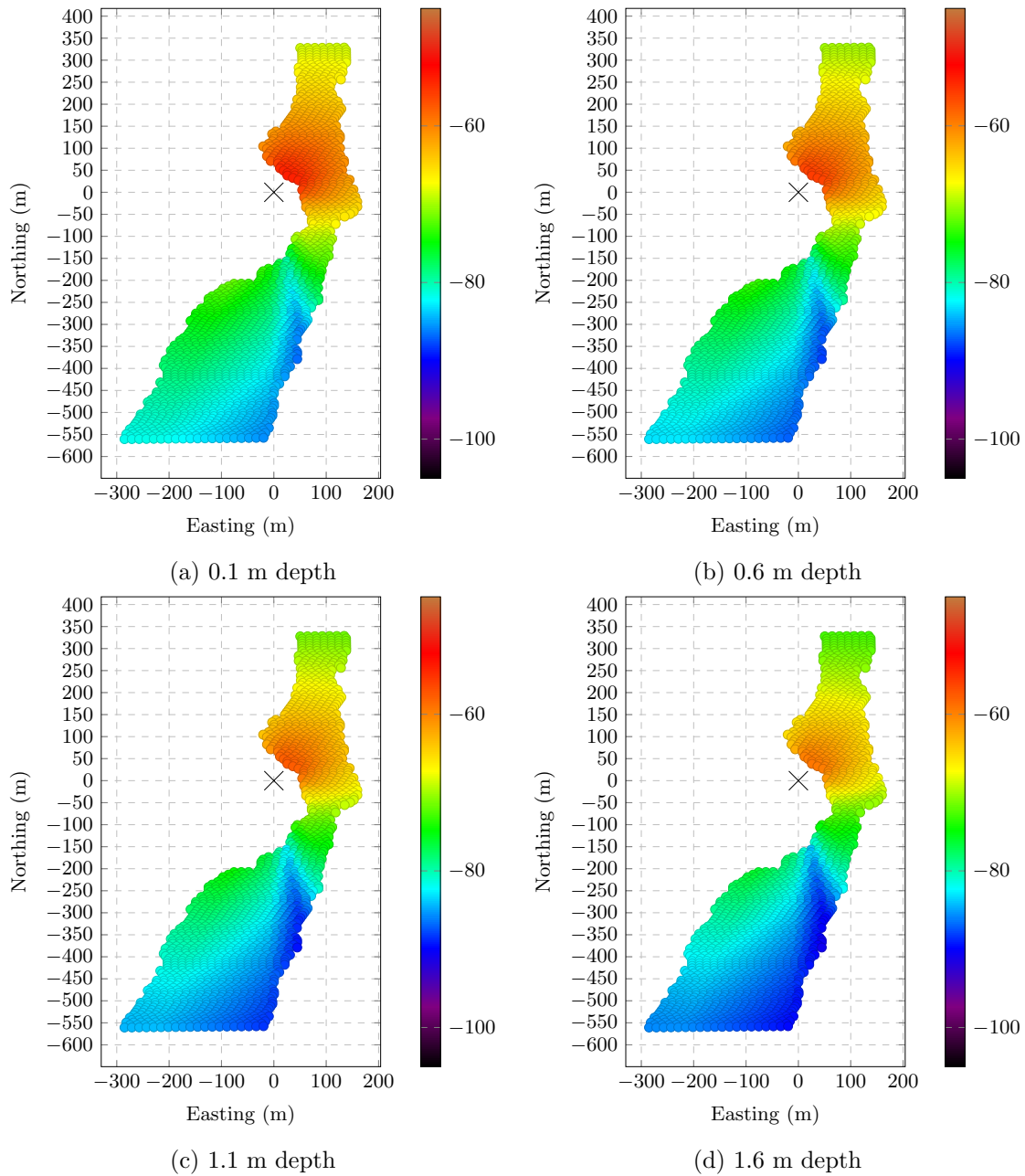


Figure A.12: Total system Loss  $0.5(\text{TE}+\text{TM})$ - Jenny Upstream site (dB). The receiver is located at 10U 559221.7604 km E, 15674302.06 km N.

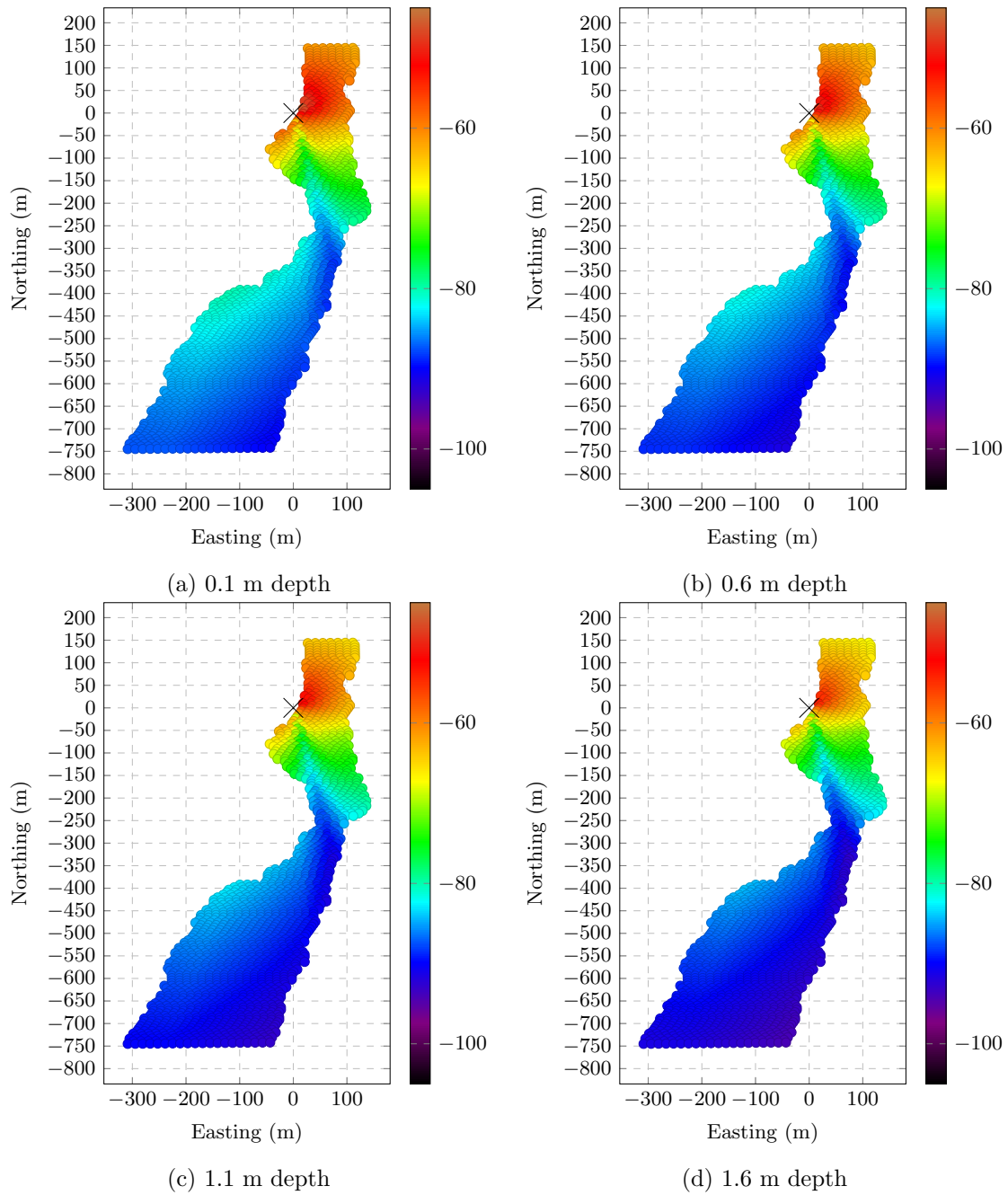


Figure A.13: Total system Loss  $0.5(Te+Tm)$ - Nose site (dB). The receiver is located at 10U 559245.1976 km E, 15674486.4 km N.

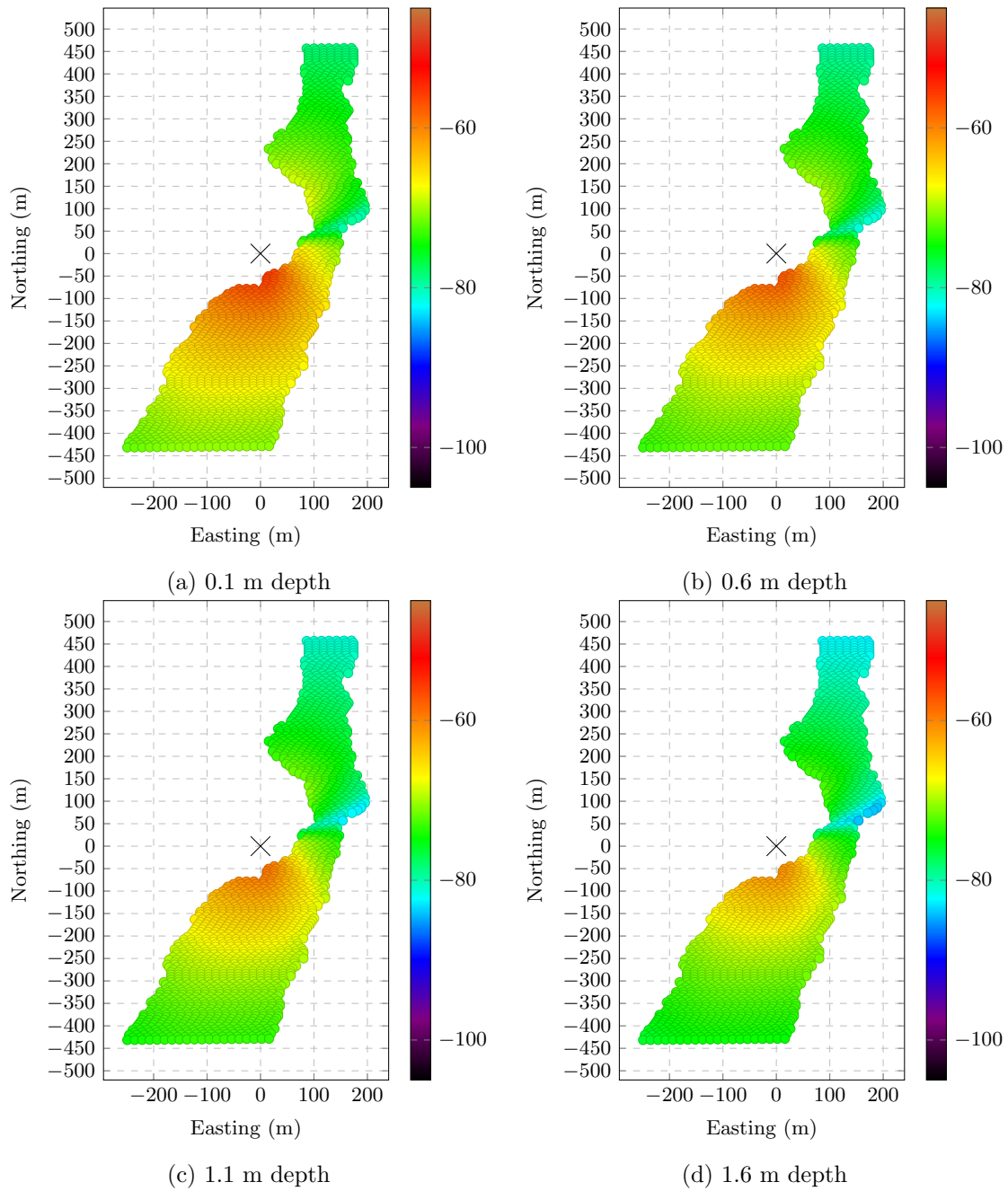


Figure A.14: Total system Loss  $0.5(TE+TM)$ - Razorback Downstream site (dB). The receiver is located at 10U 559185.8782 km E, 15674173.07 km N.

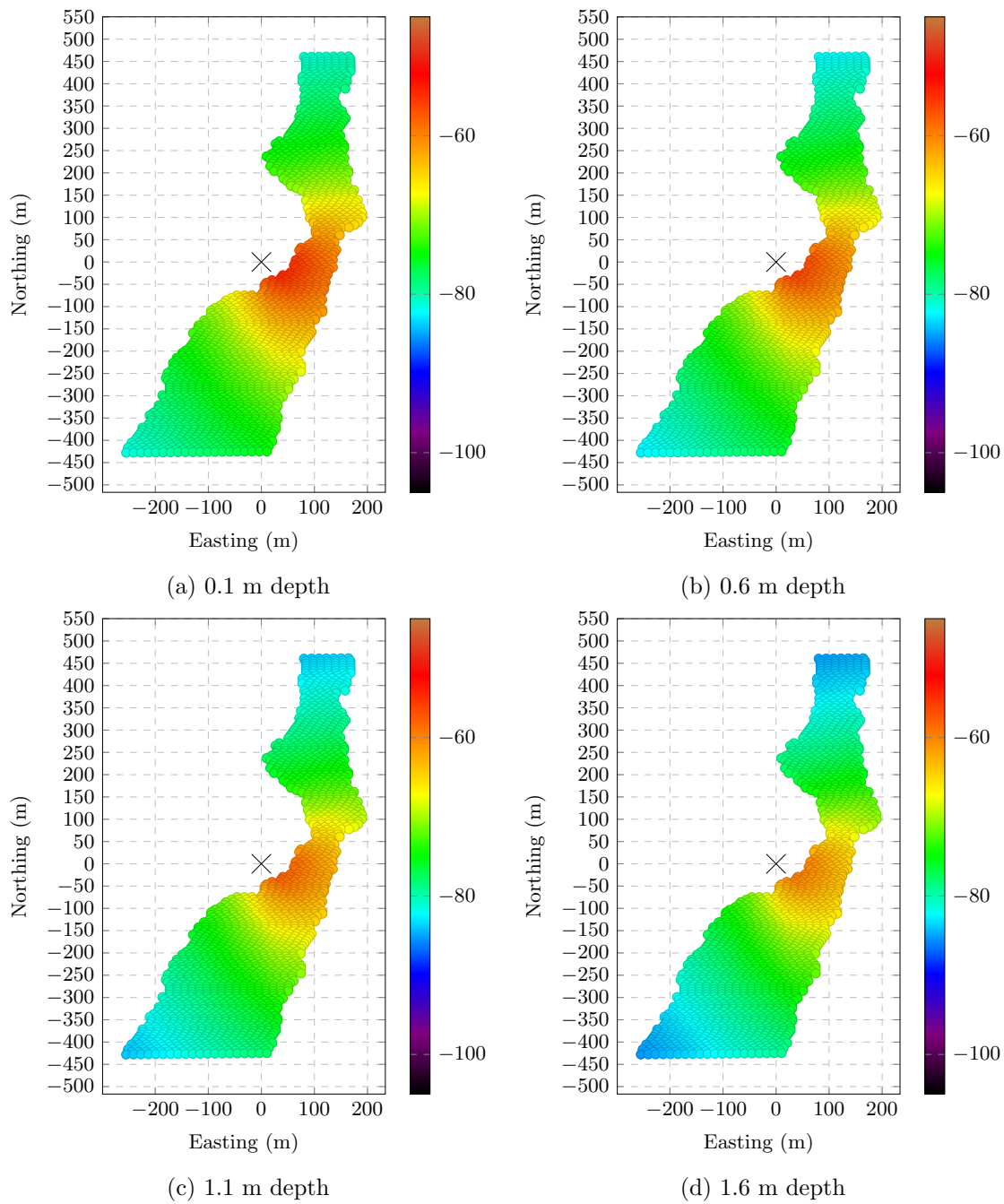


Figure A.15: Total system Loss  $0.5(TE+TM)$ - Razorback Upstream site (dB). The receiver is located at 10U 559191.6489 km E, 15674169.36 km N.

## A.2.2 TE Gain

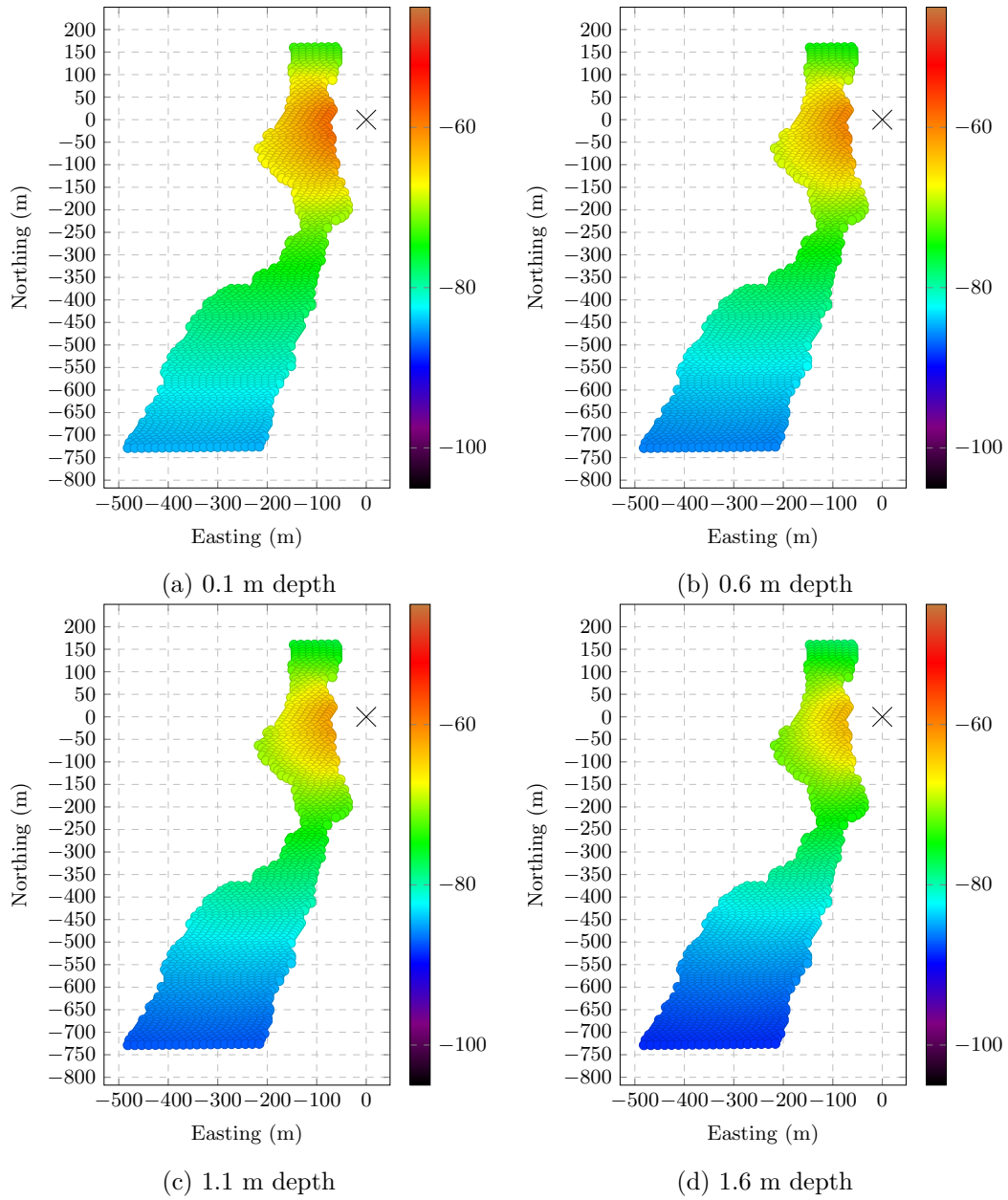


Figure A.16: Total system loss TE- Eastside Downstream site (dB).



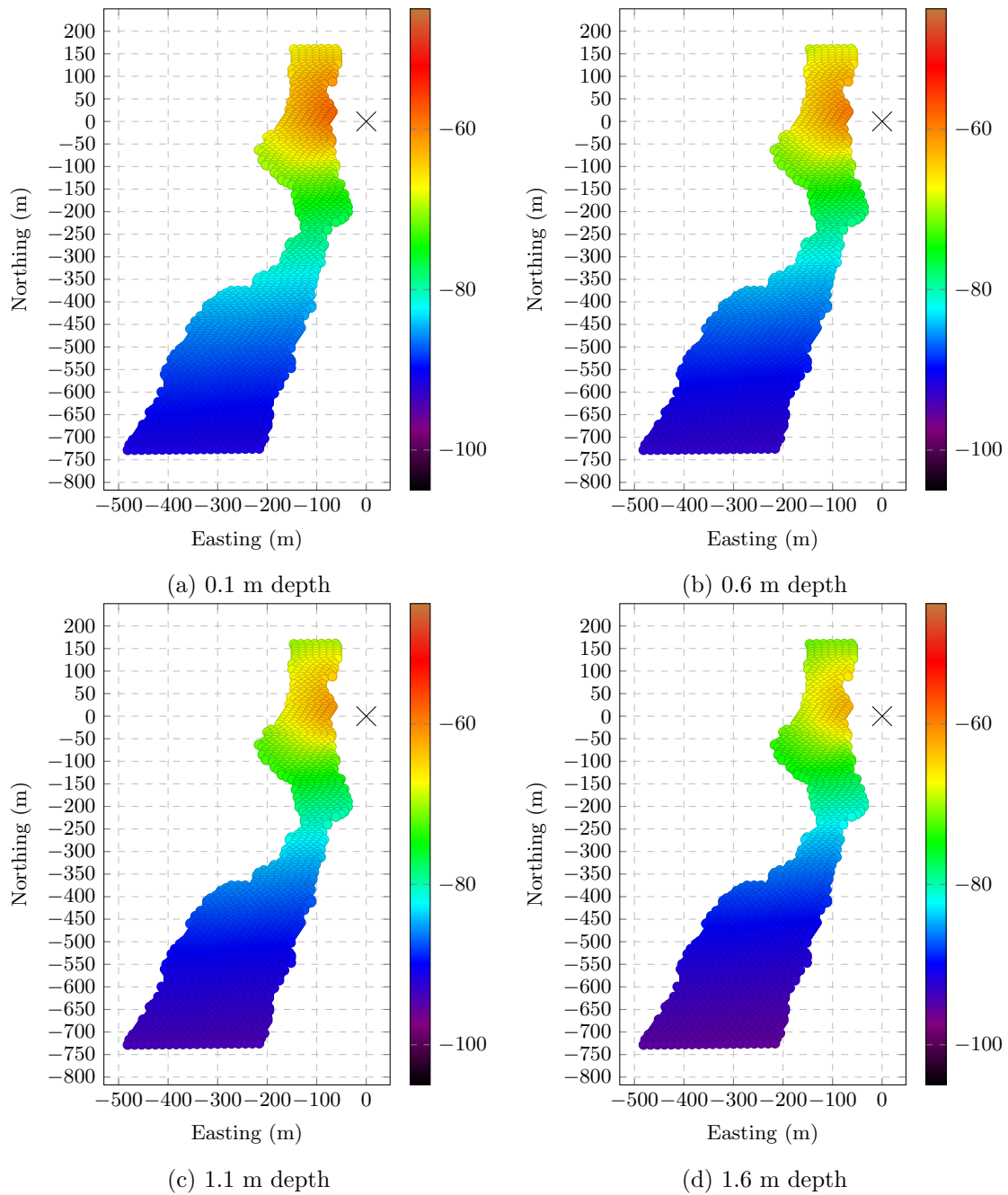


Figure A.17: Total system loss TE- Eastside Upstream site (dB).

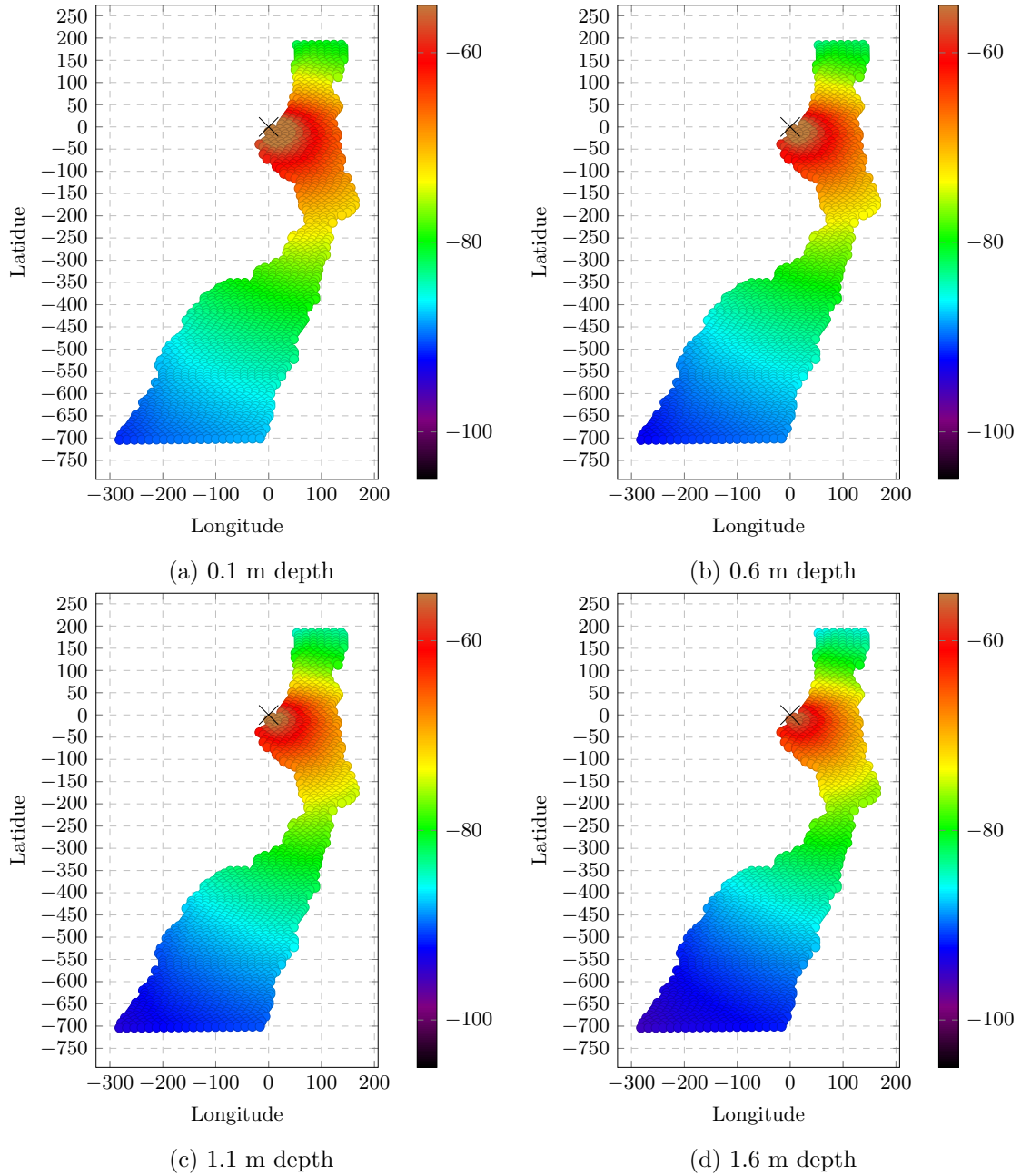


Figure A.18: Total system loss TE- Eddy Downstream site (dB).

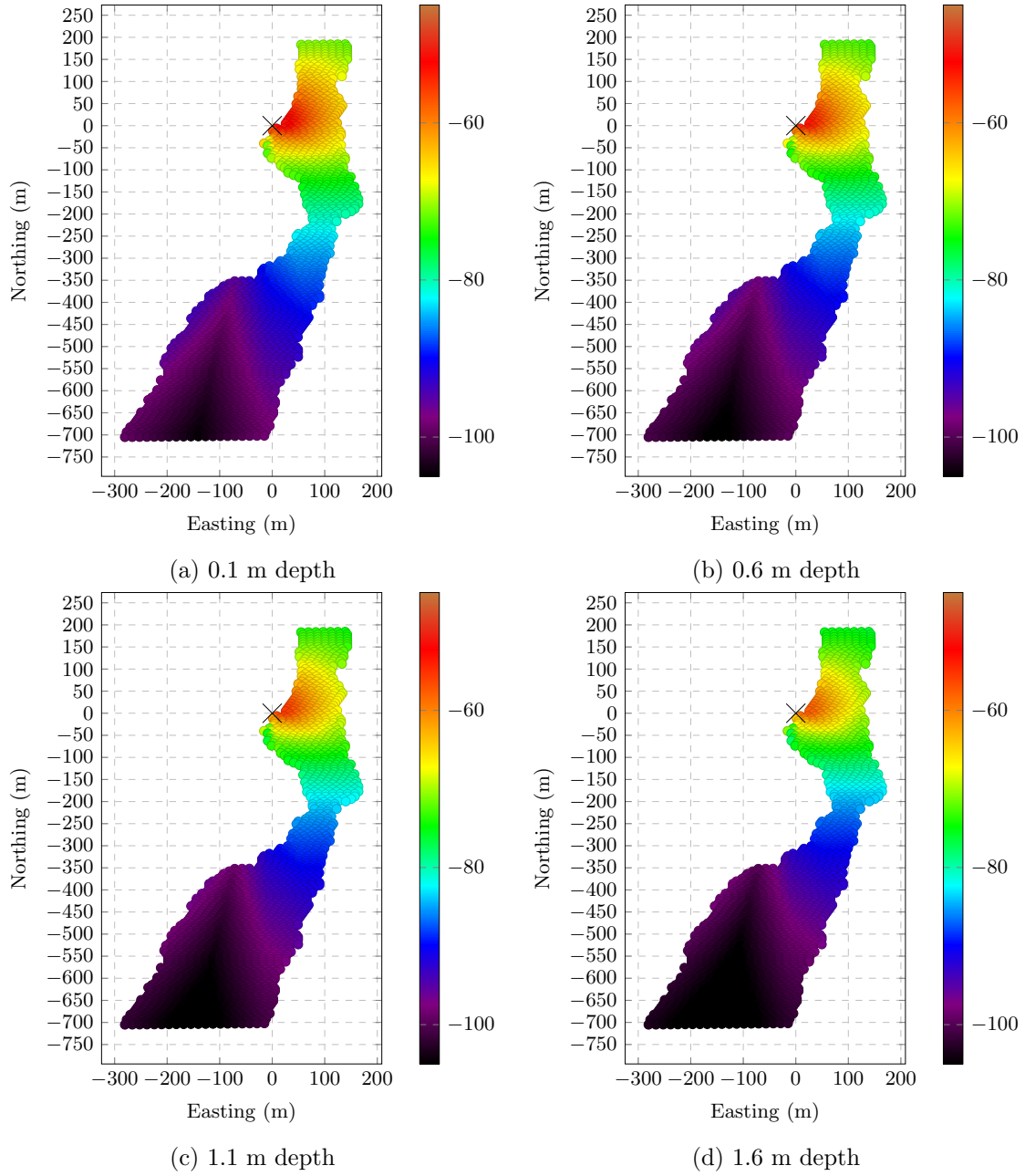


Figure A.19: Total system loss TE- Eddy Upstream site (dB).

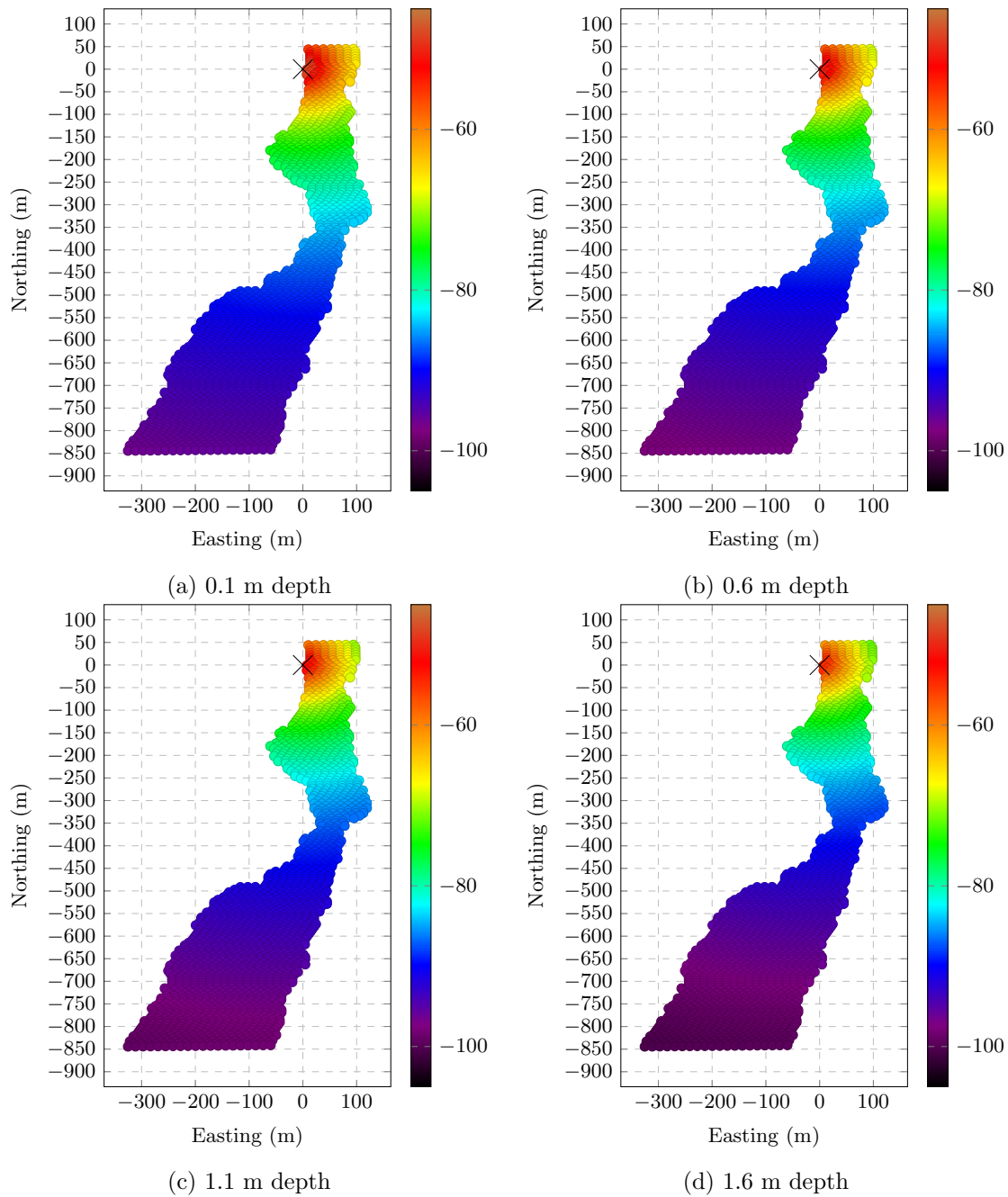


Figure A.20: Total system loss TE- iBeam p1 site (dB).

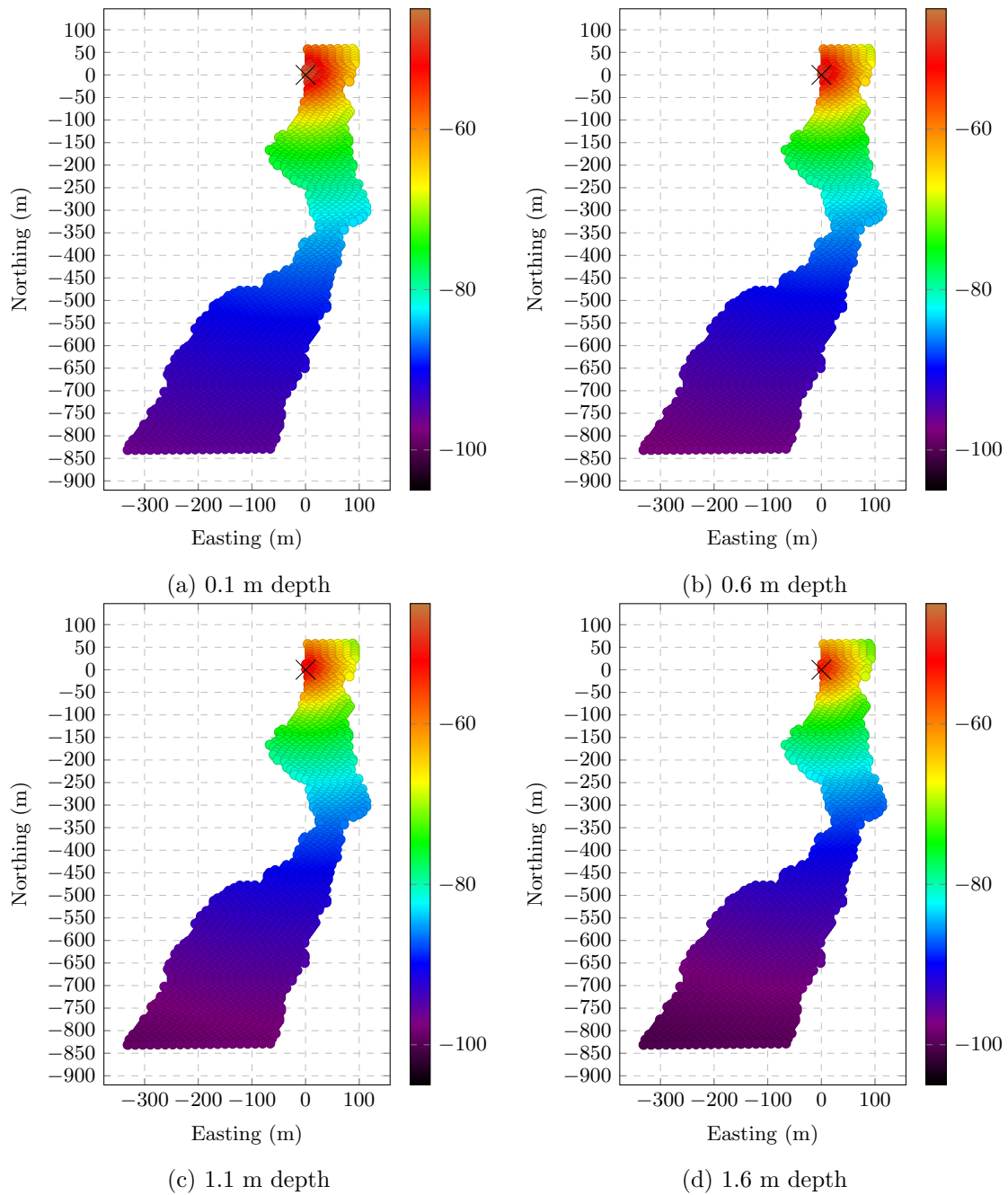


Figure A.21: Total system loss TE- iBeam p2 site (dB).

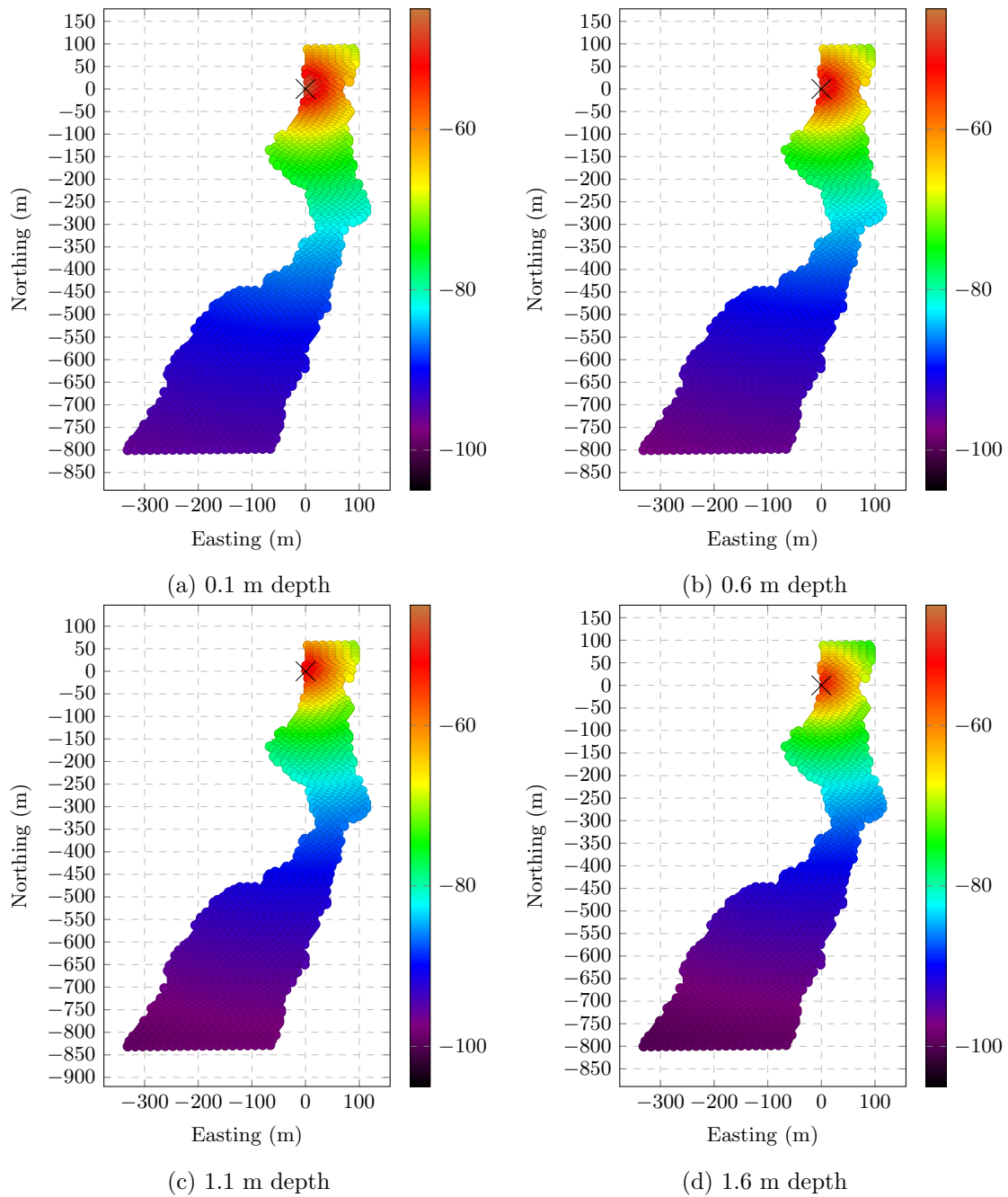


Figure A.22: Total system loss TE- iBeam p5 site (dB).

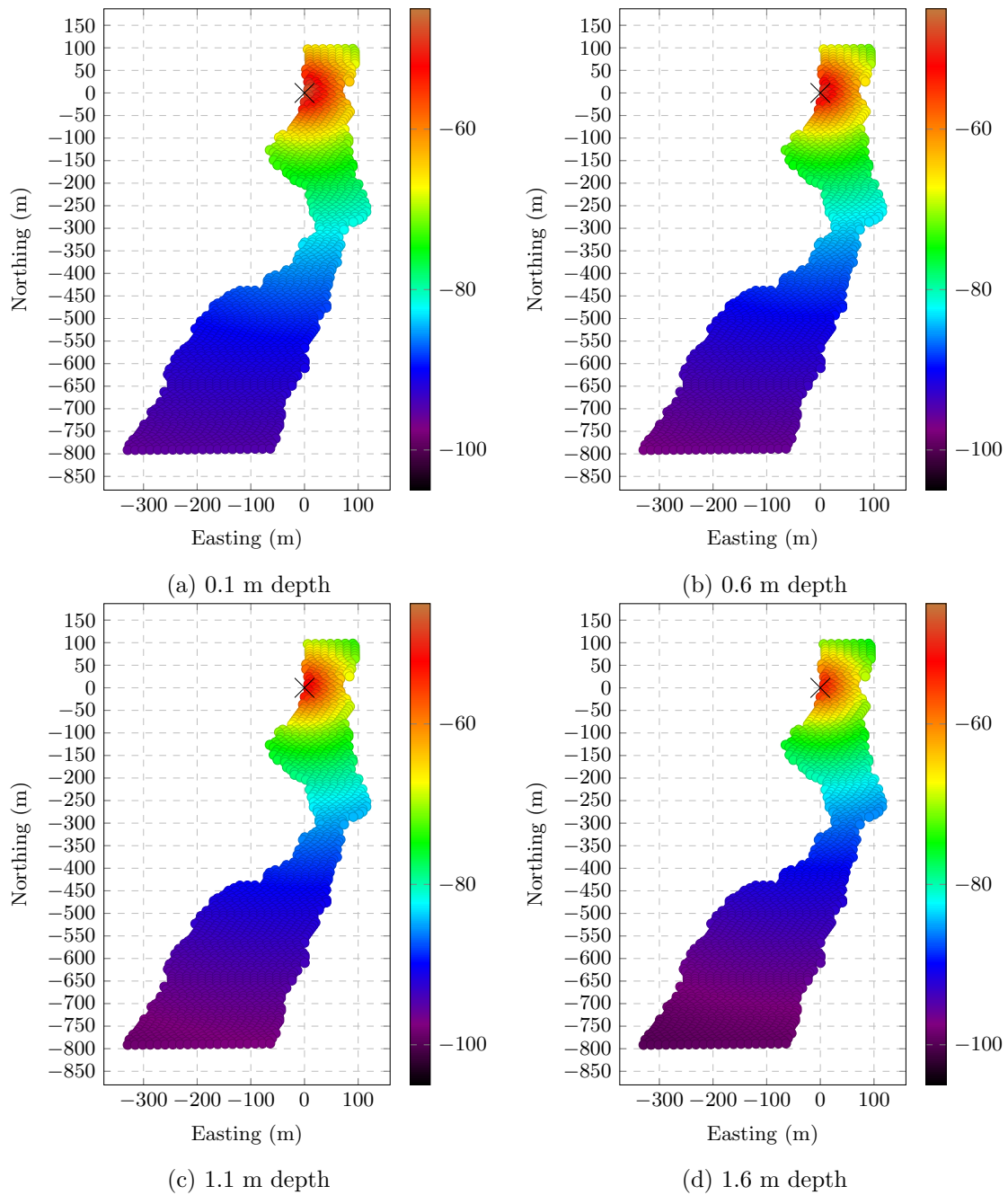


Figure A.23: Total system loss TE- iBeam p6 site (dB).

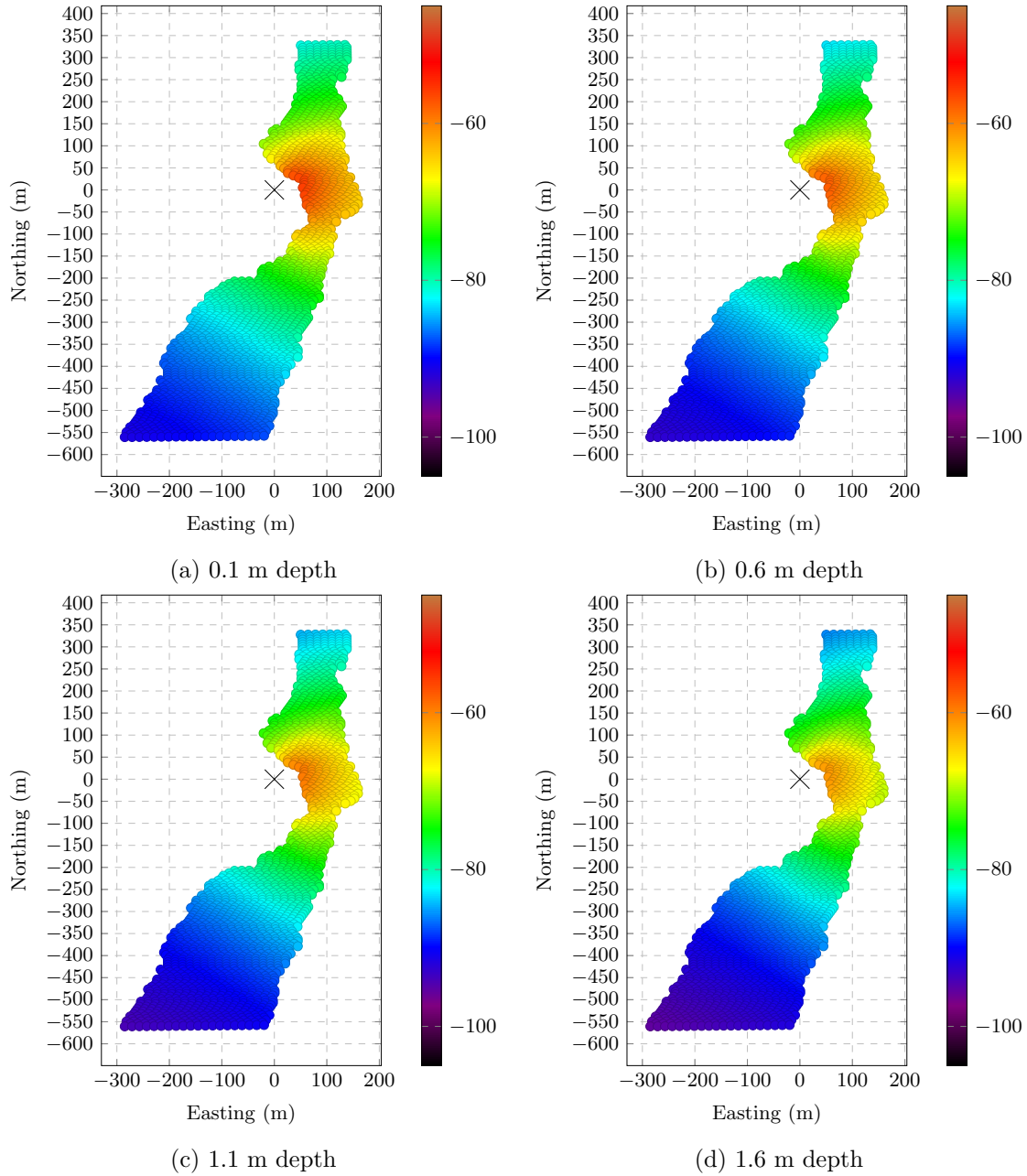


Figure A.24: Total system loss TE- Jenny Downstream site (dB).



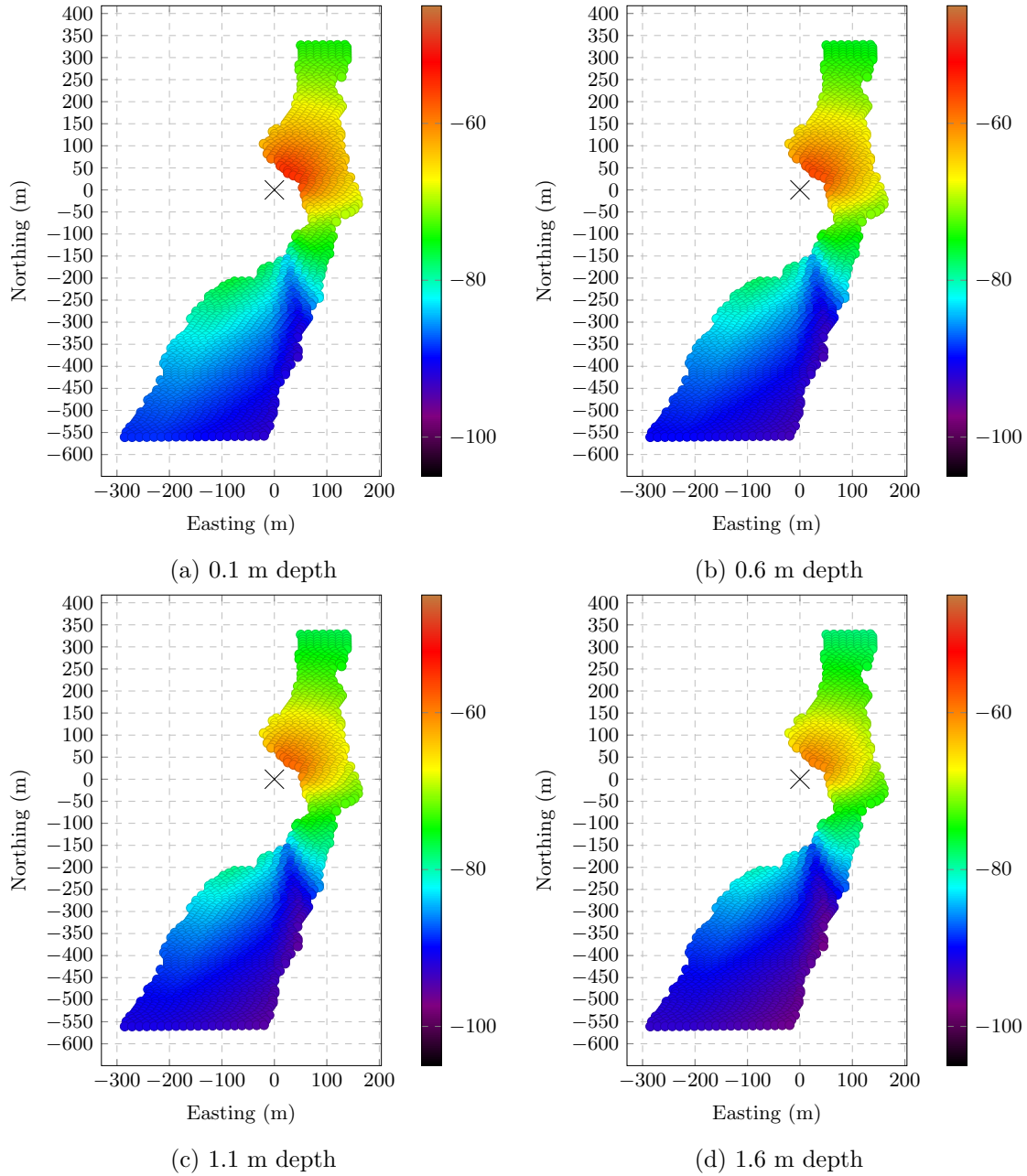


Figure A.25: Total system loss TE- Jenny Upstream site (dB).

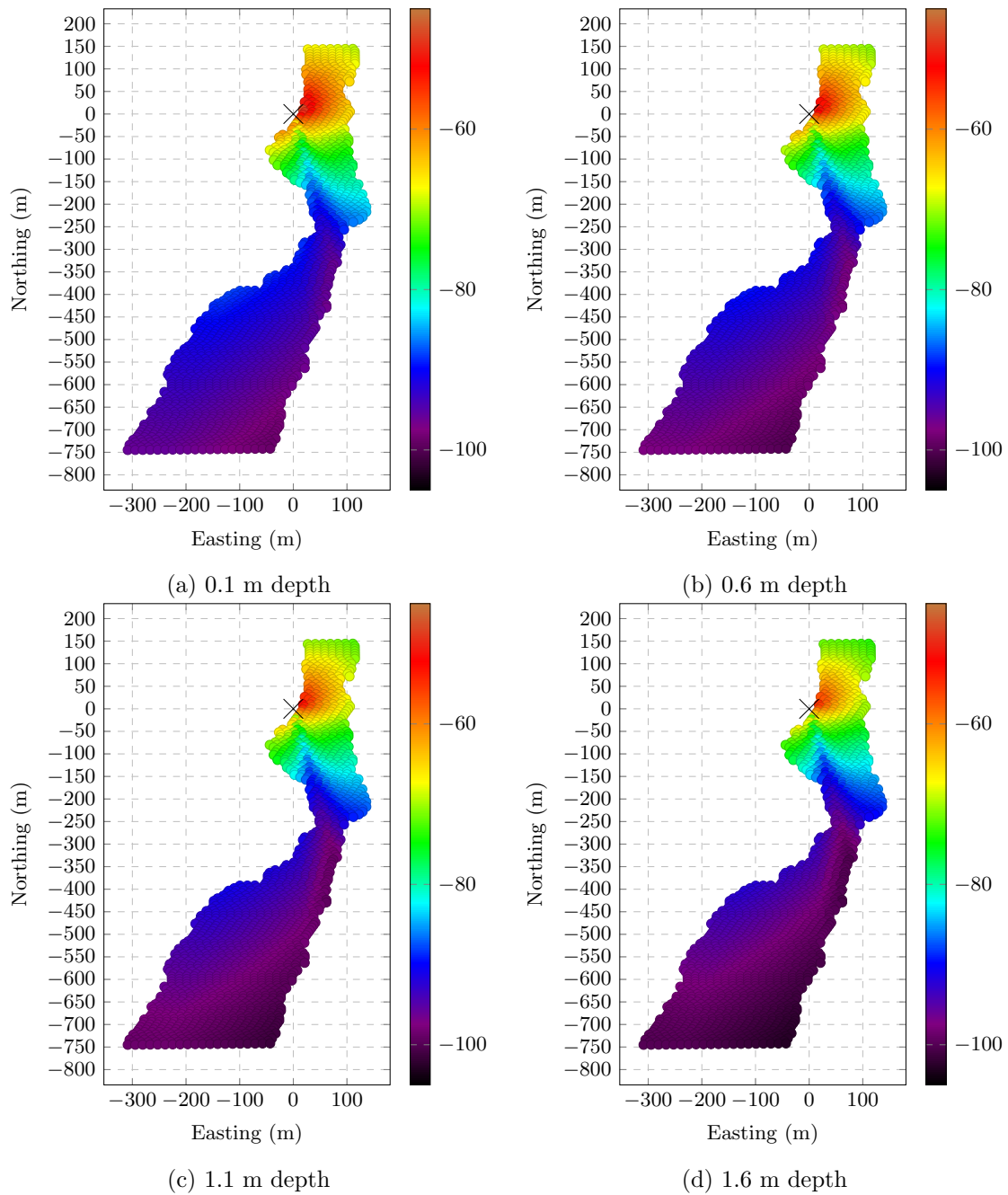


Figure A.26: Total system loss TE- Nose site (dB).

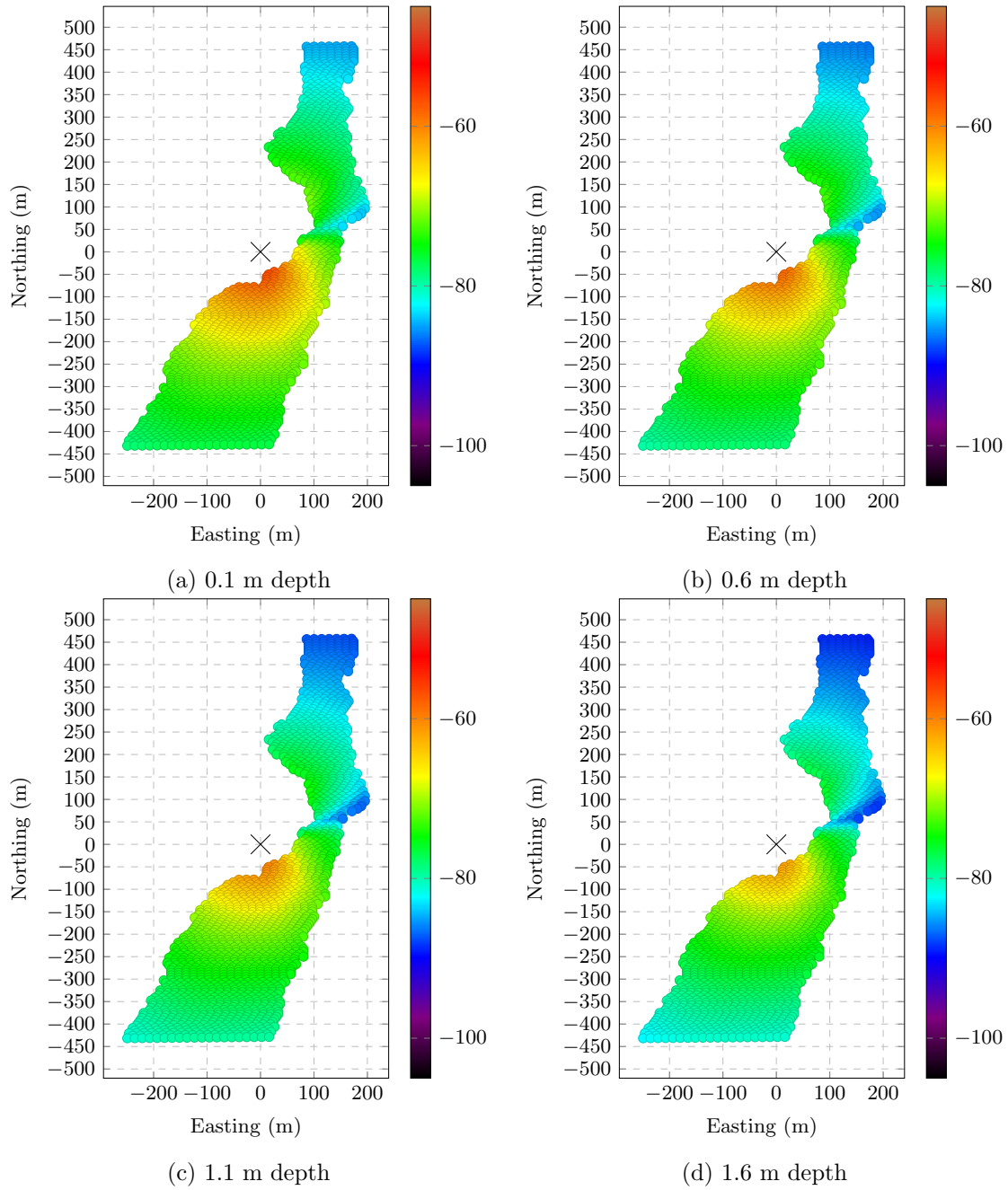


Figure A.27: Total system loss TE- Razorback Downstream site (dB).

### A.2.3 TM Gain

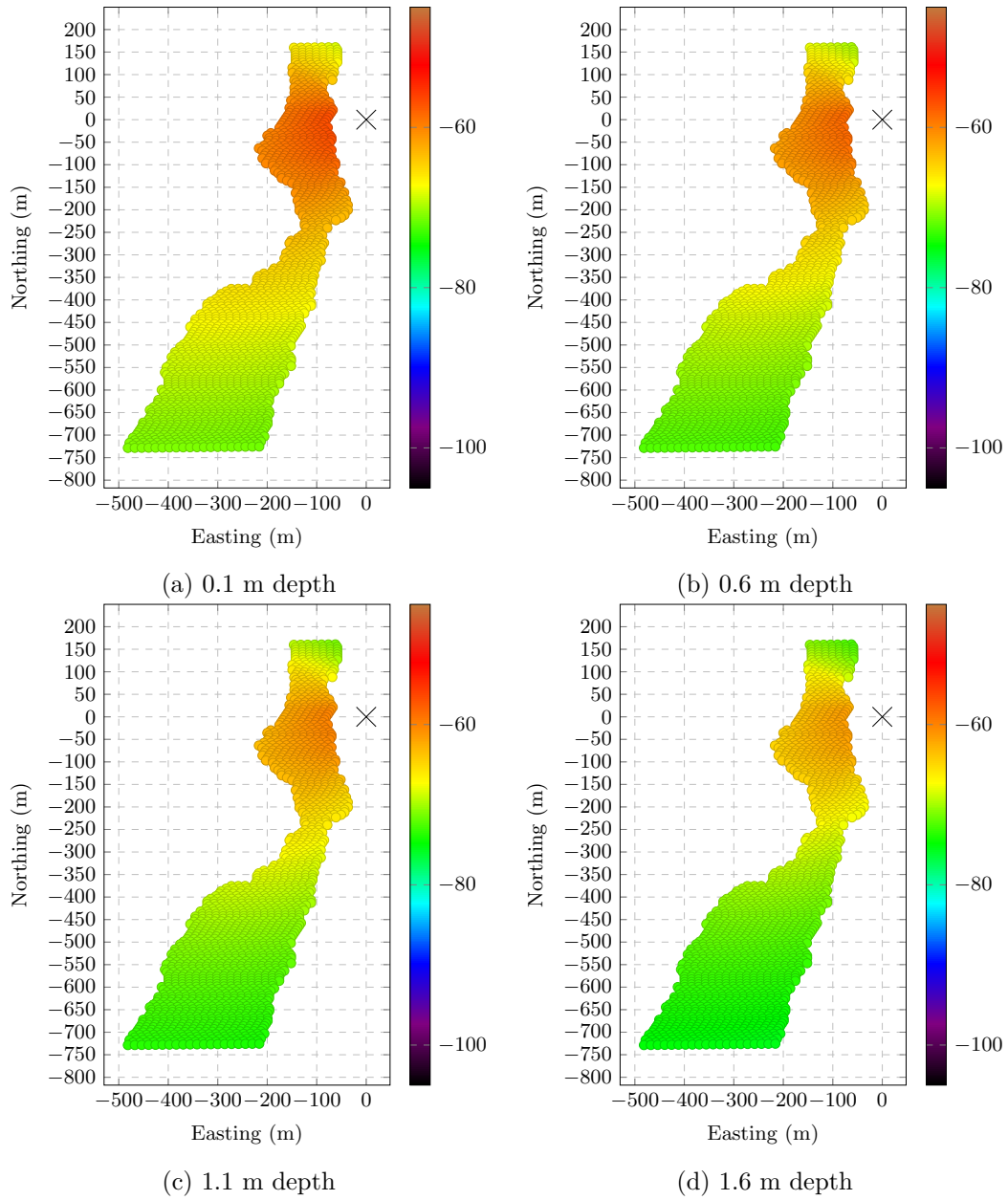


Figure A.28: Total system Loss TM- Eastside Downstream site (dB).

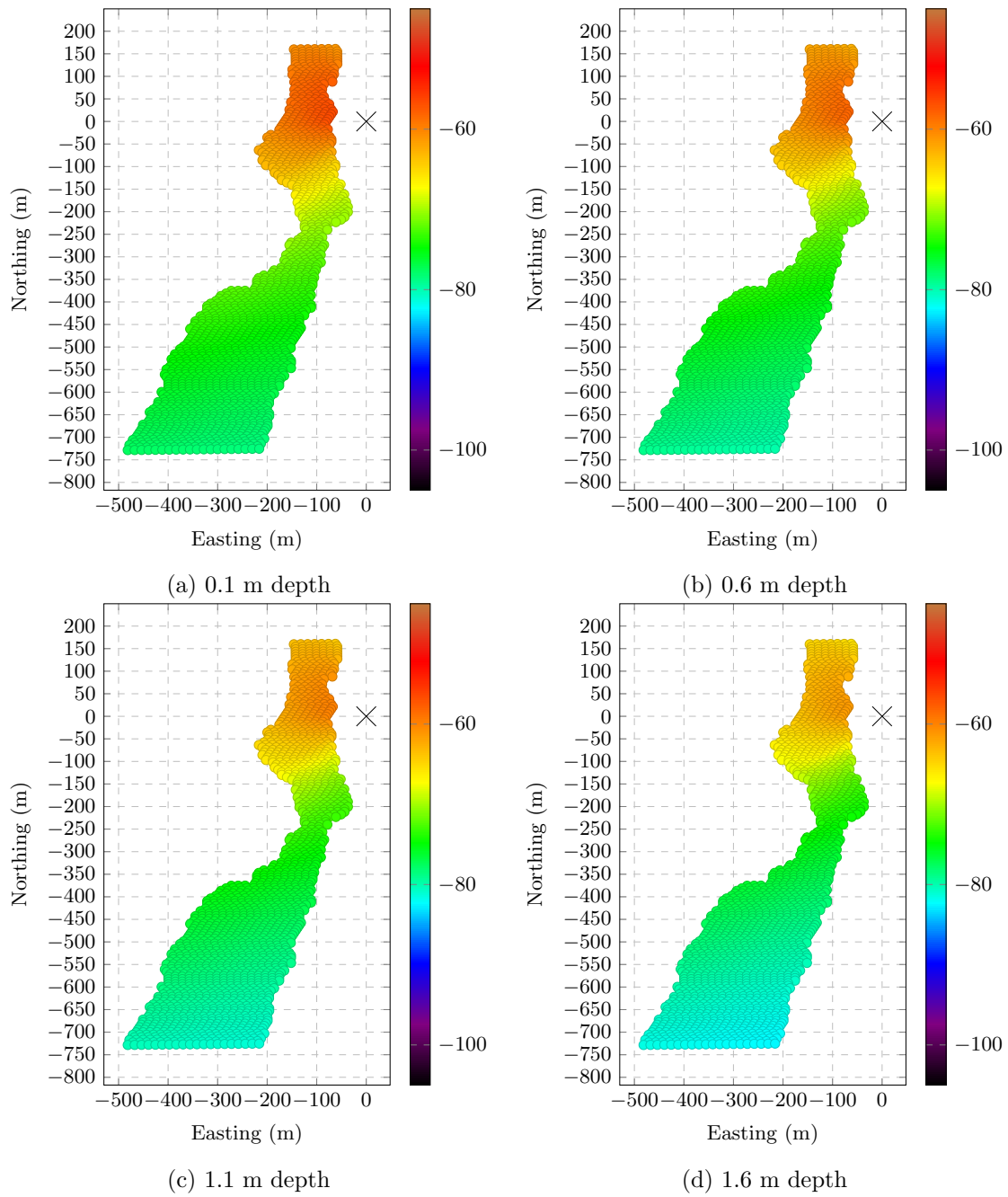


Figure A.29: Total system Loss TM- Eastside Upstream site (dB).

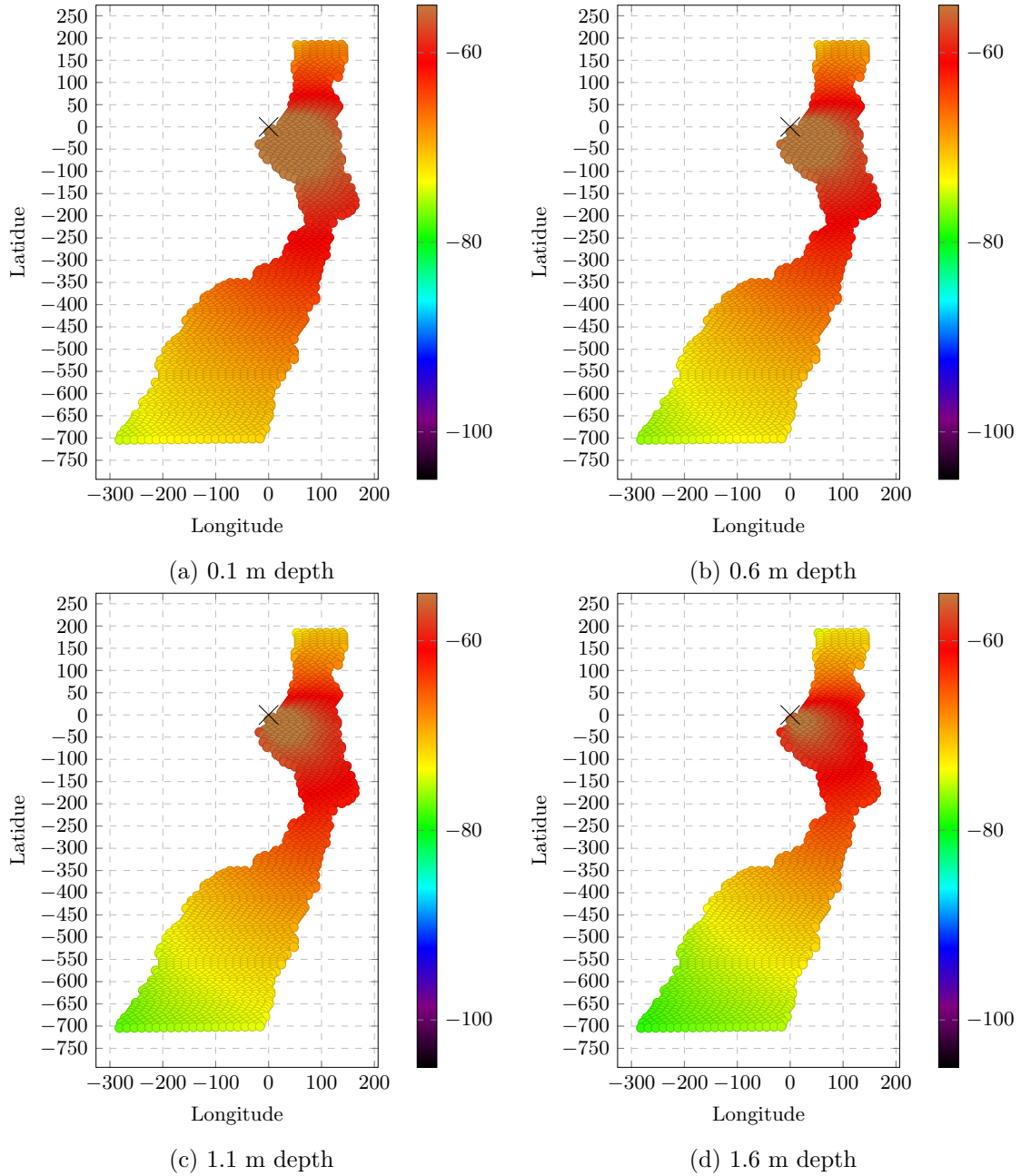


Figure A.30: Total system Loss TM- Eddy Downstream site (dB).

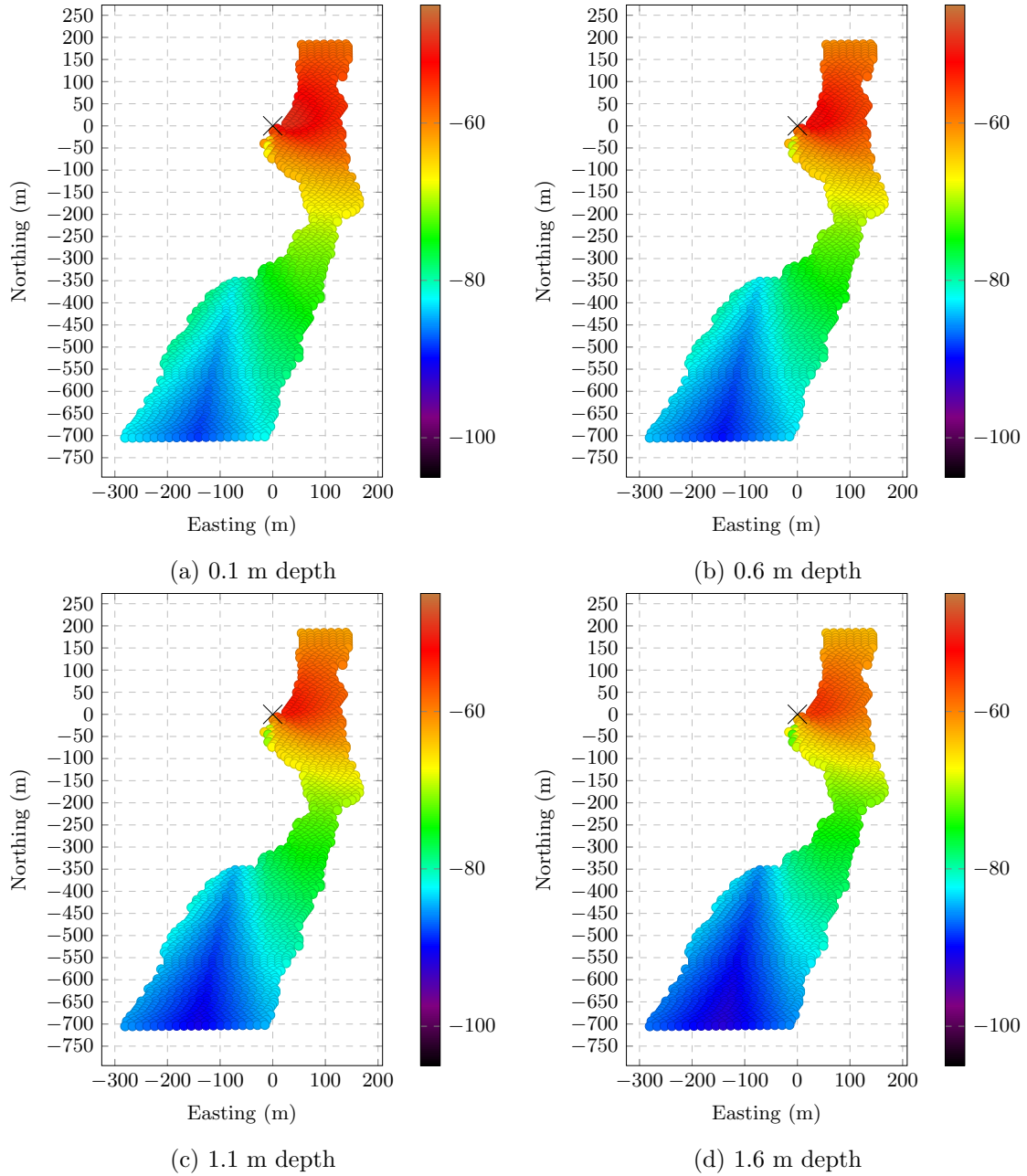


Figure A.31: Total system Loss TM- Eddy Upstream site (dB).

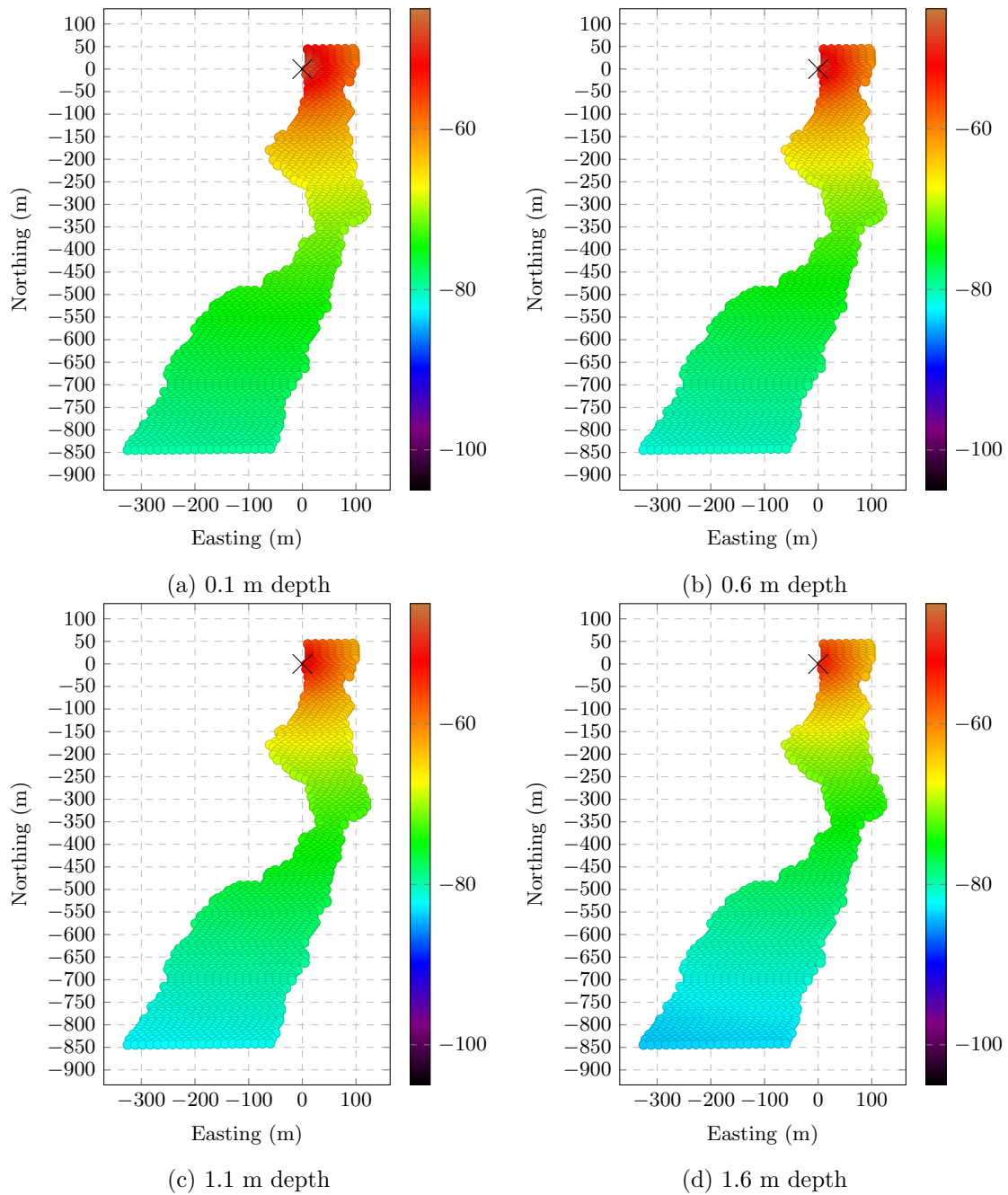


Figure A.32: Total system Loss TM- iBeam p1 site (dB).



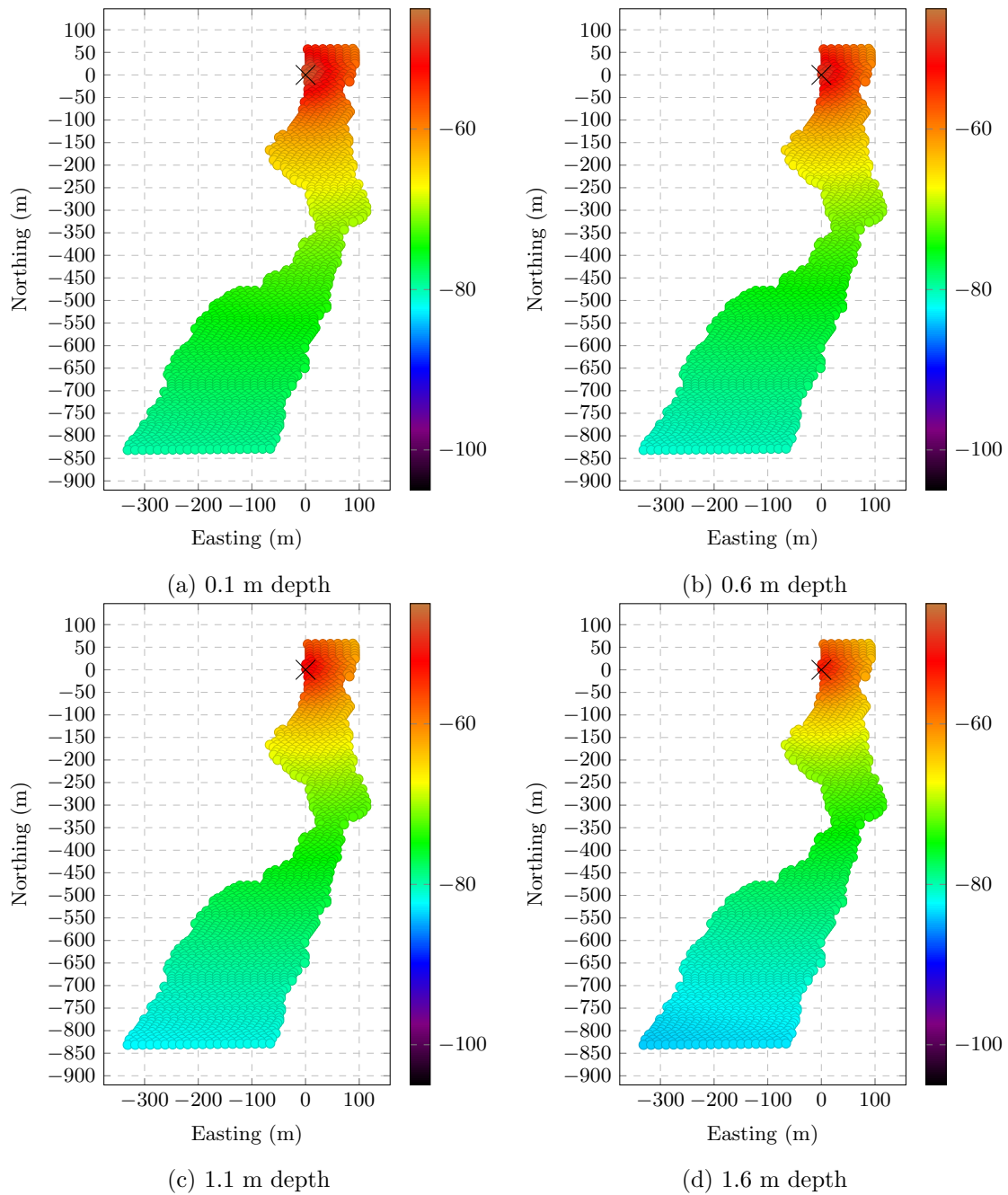


Figure A.33: Total system Loss TM- iBeam p2 site (dB).

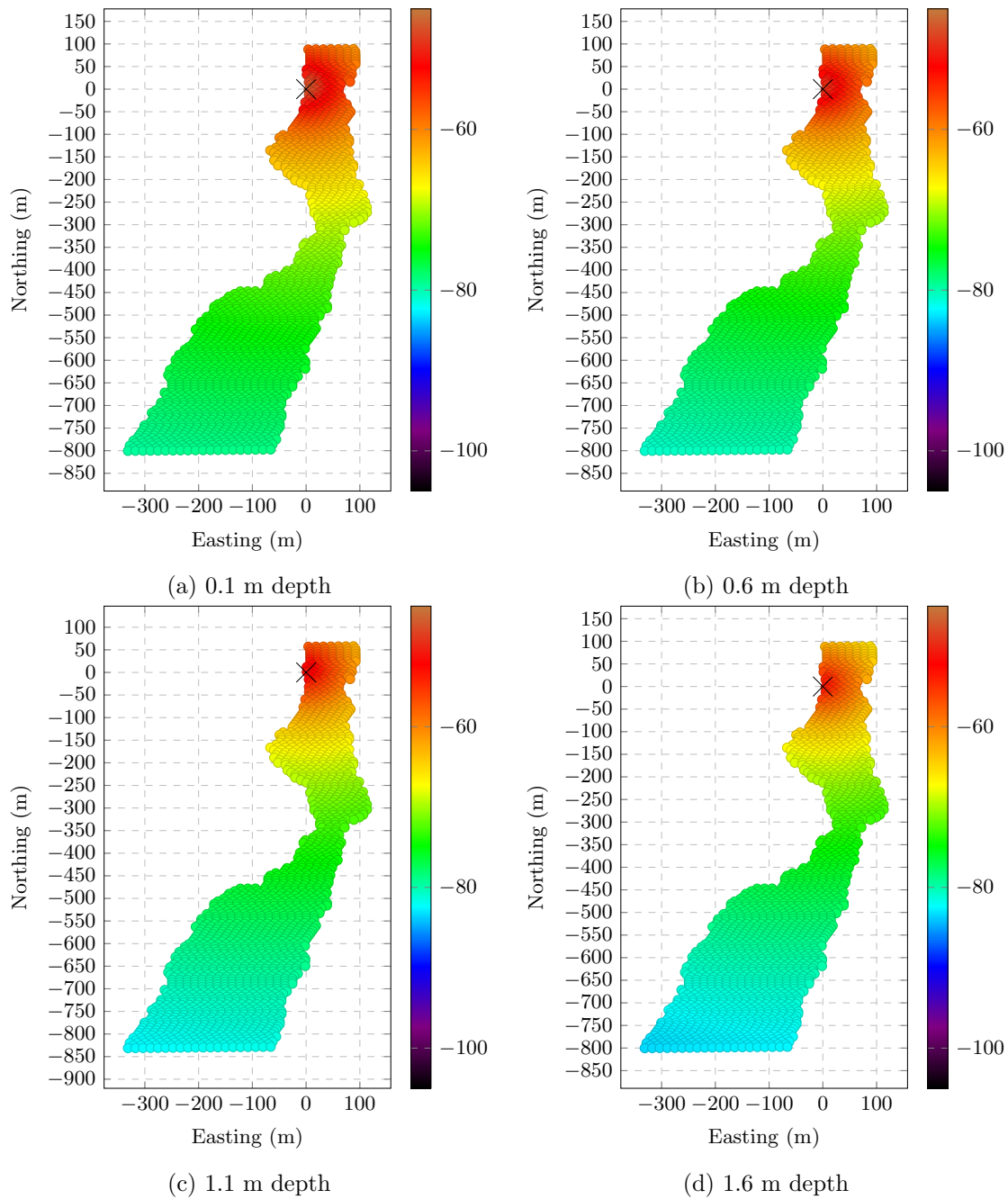


Figure A.34: Total system Loss TM- iBeam p5 site (dB).

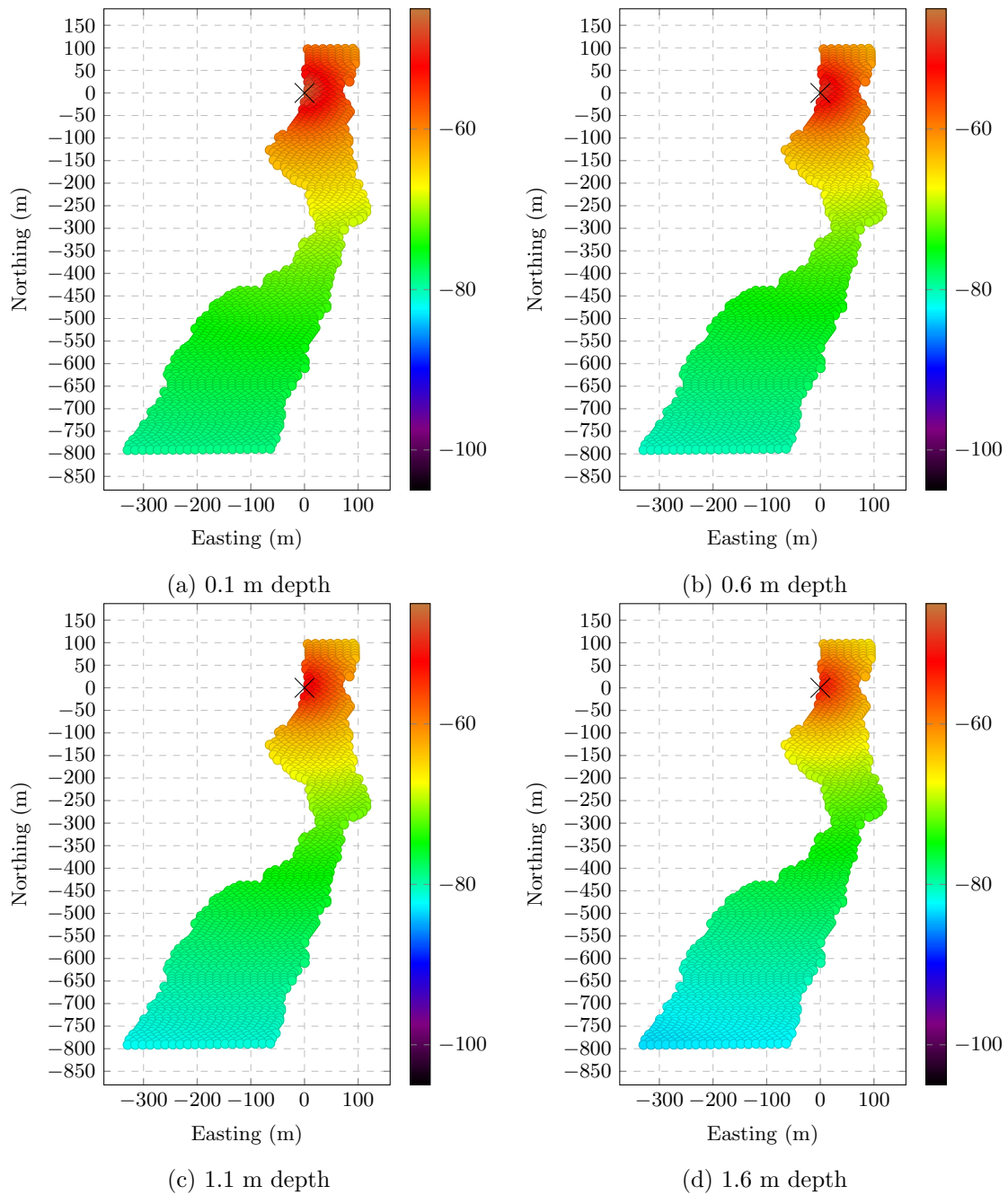


Figure A.35: Total system Loss TM- iBeam p6 site (dB).

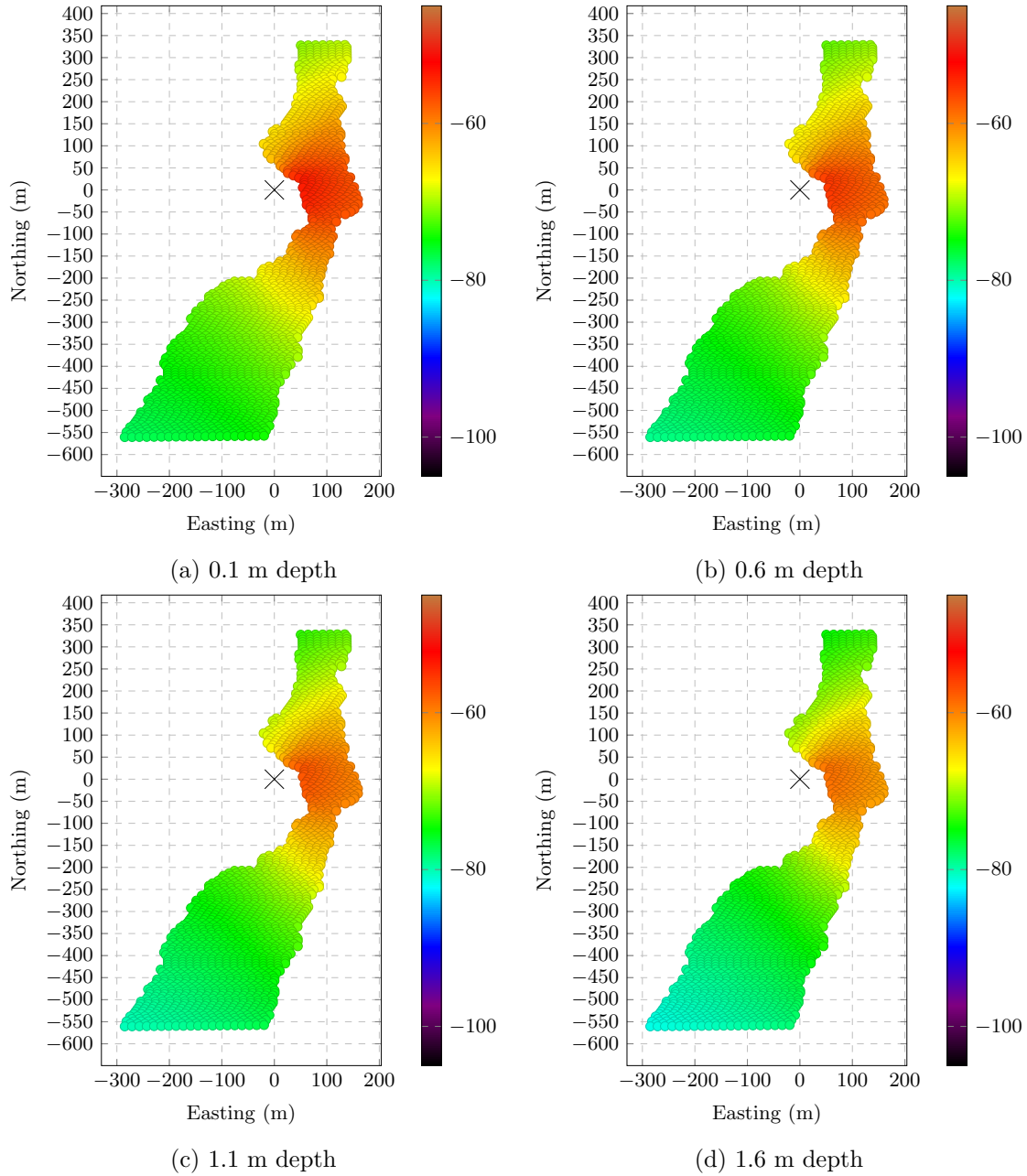


Figure A.36: Total system Loss TM- Jenny Downstream site (dB).

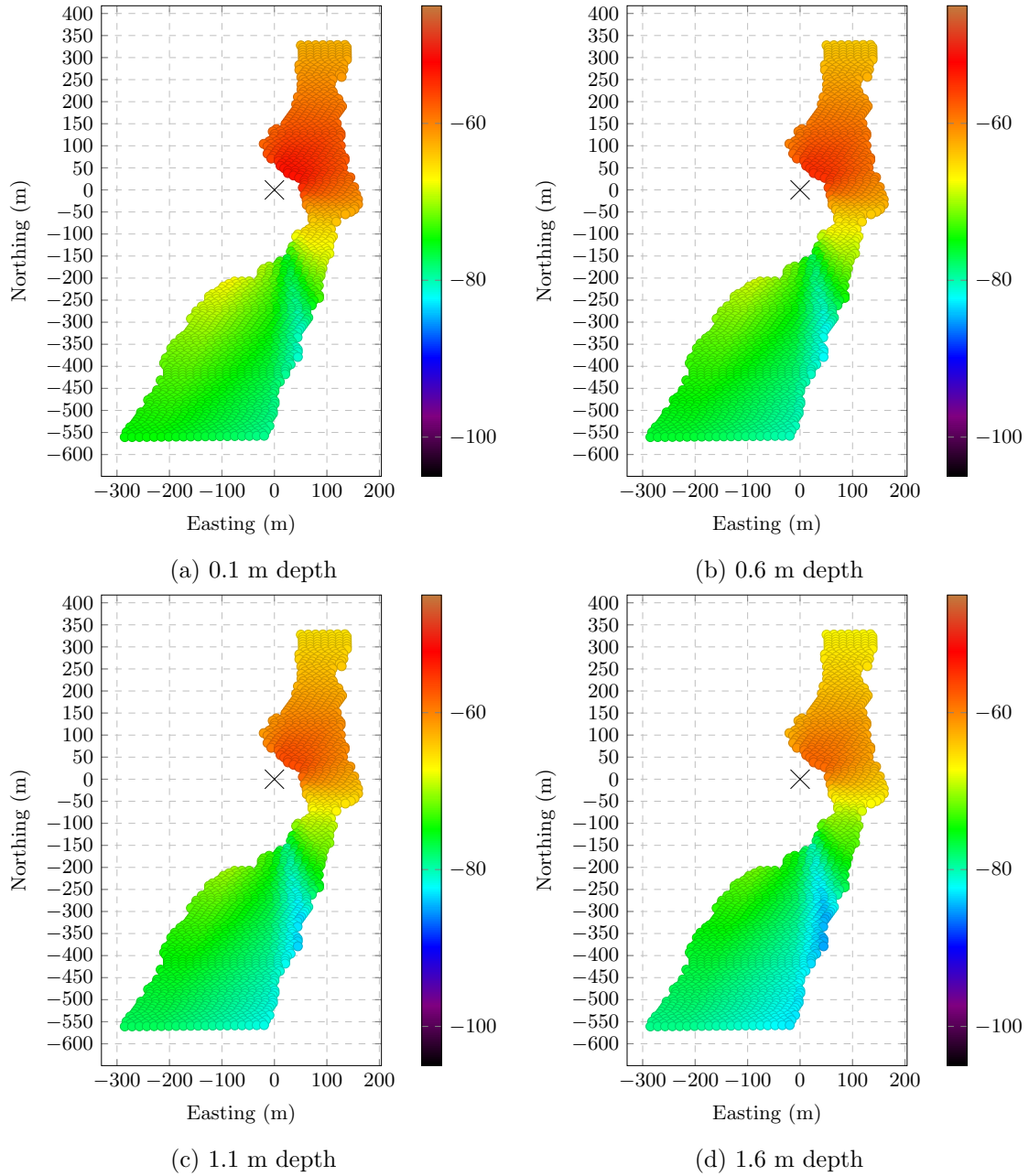


Figure A.37: Total system Loss TM- Jenny Upstream site (dB).

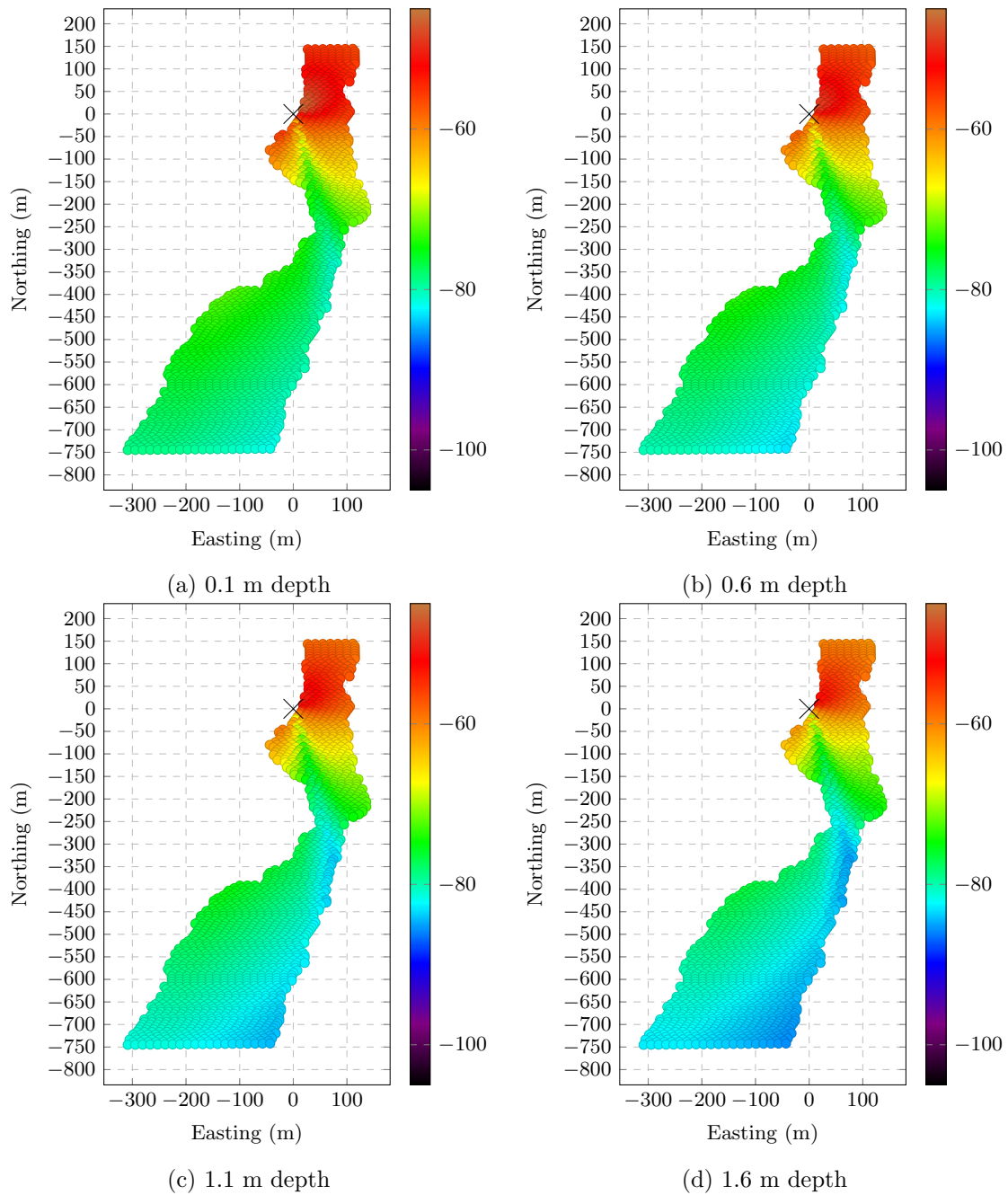


Figure A.38: Total system Loss TM- Nose site (dB).

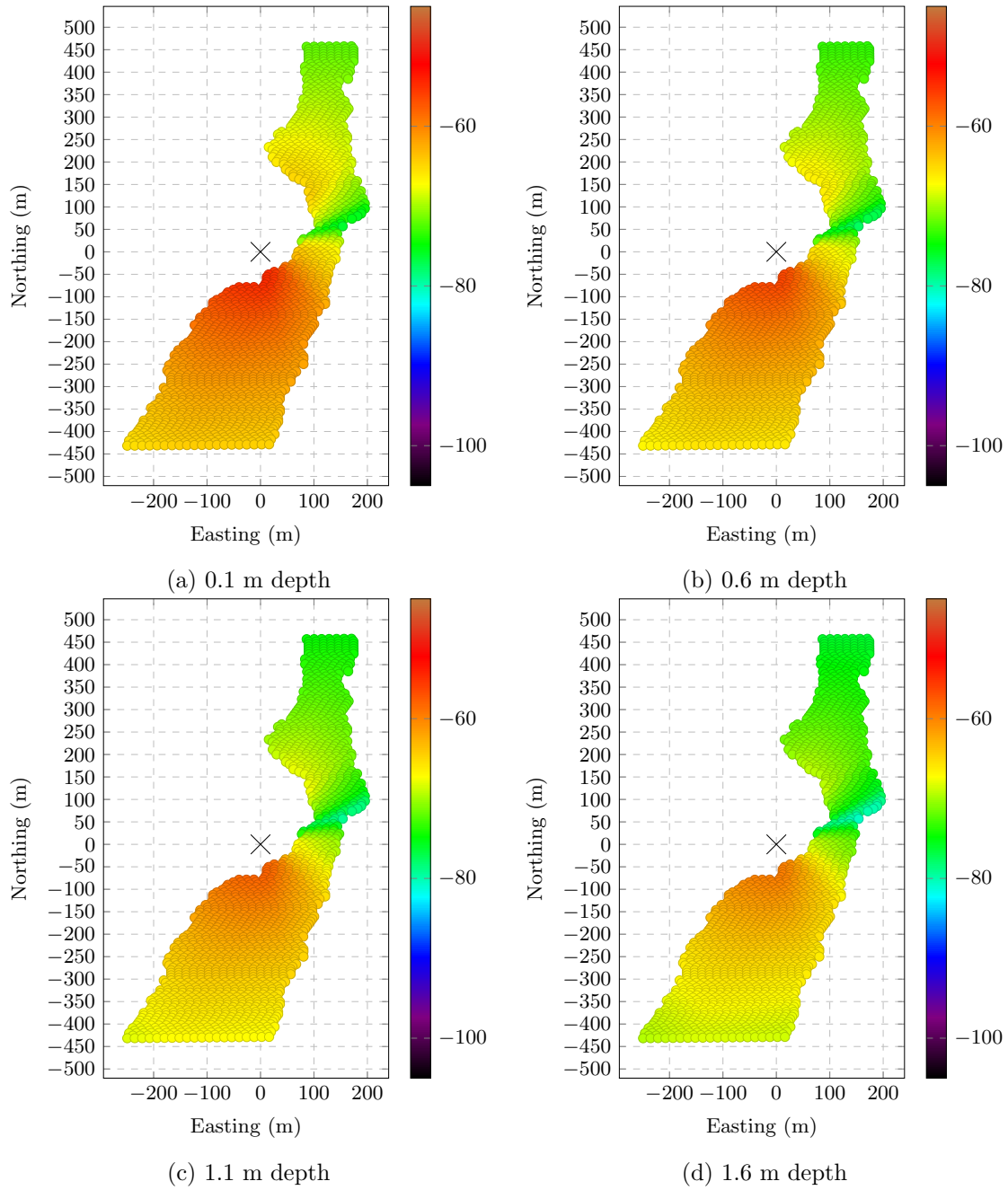


Figure A.39: Total system Loss TM- Razorback Downstream site (dB).

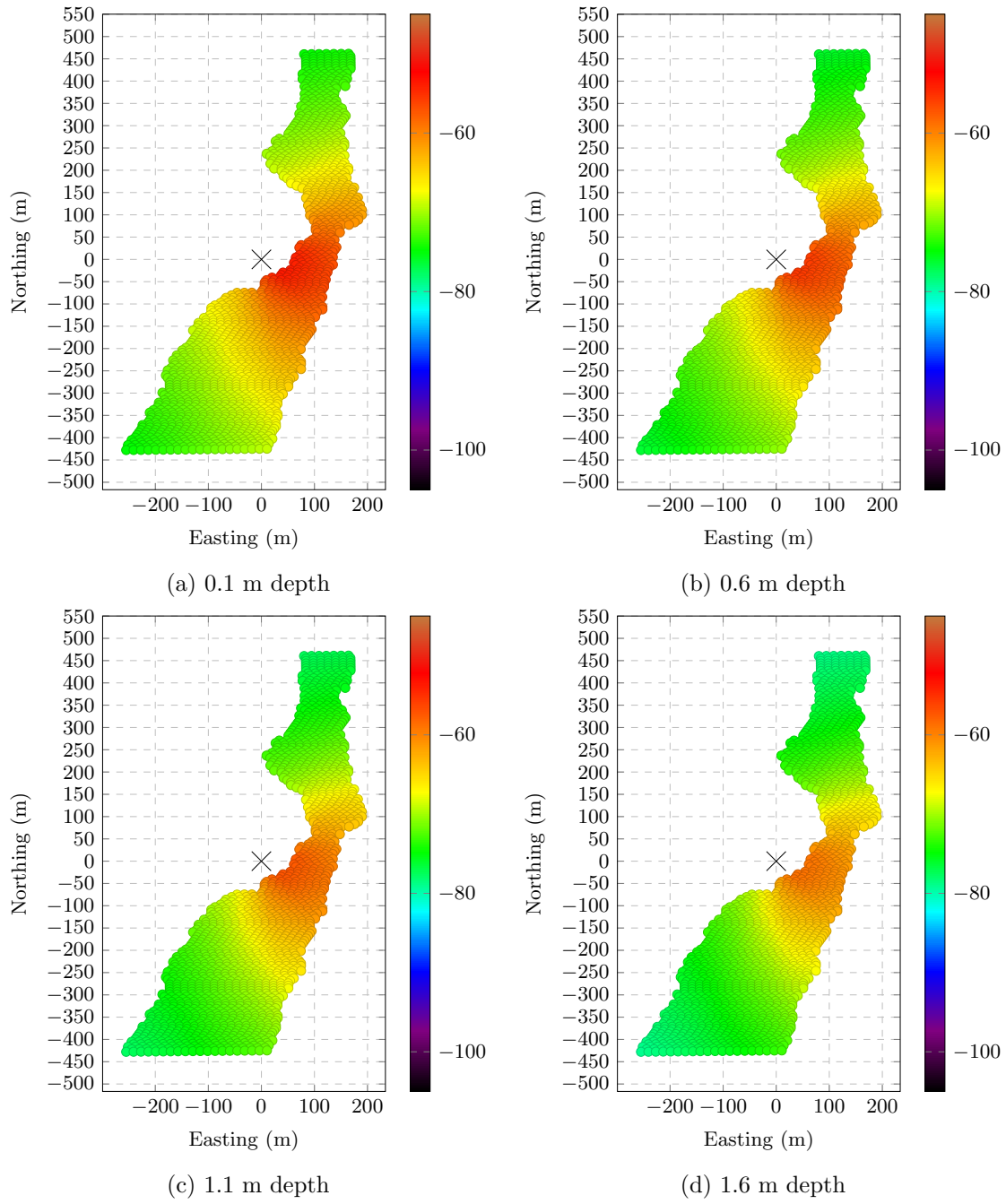


Figure A.40: Total system Loss TM- Razorback Upstream site (dB).



# Appendix B

## Code

### B.1 Fish Propagation

#### B.1.1 Fish Propagation Model

```
1 %Author: Elias Bircher
2 %Last Edited 10/18/23
3
4 %Provides colour coded map of the data
5
6 %Treats each latitude and longitude point separately and does the
7 %calculations like that. THis is the most up to date file for the
  full
8 %river. It includes a path loss calculation that encompasses both
  air time
9 %as well as river time. It also has functions.
10 clear
11 close all
12 clc
13
14 %% Writing Constants
15 ep0 = 8.854e-12;
16 mu0 = 4*pi*1e-7;
17 sigma = 0.014; %S/m
18 f = 1.5e8;
19 w = 2*pi*f;
20
21 ep1 = ep0;
22 ep2 = 81*ep0 - 1i*sigma/w;
23 k1 = w*sqrt(mu0*ep1);
24 k2 = w*sqrt(mu0*ep2);
25
26 c=2.99792458e8;
27
28 lambda1 = c./f;
29 vwater = 1/(sqrt(81*ep0*mu0));
```

```

30 lambda2 = vwater./f;
31
32 EO = 100; %Arbitrary - Makes no difference what value it is
33
34 TGain = -4; %Transmitter gain for unbalanced dipole (in dB)
35 etaPol = -3; %Polarisation Mismatch (in dB)
36
37 NumWaterPoints = 4; %Describe how many depths you want a slice of
38 NumAirPoints = 1; %Only calculates one value in air
39
40 %% If you want to do one file: Multifile = 0
41 Multifile = 1;
42
43 %% File Management
44
45 % File Management should follow the following order:
46 % Base Directory: ~/Documents/University/Thesis/FishPropagation/
47 % Input CSV:
48 % ~/Documents/University/Thesis/FishPropagation/AntennaLocations/
49 % Format of Input File: antenna_data_NameOfLocation.csv
50 % Output an empty directory has to be created: ModelLocations/
51 % Pattern of receiving antenna needs to be in FishPropagation/ with
    the
52 % name AntennaPattern.csv
53 cd ~/Documents/University/Thesis/FishPropagation/
54 files = dir('AntennaLocations/*.csv');
55
56 file = strings(size(files));
57 fileRead = strings(size(files));
58 fileWrite = strings(size(files));
59 fileWrite2 = strings(size(files));
60
61 AntennaLocations = "AntennaLocations/";
62 ModelLocations = "ModelLocations/";
63
64 for i=1:length(files)
65     file = convertCharsToStrings(files(i).name);
66     fileRead(i) = AntennaLocations+file;
67     fileWrite(i) = ModelLocations+strrep(file,'data','model');
68     fileWrite2(i) = ModelLocations+strrep(file,'data','model2');
69 end
70
71
72 if Multifile == 1
73     disp("Locked and Loaded")
74 elseif Multifile == 0
75     fileRead = fileRead(10);
76     fileWrite = fileWrite(10);
77 end
78
79
80 numFiles = 1;
81 %% Main loop that does all of the files at once

```

```

82 for file = 1:length(fileRead)
83
84 Site1 = readmatrix(fileRead(file));
85 TextSite1 =
      readtable(fileRead(file),"VariableNamingRule","preserve");
86
87 %Antenna Radiation Profile
88 AntennaGainFile = 'AntennaPattern.csv';
89
90
91 %% Initialize Empty Arrays
92 x = [];
93 y=[];
94
95 ywater = zeros(NumWaterPoints,1);
96 xwater = zeros(NumWaterPoints,1);
97 zwater = zeros(NumWaterPoints,1);
98
99 latwater = zeros(NumWaterPoints,1);
100 longwater = zeros(NumWaterPoints,1);
101
102 xair = [];
103 z = [];
104 zair = [];
105
106 PtotTE3 = [];
107 PtotTM3 = [];
108 Pinit = [];
109
110 PWaterTE = zeros(NumWaterPoints,1);
111 PWaterTM = zeros(NumWaterPoints,1);
112 PWaterTE_Engineering = zeros(NumWaterPoints,1);
113 PWaterTM_Engineering = zeros(NumWaterPoints,1);
114
115 YagiGains = zeros(NumAirPoints,1,length(Site1));
116 TransmitterGains = zeros(NumAirPoints,1,length(Site1));
117 polarisationMismatches = zeros(NumAirPoints,1,length(Site1));
118
119 MagAngleGains = zeros(NumAirPoints,1,length(Site1));
120
121 xvals = [];
122 yvals = [];
123 zvals = [];
124
125 xwaters = zeros(NumWaterPoints,1,length(Site1));
126 ywaters = zeros(NumWaterPoints,1,length(Site1));
127 zwaters = zeros(NumWaterPoints,1,length(Site1));
128
129 latwaters = zeros(NumWaterPoints,1,length(Site1));
130 longwaters = zeros(NumWaterPoints,1,length(Site1));
131
132 PinitTE = zeros(NumAirPoints,1,length(Site1));
133 PinitTM = zeros(NumAirPoints,1,length(Site1));

```

```

134
135 Pwaters = zeros(NumWaterPoints,1,length(Site1));
136 PwatersTE = zeros(NumWaterPoints,1,length(Site1));
137 PwatersTM = zeros(NumWaterPoints,1,length(Site1));
138 PwatersTE_Engineering = zeros(NumWaterPoints,1,length(Site1));
139 PwatersTM_Engineering = zeros(NumWaterPoints,1,length(Site1));
140
141 Transmission_Coefficient_te = zeros(NumAirPoints,1,length(Site1));
142 Transmission_Coefficient_tm = zeros(NumAirPoints,1,length(Site1));
143
144 Reflection = [];
145 Transmission = [];
146 Pstarter = [];
147
148 AllAngles = zeros(NumAirPoints,1,length(Site1));
149 AllAttenuationsdB = zeros(NumWaterPoints,1,length(Site1));
150 AllPathLossesdB = zeros(NumWaterPoints,1,length(Site1));
151
152 AttenuationsdB = zeros(NumWaterPoints,1);
153 PathLossesdB = zeros(NumWaterPoints,1);
154
155 Pinitial = 0;
156 Ptransmitted = 0;
157 Preflected = 0;
158
159
160 %% Following section can be altered if the input csv has a
    %% different format to the one used
161
162 Angle = Site1(:,13); %Offset Directional
163 Hypotenuse = Site1(:,12); %Hypotenuse
164 HorizontalDist = Site1(:,11); %Horizontal Distance to River
165 Latitude = Site1(:,9); %Latitude of River Piece
166 Longitude = Site1(:,10); %Longitude of River Piece
167 AntLat = Site1(:,2); %Antenna Latitude
168 AntLong = Site1(:,3); %Antenna Longitude
169 Bearing = Site1(1,6); %Bearing of Antenna: 0 indicates downward
170 Pitch = abs(Site1(1,7)); %Antenna tilt off xy plane
171 zantenna = Site1(1,8); %Height of the antenna
172 siteName = TextSite1{: ,1};
173
174 i = 1; %Index to go over every single raster point
175
176 Lengthy = length(Angle); %Go through each lat and long coordinate
177 indexAir = 1; %How many points are calculated in the air
178
179 while i<=(Lengthy)
180
181 %Each of these points will be the lat and long in the file
182 %i = 0 is the first latitude and longitude point.
183
184 %Angle in xy plane
185 phir = deg2rad(Angle(i)); %radian

```

```

186 phi = Angle(i); %degrees
187
188 % Creating distances: This would be if the bearing is pointing
189 % along the x axis.
190 xpos = cos(phir)*HorizontalDist(i);
191 ypos = sin(phir)*HorizontalDist(i);
192
193 %Theta Value - Angle of Incidence: From river to sky
194 thetar = atan(HorizontalDist(i)/zantenna); %radians
195 theta = rad2deg(thetar); %degrees
196
197 thetar_p = asin(k1.*sin(thetar)./k2); %Angle of transmission into
    water
198
199 [Gain,MaxAngleFromMaxGain] =
    AntennaGain(theta,phi,Pitch,Bearing,AntennaGainFile); %Calculate
    the Antenna Gain based on angle in xy and with z plane
200
201 [k1x,k2x,k1z,k2z] = waveNumber(thetar,w,mu0,ep1,ep2);
202
203 [rte,tte,rtm,ttm,rte_coeff,tte_coeff,rtm_coeff,ttm_coeff] =
    Coefficients(k1z,k2z,ep1,ep2);
204
205 [eta,eta_Prime,etaTE,etaTE_Prime,etaTM,etaTM_Prime] =
    EtaValues(thetar,w,mu0,k1z,k2z,ep1,ep2); %TE and TM have cosines
    baked inside
206
207 Betaz_p = real(k2z);
208 alphaz_p = -1.*imag(k2z);
209
210 dair = Hypotenuse(i); %Distance travelled in the air
211
212 [Pz,Pz_incoming,Pz_reflected] = PowerAirZ(E0,w,mu0,k1z,rte);
213
214 [E,H,Ein,Hin] =
    TE_Field(E0,k1z,k1x,zantenna,HorizontalDist(i),rte_coeff,etaTE);
215
216 [ETM,HTM,ETMin,HTMin] =
    TM_Field(E0,k1z,k1x,zantenna,HorizontalDist(i),rtm_coeff,etaTM);
217
218 PowerTEin = FieldPower(Ein,Hin).*real(cos(thetar)); %Z-direction
219 FieldsPowerIncident2 =
    0.5.*real((abs(E0).^2)./eta).*real(cos(thetar)); %Gives the Same
    Answer (Z-direction)
220
221 PowerTMin = FieldPower(ETMin,HTMin).*real(cos(thetar)); %Z-direction
222 FieldsPowerIncidentTM2 =
    0.5.*real((abs(E0).^2)./(eta.*cos(thetar).^2)).*real(cos(thetar));
    %Gives the Same Answer (Z-Direction)
223
224 PinitstE(:, :, i) = PowerTEin;
225 PinitstM(:, :, i) = PowerTMin;
226

```

```

227 YagiGain = Gain;
228 TransmitterGain = TGain;
229
230 MagAngleGain = MaxAngleFromMaxGain;
231
232 %Latitude and Longitude at the surface of the water
233 LatitudeInterface = Latitude(i);
234 LongitudeInterface = Longitude(i);
235
236 % In the water area
237 indexWater = 1;
238 for z1 = 0.1:0.5:2
239     % In the water there is a slight offset in the latitude and
240     % longitude measurements due to the fact that the ray is
241     % travelling at an angle
242     %z1 is a depth in the river
243
244     XYwater = z1.*tan(thetar_p); %Distance in xy direction in water
        - horizontal distance
245
246     % Creating distances: This would be if the bearing is pointing
247     % along the x axis. Not general to all antennas
248     xwater(indexWater,:) = cos(phir).*XYwater;
249     ywater(indexWater,:) = sin(phir).*XYwater;
250
251     %Note with Compass: 0 degree and 360 bearing (N)
252     %In compass coordinate with (y = N/S and x = E/W)
253     %Getting correct x and y variables based on the bearing of the
254     %antenna
255     xwaterref = cos(phir+(deg2rad(Bearing))).*XYwater;
256     ywaterref = sin(phir+(deg2rad(Bearing))).*XYwater;
257
258     %Decaying portion - attenuation due to conductive losses
259     Attenuation = exp(-2*alphaz_p*z1);
260     AttenuationdB = 10.*log10(Attenuation);
261
262     dwater = sqrt((z1.^2)+(XYwater.^2)); %Distance travelled in the
        water.
263
264     PathLoss_Total = pathLoss(dair,lambda1,dwater,lambda2);
        %Calculate Path loss of air and water
265
266     [ETE_Prime,HTE_Prime] =
        TE_Prime_Field(E0,k2z,k2x,z1,XYwater,tte_coeff,etaTE_Prime);
        %TE fields in water
267
268     [ETM_Prime,HTM_Prime] =
        TM_Prime_Field(E0,k2z,k2x,z1,XYwater,ttm_coeff,etaTM_Prime);
        %TM fields in water
269
270     PowerTEin_Prime =
        FieldPower(ETE_Prime,HTE_Prime).*real(cos(thetar_p))...
271     .*PathLoss_Total;

```

```

272     FieldsPowerTransmitted2 =
273         0.5.*real(((abs(tte_coeff).^2).*(abs(E0).^2).*Attenuation)./...
                eta_Prime).*real(cos(thetar_p)).*PathLoss_Total; %Gives
                same answer (z-component)
274
275     PowerTMin_Prime =
                FieldPower(ETM_Prime,HTM_Prime).*real(cos(thetar_p))...
276         .*PathLoss_Total; %Check
277     FieldsPowerTransmittedTM2 =
                0.5.*real(((abs(ttm_coeff).^2).*(abs(E0).^2).*Attenuation)./...
278         (eta_Prime.*cos(thetar_p).^2)).*real(cos(thetar_p))...
279         .*PathLoss_Total; %Gives same answer
280
281     xwater(indexWater,:) = xpos+xwater(indexWater,:);
282     ywater(indexWater,:) = ypos+ywater(indexWater,:);
283     zwater(indexWater,:) = -z1.*ones(1,length(thetar),'double');
284
285     [latnew,longnew] =
                OffsetLatitudeLongitudeCalculator(LatitudeInterface...
286         ,LongitudeInterface,...
287         xwaterref(end,:),ywaterref(end,:)); %Need to specify Lat
                and Long
288     latwater(indexWater,:) = latnew(:,:);
289     longwater(indexWater,:) = longnew(:,:);
290
291     AttenuationsdB(indexWater,:) = AttenuationdB(:,:);
292     PathLossesdB(indexWater,:) = 10.*log10(PathLoss_Total(:,:));
293
294     PWaterTE(indexWater,:) = (PowerTEin_Prime(:,:));
295     PWaterTM(indexWater,:) = (PowerTMin_Prime(:,:));
296     PWaterTE_Engineering(indexWater,:) =
                (tte).*Attenuation.*PathLoss_Total;
297     PWaterTM_Engineering(indexWater,:) =
                (ttm).*Attenuation.*PathLoss_Total;
298
299     indexWater = indexWater+1;
300 end
301 % Save the water values of the waves at a certain incoming
302 % coordinate position.
303 xvals(:,:,i) = x;
304 yvals(:,:,i) = y;
305 zvals(:,:,i) = z;
306
307 xwaters(:,:,i) = xwater;
308 ywaters(:,:,i) = ywater;
309 zwaters(:,:,i) = zwater;
310
311 latwaters(:,:,i) = latwater;
312 longwaters(:,:,i) = longwater;
313
314 PwatersTE(:,:,i) = PWaterTE;
315 PwatersTM(:,:,i) = PWaterTM;
316 PwatersTE_Engineering(:,:,i) = PWaterTE_Engineering;

```

```

317 PwatersTM_Engineering(:,:,i)= PWaterTM_Engineering;
318
319 YagiGains(:,:,i) = YagiGain;
320 TransmitterGains(:,:,i) = TransmitterGain;
321 polarisationMismatches(:,:,i) = etaPol;
322
323 MagAngleGains(:,:,i) = MagAngleGain;
324
325 AllAngles(:,:,i) = theta;
326 AllAttenuationsdB(:,:,i) = AttenuationsdB;
327 AllPathLossesdB(:,:,i) = PathLossesdB;
328
329
330 Transmission_Coefficient_te(:,:,i) = tte;
331 Transmission_Coefficient_tm(:,:,i) = ttm;
332
333 i = i+1;
334
335 x = [];
336 y=[];
337
338 xwater = zeros(NumWaterPoints,1);
339 ywater = zeros(NumWaterPoints,1);
340
341 latwater = zeros(NumWaterPoints,1);
342 longwater = zeros(NumWaterPoints,1);
343
344 xair = [];
345 z = [];
346 zwater = zeros(NumWaterPoints,1);
347 zair = [];
348
349 Pinit = [];
350 YagiGain = [];
351 TransmitterGain = [];
352
353 MagAngleGain = [];
354 AttenuationsdB =zeros(NumWaterPoints,1);
355 PathLossesdB = zeros(NumWaterPoints,1);
356
357 PWaterTE = zeros(NumWaterPoints,1);
358 PWaterTM = zeros(NumWaterPoints,1);
359 PWaterTE_Engineering = zeros(NumWaterPoints,1);
360 PWaterTM_Engineering = zeros(NumWaterPoints,1);
361
362 end
363
364 %Initializing more variables
365
366 PAirInitTE = zeros(NumAirPoints,1,length(Site1));
367 PAirInitTM = zeros(NumAirPoints,1,length(Site1));
368
369 Gain_angles = [];

```



```

370 Gain_anglesTE = zeros(NumWaterPoints,1,length(Site1));
371 Gain_anglesTM = zeros(NumWaterPoints,1,length(Site1));
372 Gain_anglesTE_Engineering = zeros(NumWaterPoints,1,length(Site1));
373 Gain_anglesTM_Engineering = zeros(NumWaterPoints,1,length(Site1));
374
375 Gain_angles_Air = zeros(NumAirPoints,1,length(Site1));
376 Gain_angles_AirTE = zeros(NumAirPoints,1,length(Site1));
377 Gain_angles_AirTM = zeros(NumAirPoints,1,length(Site1));
378 Gain_angles_AirTE3 = [];
379 Gain_angles_AirTM3 = [];
380
381 Gains = [];
382
383 %Performing the total path loss calculation
384 %For Fields equations need to divide the water power/ the air power
385 %For Engineering Equation just need to take 10*log10 of the value
386 % Note: Path Loss is already included
387 for m = 1:size(xwaters,3)
388
389 PAirInitTE(:, :, m) = PinitTE(1, :, m);
390 Gain_anglesTE(:, :, m) =
    10.*log10(PwatersTE(:, :, m)./PAirInitTE(:, :, m))+YagiGains(:, :, m)+...
391     TransmitterGains(:, :, m)+polarisationMismatches(:, :, m);
392
393 PAirInitTM(:, :, m) = PinitTM(1, :, m);
394 Gain_anglesTM(:, :, m) =
    10*log10(PwatersTM(:, :, m)./PAirInitTM(:, :, m))+YagiGains(:, :, m)+...
395     TransmitterGains(:, :, m)+polarisationMismatches(:, :, m);
396
397 Gain_anglesTE_Engineering(:, :, m) =
    10*log10(PwatersTE_Engineering(:, :, m))+YagiGains(:, :, m)+...
398     TransmitterGains(:, :, m)+polarisationMismatches(:, :, m);
399
400 Gain_anglesTM_Engineering(:, :, m) =
    10*log10(PwatersTM_Engineering(:, :, m))+YagiGains(:, :, m)+...
401     TransmitterGains(:, :, m)+polarisationMismatches(:, :, m);
402
403 end
404
405 FresnelTE = 10.*log10(Transmission_Coefficient_te);
406 FresnelTM = 10.*log10(Transmission_Coefficient_tm);
407
408 validInputs = [0,1,2,3,4,5,6,7,8,9,10];
409 meaningInputs = ["Yagi Gain","Transmission Coefficient
    TE","Transmission Coefficient TM","Angle of
    Incidence","Attenuation - Water","Path Loss","Overall
    TE","Overall TE Eng","Overall TM","Overall TM Eng","No Plot"];
410
411 % Provides a table for a user to select what type of plot is
    required
412 % or if they do not want any plot they can select 10 and it will
    save to a csv file.
413 %     TABLE = [validInputs',meaningInputs']

```

```

414 %     plottype = input('Enter a number: ');
415 plottype=10;
416
417 switch plottype
418 case 0
419     %Yagi Gain - Using longitude and latidue axis
420     n=1*numFiles+1;
421     figure(n);
422     for l = 1:size(xwaters,3)
423         hold on;
424         for s = 1:size(xwaters,2)
425             scatter3(real(longwaters(1,s,l)),real(latwaters(1,s,l)),...
426                 real(zwaters(1,s,l)),40,(YagiGains(1,s,l)),'filled');
427             xlabel("Longitude")
428             ylabel("Latitude")
429             zlabel("Height (m)")
430             title("Three Element Yagi Antenna Gain (dB)")
431         end
432     end
433     cb = colorbar;
434     scatter(AntLong(1,1),AntLat(1,1),100,'r','x')
435     % xlim([-100 100]);
436     % ylim([-100 100]);
437     % zlim([-20 0]);
438     hold off;
439 case 1
440     %Transmission Gain Coefficient TE - Using longitude and latidue
441     axis
442     n=1*numFiles+1;
443     figure(n);
444     for l = 1:size(xwaters,3)
445         hold on;
446         for s = 1:size(xwaters,2)
447             scatter3(real(longwaters(1,s,l)),real(latwaters(1,s,l)),...
448                 real(zwaters(1,s,l)),40,(FresnelTE(1,s,l)),'filled');
449             xlabel("Longitude")
450             ylabel("Latitude")
451             zlabel("Height (m)")
452             title("Transmission Gain TE (dB)")
453         end
454     end
455     cb = colorbar;
456     scatter(AntLong(1,1),AntLat(1,1),100,'r','x')
457     % xlim([-100 100]);
458     % ylim([-100 100]);
459     % zlim([-20 0]);
460     hold off;
461 case 2
462     %Transmission Gain Coefficient TM - Using longitude and latidue
463     axis
464     n=1+1*numFiles;
465     figure(n);
466     for l = 1:size(xwaters,3)

```

```

465     hold on;
466     for s = 1:size(xwaters,2)
467         scatter3(real(longwaters(1,s,1)),real(latwaters(1,s,1)),...
468                 real(zwaters(1,s,1)),40,(FresnelTM(1,s,1)),'filled');
469         xlabel("Longitude")
470         ylabel("Latitude")
471         zlabel("Height (m)")
472         title("Transmission Gain TM (dB)")
473     end
474 end
475 cb = colorbar;
476 scatter(AntLong(1,1),AntLat(1,1),100,'r','x')
477 % xlim([-100 100]);
478 % ylim([-100 100]);
479 % zlim([-20 0]);
480 hold off;
481 case 3
482     % %Angle of Incidence - Using longitude and latidue axis
483     n=1*numFiles;
484     figure(n);
485     for l = 1:size(xwaters,3)
486         hold on;
487         for s = 1:size(xwaters,2)
488             scatter3(real(longwaters(1,s,1)),real(latwaters(1,s,1)),...
489                     real(zwaters(1,s,1)),40,(AllAngles(1,s,1)),'filled');
490             xlabel("Longitude")
491             ylabel("Latitude")
492             zlabel("Height (m)")
493             title("Transmission Gain TE (dB)")
494         end
495     end
496     cb = colorbar;
497     scatter(AntLong(1,1),AntLat(1,1),100,'r','x')
498     % xlim([-100 100]);
499     % ylim([-100 100]);
500     % zlim([-20 0]);
501     hold off;
502 case 4
503     % %Attenuation in dB - Using longitude and latidue axis
504     n=1*numFiles;
505     figure(n);
506     for l = 1:size(xwaters,3)
507         hold on;
508         for s = 1:size(xwaters,2)
509             scatter3(real(longwaters(:,s,1)),real(latwaters(:,s,1)),...
510                     real(zwaters(:,s,1)),40,(AllAttenuationsdB(:,s,1))...
511                     ,'filled');
512             xlabel("Longitude")
513             ylabel("Latitude")
514             zlabel("Height (m)")
515             title("Attenuation Gain (dB)")
516         end
517     end

```

```

518     cb = colorbar;
519     scatter(AntLong(1,1),AntLat(1,1),100,'r','x')
520     % xlim([-100 100]);
521     % ylim([-100 100]);
522     % zlim([-20 0]);
523     hold off;
524 case 5
525     %Path Loss in dB - Using longitude and latidue axis
526     n=1*numFiles;
527     figure(n);
528     for l = 1:size(xwaters,3)
529         hold on;
530         for s = 1:size(xwaters,2)
531             scatter3(real(longwaters(:,s,l)),real(latwaters(:,s,l)),...
532                 real(zwaters(:,s,l)),40,(AllPathLossesdB(:,s,l))...
533                 ,'filled');
534             xlabel("Longitude")
535             ylabel("Latitude")
536             zlabel("Height (m)")
537             title("Path Loss Gain (dB)")
538         end
539     end
540     cb = colorbar;
541     scatter(AntLong(1,1),AntLat(1,1),100,'r','x')
542     % xlim([-100 100]);
543     % ylim([-100 100]);
544     % zlim([-20 0]);
545     hold off;
546 case 6
547     %Overall System (TE) - lat long
548     n=1*numFiles+1;
549     figure(n);
550     for l = 1:size(xwaters,3)
551         hold on;
552         for s = 1:size(xwaters,2)
553             scatter3(real(longwaters(:,s,l)),real(latwaters(:,s,l)),...
554                 real(zwaters(:,s,l)),10,real(Gain_anglesTE(:,s,l))...
555                 ,'filled');
556         end
557     end
558     xlabel("Longitude")
559     ylabel("Latitude")
560     zlabel("Depth (m)")
561     title("TE Link Budget Fraser River (dB) - Fields Approach")
562     cb = colorbar;
563     scatter(AntLong(1,1),AntLat(1,1),100,'r','x')
564     hold off;
565 case 7
566     %Overall System (TE) Engineering - Latitude and Longitude
567     n=1*numFiles+1;
568     figure(n);
569     for l = 1:size(xwaters,3)
570         hold on;

```

```

571     for s = 1:size(xwaters,2)
572     scatter3(real(longwaters(:,s,1)),real(latwaters(:,s,1)),...
573             real(zwaters(:,s,1)),10,real(...
574             Gain_anglesTE_Engineering(:,s,1)),'filled');
575     end
576 end
577 xlabel("Longitude")
578 ylabel("Latitude")
579 zlabel("Depth (m)")
580 title("TE Link Budget Fraser River (dB) - Engineering Approach")
581 cb = colorbar;
582 scatter(AntLong(1,1),AntLat(1,1),100,'r','x')
583 hold off;
584 case 8
585     %Overall System (TM) - Latitude and Longitude
586     n=1*numFiles+1;
587     figure(n);
588     for l = 1:size(xwaters,3)
589         hold on;
590         for s = 1:size(xwaters,2)
591             scatter3(real(longwaters(:,s,1)),real(latwaters(:,s,1)),...
592                     real(zwaters(:,s,1)),10,real(Gain_anglesTM(:,s,1))...
593                     ,'filled');
594         end
595     end
596     xlabel("Longitude")
597     ylabel("Latitude")
598     zlabel("Depth (m)")
599     title("TM Link Budget Fraser River (dB) - Fields Approach")
600     cb = colorbar;
601     scatter(AntLong(1,1),AntLat(1,1),100,'r','x')
602     hold off;
603 case 9
604     %Overall System (TM) Eng - Latitude and Longitude
605     n=numFiles*1+1;
606     figure(n);
607     for l = 1:size(xwaters,3)
608         hold on;
609         for s = 1:size(xwaters,2)
610             scatter3(real(longwaters(:,s,1)),real(latwaters(:,s,1)),...
611                     real(zwaters(:,s,1)),10,real(...
612                     Gain_anglesTM_Engineering(:,s,1)),'filled');
613         end
614     end
615     xlabel("Longitude")
616     ylabel("Latitude")
617     zlabel("Depth (m)")
618     title("TM Link Budget Fraser River (dB) - Engineering Approach")
619     cb = colorbar;
620     scatter(AntLong(1,1),AntLat(1,1),100,'r','x')
621     hold off;
622 case 10
623     disp("Skipping Plotting and saving directly");

```

```

624 otherwise
625     disp('Incorrect Entry')
626 end
627
628
629 AntLat2 = AntLat'.*[1;1;1;1];
630 AntLong2 = AntLong'.*ones(4,1);
631
632
633 %% Comment out if you don't want to write to a file
634 % %Write the data to an excel sheet
635 ToWriteData(:,1) = reshape(longwaters,[],1);
636 ToWriteData(:,2) = reshape(latwaters,[],1);
637 ToWriteData(:,3) = reshape(zwaters,[],1);
638 ToWriteData(:,4) = reshape(real(Gain_anglesTE),[],1);
639 ToWriteData(:,5) = reshape(AntLat2,[],1);
640 ToWriteData(:,6) = reshape(AntLong2,[],1);
641 ToWriteData(:,7) = reshape(real(zantenna),[],1);
642 ToWriteData(:,8) = reshape(AllAttenuationsdB,[],1);
643 ToWriteData(:,9) = reshape(AllPathLossesdB,[],1);
644 ToWriteData(:,10) = reshape(real(Gain_anglesTE_Engineering),[],1);
645 ToWriteData(:,11) = reshape(real(Gain_anglesTM),[],1);
646 ToWriteData(:,12) = reshape(real(Gain_anglesTM_Engineering),[],1);
647 ToWriteTitle = {'Longitude' 'Latitude' 'Depth (m)' 'Gain Value TE -
    Fields (dB)' 'Antenna Latitude' 'Antenna Longitude' 'Height
    Antenna' 'AllAttenuations' 'AllPathLoss' 'TE-Eng' 'TM-Fields'
    'TM-Eng'};
648 ToWrite1 = array2table(ToWriteData,"VariableNames",ToWriteTitle);
649
650 siteName2 = [siteName;siteName;siteName;siteName];
651
652 ToWrite = [siteName2 ToWrite1];
653 writetable(ToWrite,fileWrite(numFiles));
654
655 longwatersurf = longwaters(1,1,:);
656 latwatersurf = latwaters(1,1,:);
657 zantennasurf = zantenna(1,1,:);
658
659 %%For the data that has no depth variables to them
660 ToWriteData2(:,1) = reshape(longwatersurf,[],1);
661 ToWriteData2(:,2) = reshape(latwatersurf,[],1);
662 ToWriteData2(:,3) = reshape(AntLat,[],1);
663 ToWriteData2(:,4) = reshape(AntLong,[],1);
664 ToWriteData2(:,5) = reshape(real(zantennasurf),[],1);
665 ToWriteData2(:,6) = reshape(YagiGains,[],1);
666 ToWriteData2(:,7) = reshape(FresnelTE,[],1);
667 ToWriteData2(:,8) = reshape(FresnelTM,[],1);
668 ToWriteData2(:,9) = reshape(AllAngles,[],1);
669 ToWriteTitle2 = {'Longitude' 'Latitude' 'Antenna Latitude' 'Antenna
    Longitude' 'Height Antenna' ' YagiGains' 'FresnelTE' '
    FresnelTM' 'AllAngles'};
670 ToWrite2 = array2table(ToWriteData2,"VariableNames",ToWriteTitle2);
671

```

```

672 ToWrite = [siteName ToWrite2];
673 writetable(ToWrite,fileWrite2(numFiles));
674
675 numFiles = numFiles + 1;
676 end
677
678
679 function [k1x,k2x,k1z,k2z] = waveNumber(angle,w,mu0,ep1,ep2)
680     % Wave number
681     % 1 indicates in air
682     % 2 indicates in water
683     k1 = w*sqrt(mu0*ep1);
684     k2 = w*sqrt(mu0*ep2); % Eq. (7.9.2)
685     k1x = k1*sin(angle);
686     k2x = k1x;
687     k1z = k1*cos(angle);
688     k2z = sqrt(w^2*mu0*ep2 - k1x.^2); % Eq. (7.9.6)
689 end
690
691 function [rte,tte,rtm,ttm,rte_coeff,tte_coeff,rtm_coeff,ttm_coeff]
    = Coefficients(k1z,k2z,ep1,ep2)
692     % Calculate the Fresnel coefficients
693     %rte,tte,rtm,ttm are power coefficients
694     %rte_coeff and all other _coeff are the complex conjugates
695     rte_coeff = ((k1z - k2z)./(k1z + k2z));
696     rtm_coeff = ((k2z.*ep1 - k1z.*ep2)./(k2z.*ep1 + k1z.*ep2));
697
698     ttm_coeff = (2*k2z*ep1)./(k2z*ep1+k1z*ep2);
699     tte_coeff = (2*k1z)./(k1z+k2z);
700
701     %Power Values
702     rte = abs(rte_coeff).^2;
703     rtm = abs(rtm_coeff).^2;
704     ttm = 1-rtm;
705     tte = 1-rte;
706
707 end
708
709 function [eta,eta_Prime,etaTE,etaTE_Prime,etaTM,etaTM_Prime] =
    EtaValues(thetar,w,mu0,k1z,k2z,ep1,ep2)
710     %Calculate the various wave impedances
711     etaTE = w.*mu0./k1z;
712     etaTE_Prime = w.*mu0./k2z;
713     etaTM = k1z./(w.*ep1);
714     etaTM_Prime = k2z./(w.*ep2);
715     eta = sqrt(mu0./ep1);
716     eta_Prime = sqrt(mu0./ep2);
717 end
718
719 function PL = pathLoss(d1,lambda1,d2,lambda2)
720     %Calculates the path loss in air and water
721     if d1 == 0
722         PL = 1;

```

```

723     else
724         PL = (lambda1./(4.*pi.*d1)).^2.*(lambda2./(4.*pi.*d2)).^2;
725     end
726 end
727
728 function [Pz,Pz_incoming,Pz_reflected] = PowerAirZ(E0,w,mu0,k1z,rte)
729     %Calculates the incoming, reflected and total power in the
730     air
731     Pz = abs(E0)^2./(2.*w.*mu0).*k1z.*(1-(rte));
732     Pz_incoming = abs(E0)^2./(2.*w.*mu0).*k1z;
733     Pz_reflected = abs(E0)^2./(2.*w.*mu0).*k1z.*(rte);
734 end
735 function [Gain,MaxAngleFromMaxGain] =
736     AntennaGain(theta,phi,pitch,bearing,AntennaGainFile)
737     %Calculates the yagi gain
738     alpha = 90-theta-pitch;
739     % Theta measurement
740     phiPrime = phi; %Offset from antenna to water location
741
742     MaxAngleFromMaxGain = max(abs(alpha),abs(phiPrime));
743     %Calculate the maximum angle
744
745     data = readmatrix(AntennaGainFile);
746     Angle = data(:,1); %Offset Directional
747     AntGain = data(:,2);
748
749     Gain = interp1(Angle,AntGain,MaxAngleFromMaxGain);
750     %Interpolate based on manufacturers gain
751 end
752
753
754 function [E,H,Ein,Hin] = TE_Field(E0,k1z,k1x,z0,x0,rte_coeff,etaTE)
755     % TE Fields: In First medium
756     Ey = E0.*(exp(-1i.*k1z.*z0)+rte_coeff.*exp(1i.*k1z.*z0))...
757         .*exp(-1i.*k1x.*x0);
758     Hx = E0.*(-1.*exp(-1i.*k1z.*z0)+rte_coeff.*exp(1i.*k1z.*z0))...
759         .*exp(-1i.*k1x.*x0)./etaTE;
760     Hz = E0.*(k1x./k1z).*exp(-1i.*k1z.*z0)+rte_coeff.*(k1x./k1z)...
761         .*exp(1i.*k1z.*z0)).*exp(-1i.*k1x.*x0)./etaTE;
762
763     E = [0,Ey,0];
764     H = [Hx,0,Hz];
765
766     Eyin = E0.*(exp(-1i.*k1z.*z0)).*exp(-1i.*k1x.*x0);
767     Hxin = E0.*(-1.*exp(-1i.*k1z.*z0)./etaTE).*exp(-1i.*k1x.*x0);
768     Hzin =
769         E0.*((k1x./k1z).*exp(-1i.*k1z.*z0)./etaTE).*exp(-1i.*k1x.*x0);
770
771     Ein = [0,Eyin,0];
772     Hin = [Hxin,0,Hzin];
773 end

```



```

773
774 function [ETM,HTM,ETMin,HTMin] =
    TM_Field(E0,k1z,k1x,z0,x0,rtm_coeff,etaTM)
775 % TM Fields: In First medium
776 Hy_TM = E0.*(exp(-1i.*k1z.*z0)+rtm_coeff.*exp(1i.*k1z.*z0))...
777     .*exp(-1i.*k1x.*x0)./etaTM;
778 Ex_TM = E0.*(exp(-1i.*k1z.*z0)+rtm_coeff.*exp(1i.*k1z.*z0))...
779     .*exp(-1i.*k1x.*x0);
780 Ez_TM =
    E0.*(-1.*(k1x./k1z).*exp(-1i.*k1z.*z0)+rtm_coeff.*(k1x./k1z)...
781     .*exp(1i.*k1z.*z0)).*exp(-1i.*k1x.*x0);
782
783 ETM = [Ex_TM,0,Ez_TM];
784 HTM = [0,Hy_TM,0];
785
786 Hy_TMin = E0.*(exp(-1i.*k1z.*z0).*exp(-1i.*k1x.*x0))./etaTM;
787 Ex_TMin = E0.*(exp(-1i.*k1z.*z0).*exp(-1i.*k1x.*x0));
788 Ez_TMin =
    E0.*(-1.*(k1x./k1z).*exp(-1i.*k1z.*z0).*exp(-1i.*k1x.*x0));
789
790 ETMin = [Ex_TMin,0,Ez_TMin];
791 HTMin = [0,Hy_TMin,0];
792 end
793
794 function [ETE_Prime,HTE_Prime] =
    TE_Prime_Field(E0,k2z,k2x,z1,x1,tte_coeff,etaTEPrime)
795 % TE Fields: In second medium
796 EyPrime = E0.*tte_coeff.*(exp(-1i.*k2z.*z1).*exp(-1i.*k2x.*x1));
797 HxPrime =
    E0.*tte_coeff.*(-1.*exp(-1i.*k2z.*z1).*exp(-1i.*k2x.*x1))...
798     ./etaTEPrime;
799 HzPrime = E0.*tte_coeff.*((k2x./k2z).*exp(-1i.*k2z.*z1)...
800     .*exp(-1i.*k2x.*x1))./etaTEPrime;
801
802 ETE_Prime = [0,EyPrime,0];
803 HTE_Prime = [HxPrime,0,HzPrime];
804 end
805
806 function [ETM_Prime,HTM_Prime] =
    TM_Prime_Field(E0,k2z,k2x,z1,x1,ttm_coeff,etaTMPrime)
807 % TM Fields: In second medium
808 HyPrime_TM =
    E0.*ttm_coeff.*(exp(-1i.*k2z.*z1).*exp(-1i.*k2x.*x1))...
809     ./etaTMPrime;
810 ExPrime_TM =
    E0.*ttm_coeff.*(exp(-1i.*k2z.*z1).*exp(-1i.*k2x.*x1));
811 EzPrime_TM =
    E0.*ttm_coeff.*(-1.*(k2x./k2z).*exp(-1i.*k2z.*z1)...
812     .*exp(-1i.*k2x.*x1))./etaTMPrime;
813
814 ETM_Prime = [ExPrime_TM,0,EzPrime_TM];
815 HTM_Prime = [0,HyPrime_TM,0];
816 end

```

```

817
818 function [Power] = FieldPower(E,H)
819     %Calculate the poynting vector of E&H Fields
820     Power = 0.5.*real(sqrt(sum(cross(E,conj(H)).^2)));
821 end
822
823
824 function [latnew,longnew] =
    OffsetLatitudeLongitudeCalculator(Lat,Long,xoffset,yoffset)
825     rearth = 6378.137; %radius of the earth in kilometers
826     m = (1 / ((2 * pi / 360) * rearth)) / 1000; %1 meter in degree
827
828     latnew = Lat + (real(yoffset) * m);
829     longnew = Long + (real(xoffset) * m) / cos(Lat * (pi / 180));
830 end

```

## B.1.2 Fresnel Equations

### TE Polarisation

```

1 %Comparison of Multiple different textbooks for TE Oblique incidence
2 % Up to Date: NO Issues all results agree
3 % November 30th 2023 last edited
4
5 %parallel == TM == P polarization
6 %Perpendicular == TE == S polarization
7
8
9 close all;
10 clear all;
11 clc;
12
13 %% Declaring Constants
14 f = 1.5e8; %150 MHz
15 w = 2*pi*f;
16
17 %Conductivity
18 sigmaAir = 0;
19 sigmaWater = 0.014;
20
21 %Declare Permittivities epsilon_r = epsilon/epsilon_o
22 epsilon_rAir = 1;
23 epsilon_rWater = 80.10;
24 epsilon_0 = 8.85418782e-12;
25
26 %Declare Permeability mu_r = mu/mu_0
27 mu_rAir = 1;
28 mu_rWater = 0.999992;
29 mu_0 = pi*4e-7;
30
31 % Declare values that do not depend on angle
32

```

```

33 %Calculate specific permitivity: epsilon = epsilonR*epsilon0
34 epsilonAir = epsilonRAir * epsilon0;
35 epsilonWater = epsilonRWater * epsilon0;
36
37 %Calculate specific permeability: mu = muR*mu0
38 muAir = muRAir * mu0;
39 muWater = muRWater * mu0;
40
41 %% Determine Input Angle Stuff
42 thetarAir = linspace(0,pi/2,100);
43
44
45 %% James Wait Textbook
46
47 %Perpendicular
48 gammaWater =
49     sqrt(1i.*muWater.*w.*(sigmaWater+1i.*epsilonWater.*w)); %Water
50 gammaAir = sqrt(1i.*muAir.*w.*(sigmaAir+1i.*epsilonAir.*w)); %Air
51 thetarWater2 = (asin((gammaAir.*sin(thetarAir))./gammaWater));
52
53 uWater = gammaWater.*cos(thetarWater2);
54 uAir = gammaAir.*cos(thetarAir);
55 NO = (uAir)./(1i.*mu0.*w);
56 N1 = (uWater)./(1i.*mu0.*w);
57
58 %Coefficients
59 rJWTE = (NO-N1)./(NO+N1);
60 tJWTE = 1+rJWTE; %Since this is perpendicular should be able to do
61     t = 1+r
62 tJWTE2 = 2.*NO./(NO+N1);
63
64 %Power
65 RJWTE = abs(rJWTE).^2;
66 TJWTE = abs(tJWTE).^2.*real(N1)./real(NO);
67 TJWTE2 = 1-RJWTE; %Verification
68
69 %% Pozar
70 epswater = epsilonWater-1i*sigmaWater/w;
71 epsair = epsilonAir-1i*sigmaAir/w;
72
73 thetarWater =
74     asin(sin(thetarAir).*sqrt(epsair.*mu0./(epswater.*mu0)));
75 gammzWater = 1i*w*sqrt(muWater*epswater);
76 etaWater = (1i*w*muAir)/gammzWater; %Same: sqrt(mu0/epswater);
77 gammzAir = 1i*w*sqrt(muAir*epsair);
78 etaAir = (1i*w*muAir)/gammzAir;%Same: etaAir2 = sqrt(mu0/epsair);
79
80 %% Perpendicular coefficients
81 rPozarPerp =
82     (etaWater.*cos(thetarAir)-cos(thetarWater).*etaAir)./...
83     (etaWater.*cos(thetarAir)+cos(thetarWater).*etaAir);

```

```

82 tPozarPerp =
    (2.*etaWater.*cos(thetarAir))./(etaWater.*cos(thetarAir)+...
83     cos(thetarWater).*etaAir);
84 tPozarPerp2 = 1+rPozarPerp; %Verification - GOOD
85
86 %Power values
87 rPozarPerp = abs(rPozarPerp).^2;
88 TPozarPerp = abs(tPozarPerp).^2.*real(etaAir.*cos(thetarWater))./...
89     real(etaWater.*cos(thetarAir));
90 TPozarPerp2 = 1-rPozarPerp; %Verification - GOOD
91
92
93 %% MIT
94 Ni = cos(thetarAir)./etaAir;
95 Nt = cos(thetarWater)./etaWater;
96
97 %Coefficients
98 te = 2.*Ni./(Ni+Nt);
99 re=(Ni-Nt)./(Ni+Nt);
100 te2 = re+1; %Verification - GOOD
101
102 %Power Values
103 Te = abs(te).^2.*real(Nt)./real(Ni);
104 Re = abs(re).^2; % Perpendicular Power
105 Te2 = 1-Re; %Verification - GOOD
106
107 %% Ch7 Rutgers Oblique Incidence from Textbook
108 ep1 = epsilonAir;
109 ep2 = epsilonWater - 1i*sigmaWater/w;
110 k1 = w*sqrt(mu0*ep1); %Wave numbers
111 k2 = w*sqrt(mu0*ep2);
112
113 k1x = k1*sin(thetarAir);
114 k1z = k1*cos(thetarAir);
115 k2z = sqrt(w^2*mu0*ep2 - k1x.^2);
116 k2z2 = k2.*cos(thetarWater);
117 thetar_p = asin(k1.*sin(thetarAir)./k2);
118
119 % Coefficients
120 rte = ((k1z - k2z)./(k1z + k2z));
121 tte = (2*k1z./(k1z+k2z));
122 tte2 = 1+rte;
123
124 %Power Values
125 Rte = abs(rte).^2;
126 Tte = abs(tte).^2.*(real(k2z)./real(k1z));
127 Tte2 = 1-Rte;
128
129
130 %% Perpendicular Coefficient Plots
131 n = 1;
132 figure(n)
133 hold on

```

```

134 plot(rad2deg(thetarAir),(rJWTE),rad2deg(thetarAir),(tJWTE));
135 xlabel("Angle of Incidence (deg)");
136 ylabel("Transmission and Reflection Coefficients");
137 title("Coefficient-Transmission and Reflection (James Wait)");
138 legend('Reflection - RTE','Transmission - TTE');
139 hold off
140
141 n=n+1;
142 figure(n)
143 plot(rad2deg(thetarAir),(rte),rad2deg(thetarAir),(tte));
144 xlabel("Angle of Incidence (deg)");
145 ylabel("Transmission and Reflection Coefficients");
146 title("Coefficient-Transmission and Reflection (Rutgers Textbook)");
147 legend('Reflection - RTE','Transmission - TTE');
148 saveas(gcf,'../FishPropagation/Figures/Fresnel/TE/RutgersCoeff.jpg')
149
150 n=n+1;
151 figure(n)
152 plot(rad2deg(thetarAir),(rPozarPerp),rad2deg(thetarAir),tPozarPerp);
153 xlabel("Angle of Incidence (deg)");
154 ylabel("Transmission and Reflection Coefficients");
155 title("Coefficient-Transmission and Reflection (Pozar)");
156 legend('Reflection - RTE','Transmission - TTE');
157 saveas(gcf,'../FishPropagation/Figures/Fresnel/TE/PozarCoeff.jpg')
158
159 n=n+1;
160 figure(n)
161 plot(rad2deg(thetarAir),(re),rad2deg(thetarAir),(te));
162 xlabel("Angle of Incidence (deg)");
163 ylabel("Transmission and Reflection Coefficients");
164 title("Coefficient-Transmission and Reflection (MIT)");
165 legend('Reflection - RTE','Transmission - TTE');
166 saveas(gcf,'../FishPropagation/Figures/Fresnel/TE/MITCoeff.jpg')
167
168
169 %% Perpendicular Power Plots
170 n = n+1;
171 figure(n)
172 plot(rad2deg(thetarAir),(RJWTE),rad2deg(thetarAir),...
173      (TJWTE),rad2deg(thetarAir),(1-RJWTE));
174 xlabel("Angle of Incidence (deg)");
175 ylabel("Transmission and Reflection Power");
176 title("Power-TE Polarization Transmission and Reflection (James
177      Wait)");
177 legend('Reflection','Transmission','Transmission 2');
178 saveas(gcf,'../FishPropagation/Figures/Fresnel/TE/JamesWaitPower.jpg')
179
180 n=n+1;
181 figure(n)
182 plot(rad2deg(thetarAir),(Rte),rad2deg(thetarAir),...
183      (Tte),rad2deg(thetarAir),(1-Rte));
184 xlabel("Angle of Incidence (deg)");
185 ylabel("Transmission and Reflection Power");

```

```

186 title("Power-Transmission and Reflection (Rutgers Textbook)")
187 legend('Reflection','Transmission','Transmission 2');
188 saveas(gcf,'../FishPropagation/Figures/Fresnel/TE/RutgersPower.jpg')
189
190 n=n+1;
191 figure(n)
192 plot(rad2deg(thetarAir),(RPozarPerp),rad2deg(thetarAir),...
193      TPozarPerp,rad2deg(thetarAir),(1-RPozarPerp));
194 xlabel("Angle of Incidence (deg)");
195 ylabel("Transmission and Reflection Power");
196 title("Power-TE Polarization Transmission and Reflection (Pozar)")
197 legend('Reflection','Transmission','Transmission 2');
198 saveas(gcf,'../FishPropagation/Figures/Fresnel/TE/PozarPower.jpg')
199
200 n=n+1;
201 figure(n)
202 plot(rad2deg(thetarAir),(Re),rad2deg(thetarAir),...
203      (Te),rad2deg(thetarAir),(1-Re));
204 xlabel("Angle of Incidence (deg)");
205 ylabel("Transmission and Reflection Power");
206 title("Power-TE Polarization Transmission and Reflection (MIT)")
207 legend('Reflection','Transmission','Transmission 2');
208 saveas(gcf,'../FishPropagation/Figures/Fresnel/TE/MITPower.jpg')
209
210 n=n+1;
211 figure(n)
212 plot(rad2deg(thetarAir),10.*log10(Re),rad2deg(thetarAir),10.*log10(Te));
213 xlabel("Angle of Incidence (deg)");
214 ylabel("Transmission and Reflection Power");
215 title("Power-TE Polarization Transmission and Reflection (MIT)")
216 legend('Reflection - |RTE|^2','Transmission - 10*log10(|TTE|^2)');
217 saveas(gcf,'../FishPropagation/Figures/Fresnel/TE/MITPower10Log.jpg')
218
219
220
221 disp("Perpendicular")
222 TABLE = ["rJWTE","rPozar","rMIT","rRutgers"]
223 TABLE = [rJWTE',rPozarPerp',re',rte'] %Get all the same values
224 TABLE = ["tJWTE","tPozar","tMIT","tRutgers"]
225 TABLE = [tJWTE',tPozarPerp',te',tte']
226
227 disp("Perpendicular Power")
228 TABLE = ["RJWTE","RPozar","RMIT","RRutgers"]
229 TABLE = [RJWTE',RPozarPerp',Re',Rte'] %Get all the same values
230 TABLE = ["tJWTE","tPozar","tMIT","tRutgers"]
231 TABLE = [TJWTE',TPozarPerp',Te',Tte']
232
233
234 %Write to a csv file
235 labels =
    ["thetaAir","rJWTE","tJWTE","rChrisPerp","tChrisPerp","re",...
236  "te","rte","tte","RJWTE","TJWTE","RChrisPerp","TChrisPerp","Re",...
237  "Te","Rte","Tte","RdB","TdB"];

```

```

238 dataJWTE = [rad2deg(thetarAir)',real(rJWTE)',real(tJWTE)',...
239     real(rPozarPerp)',real(tPozarPerp)',real(re)',real(te)',real(rte)',...
240     real(tte)',real(RJWTE)',real(TJWTE)',real(RPozarPerp)',...
241     real(TPozarPerp)',real(Re)',real(Te)',real(Rte)',real(Tte)',...
242     (10.*log10((Rte)))',(10.*log10(Rte))'];
243 togo = [labels;dataJWTE];
244 writematrix(togo,'../FishPropagation/Figures/Fresnel/TE/FresnelTE.csv');

```

## TM Polarisation

```

1 %%Comparison of Multiple different textbooks for TM Oblique incidence
2 %% UP to Date:
3 %% November 30th 2023 last edited
4
5 %%parallel == TM == P polarization
6 %%Perpendicular == TE == S polarization
7
8 close all;
9 clear all;
10 clc;
11
12 %% Declaring Constants
13 f = 1.5e8;
14 w = 2*pi*f;
15
16 %%Conductivity
17 sigmaAir = 0;
18 sigmaWater = 0.014;
19
20 %%Declare Permittivities epsilon_r = epsilon/epsilon_0
21 epsilonAir = 1;
22 epsilonWater = 80.10;
23 epsilon0 = 8.85418782e-12;
24
25 %%Declare Permeability mu_r = mu/mu_0
26 murAir = 1;
27 murWater = 0.999992;
28 mu0 = pi*4e-7;
29
30 %% Declare values that do not depend on angle
31 %%Calculate specific permittivity: epsilon = epsilon_r*epsilon0
32 epsilonAir = epsilonAir * epsilon0;
33 epsilonWater = epsilonWater * epsilon0;
34
35 %%Calculate specific permeability: mu = mu_r*mu0
36 muAir = murAir * mu0;
37 muWater = murWater * mu0;
38
39
40
41 %% Determine Input Angle Stuff
42 thetarAir = linspace(0,pi/2,100);
43

```

```

44 %% James Wait Textbook
45 gammaWater =
    sqrt(1i.*muWater.*w.*(sigmaWater+1i.*epsilonWater.*w));%Water
46 gammaAir = sqrt(1i.*muAir.*w.*(sigmaAir+1i.*epsilonAir.*w)); %Air
47
48 thetarWater = (asin((gammaAir.*sin(thetarAir))./gammaWater));
49 uWater = gammaWater.*cos(thetarWater);
50 uAir = gammaAir.*cos(thetarAir);
51 KAir = uAir./(sigmaAir+1i.*epsilonAir.*w);
52 KWater = uWater./(sigmaWater+1i.*epsilonWater.*w);
53 ZWater = KWater; %For the semi-infinite 2 layer case
54
55
56 %Coefficients
57 rJWTM = -(ZWater-KAir)./(ZWater+KAir);
58 tJWTM = 2*KAir./(KAir+ZWater);
59 tJWTM2 = (1+rJWTM);
60
61 % Power
62 TJWTM = abs(tJWTM).^2.*real(KWater)./real(KAir);
63 RJWTM = abs(rJWTM).^2;
64 TJWTM2 = 1-RJWTM;
65
66
67 %% Pozar
68
69 thetarWater = asin(sin(thetarAir).*sqrt(epsilonAir.*mu0./...
70     (epsilonWater.*mu0)));
71
72 epswater = epsilonWater-1i*sigmaWater/w;
73 epsair = epsilonAir-1i*sigmaAir/w;
74 gammzWater = 1i*w*sqrt(muWater*epswater);
75 etaWater = (1i*w*muAir)/gammzWater; %Same: sqrt(mu0/epswater);
76 gammzAir = 1i*w*sqrt(muAir*epsair);
77 etaAir = (1i*w*muAir)/gammzAir;%Same: etaAir2 = sqrt(mu0/epsair);
78
79 %Coefficients
80 rPozarPara =
    (etaWater.*cos(thetarWater)-cos(thetarAir).*etaAir)./...
81     (etaWater.*cos(thetarWater)+etaAir.*cos(thetarAir));
82 tPozarPara = (2.*etaWater.*cos(thetarWater))./...
83     (etaWater.*cos(thetarWater)+cos(thetarAir).*etaAir);
84 tPozarPara2 = (1+rPozarPara);
85
86
87 %Power Equations
88 RPozarPara = abs(rPozarPara).^2;
89 TPozarPara = real(etaAir.*cos(thetarAir))./...
90     real(etaWater.*cos(thetarWater)).*abs(tPozarPara).^2;
91 TPozarPara2 = 1-RPozarPara;
92
93
94

```



```

95 %% MIT
96 Mi = etaAir.*cos(thetarAir);
97 Mt = etaWater.*cos(thetarWater);
98
99 %Coefficients
100 th = 2.*Mi./(Mi+Mt);
101 rh = (Mi-Mt)./(Mi+Mt);
102 th2 = (1+rh);
103
104 %Power
105 Th = abs(th.^2).*real(Mt)./real(Mi);
106 Rh = abs(rh).^2;
107 Th2 = 1-Rh;
108
109
110
111 %% Ch7 Rutgers Oblique Incidence from Textbook
112 ep1 = epsilonAir;
113 ep2 = epsilonWater - 1i*sigmaWater/w;
114 k1 = w*sqrt(mu0*ep1); %Wave numbers
115 k2 = w*sqrt(mu0*ep2);
116
117 k1x = k1*sin(thetarAir);
118 k1z = k1*cos(thetarAir);
119 k2z = sqrt(w^2*mu0*ep2 - k1x.^2);
120 k2z2 = k2.*cos(thetarWater);
121
122 % Coefficients
123 rtm = ((k2z.*ep1 - k1z.*ep2)./(k2z.*ep1 + k1z.*ep2));
124 ttm = (2*k2z*ep1)./(k2z*ep1+k1z*ep2);
125 ttm2 = (1+rtm);
126
127
128 %Power Values
129 Rtm = abs(rtm).^2;
130 Ttm = abs(ttm2).^2.*(real(k1z*ep2)./real(k2z*ep1));
131 Ttm2 = 1-Rtm;
132
133
134 %% Parallel Coefficients
135 n= 1;
136 figure(n)
137 plot(rad2deg(thetarAir),(rJWtm),rad2deg(thetarAir),(tJWtm));
138 xlabel("Angle of Incidence (deg)");
139 ylabel("Transmission and Reflection Coefficients");
140 title("Coefficients-Transmission and Reflection (James Wait)")
141 legend('Reflection - RTM','Transmission - TTM');
142 saveas(gcf,'../FishPropagation/Figures/Fresnel/TM/JamesWait.jpg')
143
144
145 n=n+1;
146 figure(n)
147 plot(rad2deg(thetarAir),(rPozarPara),rad2deg(thetarAir),tPozarPara);

```

```

148 xlabel("Angle of Incidence (deg)");
149 ylabel("Transmission and Reflection Coefficients");
150 title("Coefficients-Transmission and Reflection (Pozar)");
151 legend('Reflection - RTM','Transmission - TTM');
152 saveas(gcf,'../FishPropagation/Figures/Fresnel/TM/Pozar.jpg')
153
154 n=n+1;
155 figure(n)
156 plot(rad2deg(thetarAir),(rtm),rad2deg(thetarAir),(ttm));
157 xlabel("Angle of Incidence (deg)");
158 ylabel("Transmission and Reflection Coefficients");
159 title("Coefficients-Transmission and Reflection (Rutgers Textbook)");
160 legend('Reflection - RTM','Transmission - TTM');
161 saveas(gcf,'../FishPropagation/Figures/Fresnel/TM/Rutgers.jpg')
162
163 n=n+1;
164 figure(n)
165 plot(rad2deg(thetarAir),(rh),rad2deg(thetarAir),(th));
166 xlabel("Angle of Incidence (deg)");
167 ylabel("Transmission and Reflection Coefficients");
168 title("Coefficients-Transmission and Reflection (MIT)");
169 legend('Reflection - RTM','Transmission - TTM');
170 saveas(gcf,'../FishPropagation/Figures/Fresnel/TM/MIT.jpg')
171
172 %% Parallel Power Plots
173 n= n+1;
174 figure(n)
175 plot(rad2deg(thetarAir),(RJWTM),rad2deg(thetarAir),(TJWTM));
176 xlabel("Angle of Incidence (deg)");
177 ylabel("Transmission and Reflection Coefficients");
178 title("Power-Transmission and Reflection (James Wait)");
179 legend('Reflection','Transmission');
180 saveas(gcf,'../FishPropagation/Figures/Fresnel/TM/JamesWaitPower.jpg')
181
182
183 n=n+1;
184 figure(n)
185 plot(rad2deg(thetarAir),(RPozarPara),rad2deg(thetarAir),TPozarPara);
186 xlabel("Angle of Incidence (deg)");
187 ylabel("Transmission and Reflection Coefficients");
188 title("Power-Transmission and Reflection (Pozar)");
189 legend('Reflection','Transmission');
190 saveas(gcf,'../FishPropagation/Figures/Fresnel/TM/PozarPower.jpg')
191
192 n=n+1;
193 figure(n)
194 plot(rad2deg(thetarAir),(Rtm),rad2deg(thetarAir),(Ttm));
195 xlabel("Angle of Incidence (deg)");
196 ylabel("Transmission and Reflection Coefficients");
197 title("Power-TM/Parallel Polarization Transmission and " + ...
198       "Reflection (Rutgers)");
199 legend('Reflection','Transmission');
200 saveas(gcf,'../FishPropagation/Figures/Fresnel/TM/RutgersPower.jpg')

```

```

201
202 n=n+1;
203 figure(n)
204 plot(rad2deg(thetarAir),(Rh),rad2deg(thetarAir),(Th));
205 xlabel("Angle of Incidence (deg)");
206 ylabel("Transmission and Reflection Coefficients");
207 title("Power-Transmission and Reflection (MIT)");
208 legend('Reflection','Transmission');
209 saveas(gcf,'../FishPropagation/Figures/Fresnel/TM/MITPower.jpg')
210
211 n=n+1;
212 figure(n)
213 plot(rad2deg(thetarAir),10*log10(Rh),rad2deg(thetarAir),10.*log10(Th));
214 xlabel("Angle of Incidence (deg)");
215 ylabel("Transmission and Reflection Coefficients");
216 title("Power-Transmission and Reflection (MIT)");
217 legend('Reflection - 10*log10|RTM|^2','Transmission -
        10*log10|TTM|^2');
218 saveas(gcf,'../FishPropagation/Figures/Fresnel/TM/MITPowerdB.jpg')
219
220
221
222
223
224 %parallel == TM
225 %Perpendicular == TE
226
227 disp("Parallel Coefficients")
228 TABLE = ["rJWTM","rPozar","rMIT","rRutgers"]
229 TABLE = [rJWTM',rPozarPara',rh',rtm'] %A Pesky sign issue remains
230 TABLE = ["tJWTM","tPozar","tMIT","tRutgers"]
231 TABLE = [tJWTM',tPozarPara',th',ttm']
232
233
234 disp("Parallel Power")
235 TABLE = ["rJWTM","rPozar","rMIT","rRutgers"]
236 TABLE = [RJWTM',RPozarPara',Rh',Rtm'] %A Pesky sign issue remains
237 TABLE = ["tJWTM","tJW2TM","tPozar","tMIT","tRutgers"] %
238 TABLE = [TJWTM',TPozarPara',Th',Ttm']%
239 TABLE = ["tJWTM","tMIT","tRutgers"]
240 TABLE = [TJWTM',Th2',Ttm2']
241
242 labels =
        ["thetaAir","rJWTM","tJWTM","rChrisPara","tChrisPara","rh"...
243         ,"th","rtm","ttm","RJWTM","TJWTM","RChrisPara","TChrisPara","Rh"...
244         ,"Th","Rtm","Ttm","RdB","TdB"];
245 dataJWTE = [rad2deg(thetarAir)',real(rJWTM)',real(tJWTM)']...
246         ,real(rPozarPara)',real(tPozarPara)',real(rh)',real(th)',real(rtm)']...
247         ,real(ttm)',real(RJWTM)',real(TJWTM)',real(RPozarPara)',...
248         real(TPozarPara)',real(Rh)',real(Th)',real(Rtm)',real(Ttm)',...
249         (10.*log10((Rtm)))',(10.*log10(Ttm))'];
250 togo = [labels;dataJWTE];
251 writematrix(togo,'../FishPropagation/Figures/Fresnel/TM/FresnelTM.csv');

```

## B.2 Acoustic Propagation

### B.2.1 Fitting to Single-layer

```
1 %% Window Propagation
2 % Fits the averaged data obtained by multiple sources for the
  absorption
3 % coefficient and for the transmission loss to a transmission line
  model.
4 % Three different fitting approaches are used. Linear fit,
  polynomial fit
5 % and spline fit. These results can then be used in calculating
  other
6 % transmission line models that we come up with.
7
8 % Although there is more transmission loss data, we had to reduce
  the
9 % number of points to match the number of points we had for the
  absorption
10 % coefficient.
11
12 clear;
13 clc;
14
15 f=[125,250,500,1000,2000,4000];
16
17 %%3 mm
18 % Single Pane 3 mm - Sound Reduction (dB)
19 R = [-20.175,-21.25,-25.55,-28.9,-33.175,-26.6];
20
21 % Single Pane 3 mm - Absorption Coefficient
22 alpha = [0.0702,0.04,0.03,0.03,0.02,0.02];
23
24 % %% 6 mm
25 % % Single Pane 6 mm - Sound Reduction (dB)
26 % R = [-23.4,-27.4,-31.8,-35.2,-26.8,-35.5];
27 %
28 % % Single Pane 6 mm - Absorption Coefficient
29 % alpha = [0.08,0.04,0.03,0.03,0.02,0.02,0.02];
30
31 ZGlasses = [];
32 gammaGlasses = [];
33
34 for i = 1:length(f)
35     w = 2*pi*f(i);
36     c = 343; %In Air
37     cglass = 4540;
38     rho0 = 1.293; %Density of Air
39     rhoglass = 2500;
40
41     %% Transmission Line Calculation
42     ZAir = rho0.*c; %Impedance of Air (considered to be lossless)
```

```

43 ZAir2 = rho0.*c;
44
45 ZGlassRe = rhoglass.*cglass;
46 syms ZGlassIm %What we are trying to solve for
47 ZGlass = ZGlassRe+1i.*ZGlassIm;
48
49 %k = Beta-1i*alpha
50 %ik = gamma = alpha+iBeta
51 gammaAir = 1i.*w./c; %Lossless portion of the propagation
    constant
52 gammaGlassIm = 1i.*w./cglass;
53 syms gammaGlassRe %What we are solving for (attenuation)
54
55 %Fitting to single pane scenario where the glass is 3 mm thick
56 lair = 0;
57 lglass = 0.003;
58 lair2 = 0;
59
60 %Calculate the input impedance and the total Reflection
61 Zin =
    ZGlass.*((ZAir2+ZGlass.*tanh((gammaGlassRe+gammaGlassIm)...
62     .*lglass))./(ZGlass+ZAir2.*tanh((gammaGlassRe+gammaGlassIm)...
63     .*lglass)));
64 gammaTotal = (Zin-ZAir)./(Zin+ZAir);
65
66
67 % Transmission Line
68 Vs = 10;
69 IncidentPower =
    0.5.*abs(Vs).^2.*real(1./ZAir).*(1-abs(gammaTotal).^2);
70 Pin = 0.5.*abs(Vs).^2.*real(1./ZAir);
71 Pref = 0.5.*abs(Vs).^2.*real(1./ZAir).*(abs(gammaTotal).^2);
72
73 %Equations for three layer transmission line from Bound.Cond.
74 V1m = -0.5.*Vs.*((ZGlass./ZAir).*(1-gammaTotal)-(1+gammaTotal));
75 V1p = 0.5.*Vs.*((ZGlass./ZAir).*(1-gammaTotal)+(1+gammaTotal));
76
77 %Wave leaving the middle layer
78 V2p = V1p.*exp(-(gammaGlassRe+gammaGlassIm).*lglass)+V1m...
79     .*exp((gammaGlassRe+gammaGlassIm).*lglass);
80
81 LoadPower = 0.5.*real(1./ZAir).*abs(V2p).^2;
82
83 LossPower = IncidentPower-LoadPower;
84
85 eqn1 = abs(gammaTotal).^2 == (1-alpha(i));
86 eqn2 = (LoadPower./Pin) == 10^(R(i)/10); %R
    =10.*log10(Iout./Iin)
87
88 eqns =[eqn1,eqn2]; %eqn3
89
90 %Want both the variables we are solving for to be positive.
91 assume(gammaGlassRe>0)

```

```

92     assumeAlso(ZGlassIm>0)
93     %Solve the system of equations
94     S = vpasolve(eqns,[ZGlassIm,gammaGlassRe]);
95
96
97
98     %% Check - Solving the values at each frequency and making sure
99     %% Re-do with calculated values for transmission Line
100     Calculations
101     ZAir = rho0.*c;
102     ZGlasssym = S.ZGlassIm;
103     dZGlassIm = double(ZGlasssym);
104     ZGlass = ZGlassRe+1i.*dZGlassIm;
105
106     gammaAir = w./c;
107     gammaGlassIm = 1i.*w./cglass;
108     gammaGlassRe = S.gammaGlassRe;
109     dgammaGlassRe = double(gammaGlassRe);
110     gammaGlass = dgammaGlassRe+gammaGlassIm;
111     gammaAir2 = w./c;
112
113     lair = 0;
114     lglass = 0.003;
115     lair2 = 0;
116
117     Zin = ZGlass.*((ZAir2+ZGlass.*tanh(gammaGlass.*lglass))...
118     ./((ZGlass+ZAir2.*tanh(gammaGlass.*lglass)));
119     gammaTotal = (Zin-ZAir)./(Zin+ZAir);
120
121     % Transmission Line
122     Vs = 10;
123     IncidentPower =
124     0.5.*abs(Vs).^2.*real(1./ZAir).*(1-abs(gammaTotal).^2);
125     Pin = 0.5.*abs(Vs).^2.*real(1./ZAir);
126     Pref = 0.5.*abs(Vs).^2.*real(1./ZAir).*(abs(gammaTotal).^2);
127
128     V1m = -0.5.*Vs.*((ZGlass./ZAir).*(1-gammaTotal)-(1+gammaTotal));
129     V1p = 0.5.*Vs.*((ZGlass./ZAir).*(1-gammaTotal)+(1+gammaTotal));
130
131     V2p =
132     V1p.*exp(-gammaGlass.*lglass)+V1m.*exp(gammaGlass.*lglass);
133
134     LoadPower = 0.5.*real(1./ZAir).*abs(V2p).^2;
135
136     LossPower = IncidentPower-LoadPower;
137
138     if (abs(gammaTotal).^2 - (1-alpha(i)) <=1E-10) ...
139     && (10.*log10(LoadPower./Pin)-R(i) <=1E-10)
140         disp("Plugging solved variables back into the equation it
141         works.")

```

```

140     else
141         disp("We get the wrong answer for some reason?")
142         disp(abs(gammaTotal).^2 - (1-alpha(i)))
143         disp(10.*log10(LoadPower./Pin)-R(i))
144     end
145
146     ZGlasses(end+1) = ZGlass;
147     gammaGlasses(end+1) = gammaGlass;
148
149
150
151
152
153 end
154
155
156 freq = linspace(125,4000,100);
157
158
159 %% Polynomial Fit
160 %Carry out the polynomial fit
161 ZGlassesPoly = polyfit(f,ZGlasses,3);
162 gammaGlassesPoly = polyfit(f,gammaGlasses,3);
163
164 %Evaluate the polynomial fit
165 ZGlassesPolyVal = polyval(ZGlassesPoly,freq);
166 gammaGlassesPolyVal = polyval(gammaGlassesPoly,freq);
167
168 %% Linear interpolation
169 %Makes an array with the interpolated results immediately
170 ZGlassesLinInterp = interp1(f, ZGlasses, freq, 'linear');
171 gammaGlassesLinInterp = interp1(f, gammaGlasses, freq, 'linear');
172
173 %% Spline interpolation
174 %Makes an array with the interpolated results immediately
175 ZGlassesSplineInterp = interp1(f, ZGlasses, freq, 'spline');
176 gammaGlassesSplineInterp = interp1(f, gammaGlasses, freq, 'spline');
177
178 %% Uncomment if you want to run on its own
179
180 labels = ["FitFreq","ReZGlassPolyFit","ImZGlassPolyFit"...
181         ,"RegammaGlassPolyFit","ImgammaGlassPolyFit","ReZGlassLinearFit"...
182         ,"ImZGlassLinearFit","RegammaGlassLinearFit","ImgammaGlassLinearFit"...
183         ,"ReZGlassSplineFit","ImZGlassSplineFit","RegammaGlassSplineFit"...
184         ,"ImgammaGlassSplineFit"];
185 labels2 =
186     ["Frequencies","ReZGlass","ImZGlass","RegammaGlass","ImgammaGlass"];
187 FittingOptions =
188     [freq',real(ZGlassesPolyVal)',imag(ZGlassesPolyVal)']...
189     ,real(gammaGlassesPolyVal)',imag(gammaGlassesPolyVal)']...
190     ,real(ZGlassesLinInterp)',imag(ZGlassesLinInterp)']...
191     ,real(gammaGlassesLinInterp)',imag(gammaGlassesLinInterp)']...

```

```

191     ,real(ZGlassesSplineInterp)', imag(ZGlassesSplineInterp)'...
192     ,real(gammaGlassesSplineInterp)', imag(gammaGlassesSplineInterp)'];
193 FittingOptions2 =
194     [f', real(ZGlasses)', imag(ZGlasses)', real(gammaGlasses)'...
195     , imag(gammaGlasses)'];
196 togo = [labels;FittingOptions];
197 togo2 = [labels2;FittingOptions2];
198 writematrix(togo, "..../Acoustics/Figures/FittedImpedanceandWave.csv");
199 writematrix(togo2, "..../Acoustics/Figures/ActualImpedanceandWave.csv");
200
201 %% Polyfit comparison
202 figure(1)
203 scatter(f, real(ZGlasses))
204 hold on
205 plot(freq, real(ZGlassesPolyVal))
206 legend("Actual Values", "Polyval")
207 hold off
208 grid
209 xlabel('Frequency')
210 ylabel('Real ZGlasses Polyval')
211
212 figure(2)
213 scatter(f, imag(ZGlasses))
214 hold on
215 plot(freq, imag(ZGlassesPolyVal))
216 legend("Actual Values", "Polyval")
217 hold off
218 grid
219 xlabel('Frequency')
220 ylabel('Imag ZGlasses Polyval')
221
222 figure(3)
223 scatter(f, real(gammaGlasses))
224 hold on
225 plot(freq, real(gammaGlassesPolyVal))
226 legend("Actual Values", "Polyval")
227 hold off
228 grid
229 xlabel('Frequency')
230 ylabel('Real gammaGlasses Polyval')
231
232 figure(4)
233 scatter(f, imag(gammaGlasses))
234 hold on
235 plot(freq, imag(gammaGlassesPolyVal))
236 legend("Actual Values", "Polyval")
237 hold off
238 grid
239 xlabel('Frequency')
240 ylabel('Imag gammaGlasses Polyval')
241
242

```



```

243
244
245 %% Interp comparison
246 figure(5)
247 scatter(f, real(ZGlasses))
248 hold on
249 plot(freq, real(ZGlassesInterp))
250 legend("Actual Values","Interp")
251 hold off
252 grid
253 xlabel('Frequency')
254 ylabel('Real ZGlasses Interp')
255
256 figure(6)
257 scatter(f, imag(ZGlasses))
258 hold on
259 plot(freq, imag(ZGlassesInterp))
260 legend("Actual Values","Interp")
261 hold off
262 grid
263 xlabel('Frequency')
264 ylabel('Imag ZGlasses Interp')
265
266 figure(7)
267 scatter(f, real(gammaGlasses))
268 hold on
269 plot(freq, real(gammaGlassesInterp))
270 legend("Actual Values","Interp")
271 hold off
272 grid
273 xlabel('Frequency')
274 ylabel('Real gammaGlasses Interp')
275
276 figure(8)
277 scatter(f, imag(gammaGlasses))
278 hold on
279 plot(freq, imag(gammaGlassesInterp))
280 legend("Actual Values","Interp")
281 hold off
282 grid
283 xlabel('Frequency')
284 ylabel('Imag gammaGlasses Interp')

```

## B.2.2 Multi-layer Transmission Line

```

1 % Multi layer Perpendicular Polarization
2 % Does the actual calculations for the multilayer transmission line
3 % Reads in the impedance values from the
4 % AuralizationEquatingTransmissionLine
5
6 %Last Updated Oct 23 - Works well - can do multiple frequencies
7

```

```

8
9 clear;
10 close all;
11 clc;
12
13 AuralizationEquatingTransmissionLine;
14
15 ZGlass =
    [ZGlassesPolyVal',ZGlassesLinInterp',ZGlassesSplineInterp'];
16 gammaGlass = [gammaGlassesPolyVal',gammaGlassesLinInterp'...
17               ,gammaGlassesSplineInterp'];
18 typeInterpolation = ["polynomial","linear","spline"];
19
20 numlayers = 3;
21 numangles = 1;
22 numfrequencypoints = 100;
23 %%
24 % 0 - Triple Pane: Air
25 % 1 - Double Pane: Air
26 % 2 - Single Pane
27 % 3 - Triple Pane: Argon
28 % 4 - Double Pane: Argon
29 windowtype = 2;
30
31 %% Values that AuralizationEquatingTransmissionLine produces
32 % ZGlassesPolyVal
33 % gammaGlassesPolyVal
34 % ZGlassesLinInterp
35 % gammaGlassesLinInterp
36 % ZGlassesSplineInterp
37 % gammaGlassesSplineInterp
38
39 lengthbetweenpane = [0.003,0.006,0.009,0.03,0.06,0.09,0.3,0.6,0.9];
40 InterpolationStyles = 3;
41 for a=1:InterpolationStyles
42 for q = 1:length(lengthbetweenpane)
43
44     lspacing = lengthbetweenpane(q);
45     [freq,w,theta,etaT,nT,Z,l,smallgamma,smallgamma2,del,u,N] = ...
46         InitializeVariables(numlayers, numangles,...
47             numfrequencypoints,ZGlass(:,a),gammaGlass(:,a),...
48             lspacing,windowtype);
49
50     thetaAir = theta(1,:,:) ;
51
52     %% Rutgers Stuff
53     etaT_in = ImpedanceCalculatorRut(etaT,del,numlayers);
54     etaT_end = etaT_in(end,:,:) ;
55     etaTAir = etaT(1,:,:) ;
56     gammaT1 = (etaT_end-etaTAir)./(etaT_end+etaTAir);
57
58
59     %% Transmission Line

```

```

60   ZAir = Z(1, :, :);
61
62   Zin = ImpedanceCalculatorTLin(Z, smallgamma, l, numlayers);
63   ZinEnd = Zin(end, :, :);
64
65   gammaTotal = (ZinEnd - ZAir) ./ (ZinEnd + ZAir);
66
67   %% Power
68
69   %% Rutgers Stuff
70   E0 = 10;
71   E = [];
72   H = [];
73   Power = [];
74   AbsPower = [];
75
76   ETa = E0 .* (1 + gammaT1);
77   HTa = (E0 ./ etaTAir) .* (1 - gammaT1);
78   E = ETa;
79   H = HTa;
80
81   Pinc = 1/2 .* real(ETa .* conj(HTa)); %1 - |gammaT1|^2
82   Pins = 1/2 .* real(abs(E0).^2 ./ etaTAir);
83   Power = Pinc;
84
85   for i = 1:numlayers %Calculate ET2 and ET3
86       deli = del(i, :, :);
87       etaTi = etaT(i, :, :);
88       HTi = H(i, :, :);
89       ETi = E(i, :, :);
90       ETi_1 = cos(deli) .* ETi - 1i .* etaTi .* sin(deli) .* HTi;
91       HTi_1 = -1i .* (1 ./ etaTi) .* sin(deli) .* ETi + cos(deli) .* HTi;
92       E(end+1, :, :) = ETi_1;
93       H(end+1, :, :) = HTi_1;
94       Power(end+1, :, :) = 1/2 .* real(ETi_1 .* conj(HTi_1));
95   end
96
97   InputPower = Pins ./ Pins;
98   TransmittedPower = Power(end, :, :) ./ Pins;
99   ReflectedPower = (Pins - Pinc) ./ Pins;
100  ReflectPower2 = abs(gammaT1).^2;
101
102  % for s = 2:numlayers
103  %     AbsPower(end+1, :, :) = Power(s-1, :, :) - Power(s, :, :);
104  % end
105  AbsPower = Power ./ Pins;
106  TotAbsorbedPower = InputPower - TransmittedPower - ReflectedPower;
107
108
109  %% Transmission Line Generalized
110
111  V = [];
112  I = [];

```

```

113 Vs = 10;
114
115 PowerTLin = [];
116 AbsPowerTLin = [];
117
118 Va = Vs.*(1+gammaTotal);
119 Ia = (Vs./etaTAir).*(1-gammaTotal);
120 V = Va;
121 I = Ia;
122
123 Pinc = 1/2.*real(Va.*conj(Ia)); %1-|gammaT1|^2
124 Pins = 1/2.*real(abs(Vs).^2./etaTAir); %1
125 PowerTLin = Pinc;
126
127 for i = 1:numlayers %Calculate ET2 and ET3
128     smallgammai = smallgamma(i, :, :).*l(i, :, :)./(1i);
129     etaTi = etaT(i, :, :);
130     Ii = I(i, :, :);
131     Vi = V(i, :, :);
132     Vi_1 = cos(smallgammai).*Vi-1i.*etaTi.*sin(smallgammai).*Ii;
133     Ii_1 =
134         -1i.*(1./etaTi).*sin(smallgammai).*Vi+cos(smallgammai).*Ii;
135     V(end+1, :, :) = Vi_1;
136     I(end+1, :, :) = Ii_1;
137     PowerTLin(end+1, :, :) = 1/2.*real(Vi_1.*conj(Ii_1));
138 end
139
140 % for l = 2:numlayers
141 %     AbsPowerTLin(end+1, :, :) = Pins-PowerTLin(l, :, :);
142 % end
143
144 AbsPowerTLin = PowerTLin./Pins;
145 InputPowerTLin = Pins./Pins;
146 TransmittedPowerTLin = PowerTLin(end, :, :)./Pins;
147 ReflectedPowerTLin = (Pins - Pinc)./Pins;
148 TotAbsorbedPowerTLin = InputPowerTLin-TransmittedPowerTLin...
149     -ReflectedPowerTLin;
150
151 for f = 1:length(freq)
152     disp("Frequency: ")
153     disp(freq(f, :))
154
155     disp("Rutgers - Impedance and Reflection")
156     disp("Incident Angle, Reflection Coefficient , Input
157         Impedance")
158     table = [rad2deg(thetaAir(:, :, f))', gammaT1(:, :, f)'...
159         , etaT_end(:, :, f)']
160
161     disp("Transmission Line - Impedance and Reflection")
162     disp("Incident Angle , Reflection Coefficient , Input
163         Impedance")
164     table = [rad2deg(thetaAir(:, :, f))', gammaTotal(:, :, f)'...

```

```

163         ,ZinEnd(:,:,f)']
164
165     disp("Rutgers - Normalized")
166     disp("Angle,Incident Power,Ref. Power,Transm. Pow,
167         Absorbed")
167     table = [rad2deg(thetaAir(:,:,f))',InputPower(:,:,f)']...
168             ,ReflectedPower(:,:,f)'] ,TransmittedPower(:,:,f)']...
169             ,TotAbsorbedPower(:,:,f)']
170
171     disp("Transmission Line Technique - Generalized")
172     disp("Angle,Incident Power,Ref. Power,Transm. Pow,
173         Absorbed")
173     table =
174         [rad2deg(thetaAir(:,:,f))',(InputPowerTLin(:,:,f))']...
175         ,(ReflectedPowerTLin(:,:,f))',(TransmittedPowerTLin(:,:,f))']...
176         ,(TotAbsorbedPowerTLin(:,:,f))']
176
177 end
177
178
179 TPower = real(10.*log10(reshape(TransmittedPower,1,...
180     length(TransmittedPower))));
180
181 TPowerTlin = real(10.*log10(reshape(TransmittedPowerTLin,1,...
182     length(TransmittedPowerTLin))));
181
183 RPower = real(10.*log10(reshape(ReflectedPower,1,...
184     length(ReflectedPower))));
182
185 RPowerTlin = real(10.*log10(reshape(ReflectedPowerTLin,1,...
186     length(ReflectedPowerTLin))));
183
187 AbsolutePowerIntermed = real(10.*log10(reshape(AbsPower,...
188     size(AbsPower,1),size(AbsPower,3))));
184
189 AbsolutePower = AbsolutePowerIntermed(2:end,:);
185
190
191 n = 1;
192 figure(n)
193 plot(freq,(TPower))
194 xlabel("Frequencies")
195 ylabel("Transmitted Power (dB)")
191
196
197 n=n+1;
198 figure(n)
199 plot(freq,(TPowerTlin))
200 xlabel("Frequencies")
201 ylabel("Transmitted Power (dB)")
196
202
203 Layer = linspace(1,numlayers,numlayers);
204 labels =
205     ["Frequencies","TPower","TPowerTlin","RPower","RPowerTlin"];
202
206 dataWindowModel =
207     [freq,TPower',TPowerTlin',RPower',RPowerTlin'];
203
208 togo = [labels;dataWindowModel];
204
209
210 frequencylabel = string(freq);
205
211 labels2 = [frequencylabel',"Layer"];
206

```

```

211 dataWindowModel2 = [(AbsolutePower),Layer'];
212 togo2 = [labels2;dataWindowModel2];
213
214 switch windowtype
215     case 0
216         config = "TripleAir";
217     case 1
218         config = "DoubleAir";
219     case 2
220         config = "Single";
221     case 3
222         config = "TripleArgon";
223     case 4
224         config = "DoubleArgon";
225 end
226
227 writematrix(togo,".././Accoustics/Figures/"+config...
228     +typeInterpolation(a)+"Pane3mmGlass"+string(lspacing*1000)...
229     +"mmSpace.csv");
230 writematrix(togo2,".././Accoustics/Figures/"+config...
231     +typeInterpolation(a)+"PaneAbs3mmGlass"+string(lspacing*1000)...
232     +"mmSpace.csv");
233
234 end
235 end
236
237 %% Necessary Functions for James Wait Approach
238
239 function [Tperp,Rperp,Y] = Coefficient(N,u,l,numLayer)
240     Y = ImpedanceCalculatorJW(N,u,l,numLayer);
241     tsubcoeff = tCoeffs(N,numLayer);
242     d = dval(N,Y,u,l,numLayer);
243     expPart = exponential(u,l);
244
245     Tperp = tsubcoeff.*d.*expPart;
246     Rperp = (N(end,::)-Y(end,::))./(N(end,::)+Y(end,::));
247 end
248
249 function d = dval(N,Y,u,l,numLayer)
250     %Note N = [NM,NM_m1,...,Nm,...,N0]; N = [N2,N1,N0];
251     %Note Y = [YM,....,Y1]; Y = [Y2,Y1];
252     d = ones(1,size(N,2));
253     for currentlayer = 2:numLayer-1 %Starts at M-1 and ends at m = 1
254         Nm_m1 = N(currentlayer+1,::);%m-1 is one lower than m
255         Nm = N(currentlayer,::);
256         Ym_1 = Y(currentlayer-1,::);%Actually is Ym+1
257         u_m = u(currentlayer,::);
258         l_m = l(currentlayer,::);
259
260
261         dm = (((1-((Nm_m1-Nm)./(Nm_m1+Nm)).*((Ym_1-Nm)./(Ym_1+Nm))...
262             .*exp(-2.*u_m.*l_m)));
263         d = dm.*d;

```

```

264     end
265     d = 1./d;
266 end
267 %Y = [Y_M_theta1,Y_M_theta2,Y_M_theta3,Y_M_theta4]
268 %     [Y_m+1_theta1,Y_m+1_theta2,Y_m+1_theta3,Y_m+1_theta4]
269
270 function tsubcoeff = tCoeffs(N,numLayer)
271     tsubcoeff = ones(1,size(N,2));
272     for currentlayer =1:numLayer-1 %Starts at M
273         Nm_m1 = N(currentlayer+1,,:); %m-1 is one lower than m
274         Nm = N(currentlayer,,:);
275         t = (2.*Nm_m1)./(Nm+Nm_m1);
276         tsubcoeff = tsubcoeff.*t;
277     end
278 end
279 %Y = [Y_M_theta1,Y_M_theta2,Y_M_theta3,Y_M_theta4]
280 %     [Y_m+1_theta1,Y_m+1_theta2,Y_m+1_theta3,Y_m+1_theta4]
281
282 function expPart = exponential(u,l)
283     um_m1 = u(2:end,,:);
284     lm_m1 = l(2:end,,:);
285     expPart = exp(-sum(um_m1.*lm_m1));
286 end
287
288 function Y = ImpedanceCalculatorJW(N,u,l,numLayer)
289     Y = [];
290     N_M = N(1,,:);
291     Y_M = N_M.*ones(1,size(u,2),size(u,3));
292     Y = Y_M;
293     for currentlayer = 2:numLayer-1
294         u_m = u(currentlayer,,:);
295         l_m = l(currentlayer,,:);
296         N_m = N(currentlayer,,:); %organized so top is last slab
297         Y_m = ImpedanceJW(Y(end,,:),N_m,u_m,l_m);
298         Y(end+1,,:) = Y_m;
299     end
300
301 end
302 %Y = [Y_M_theta1,Y_M_theta2,Y_M_theta3,Y_M_theta4]
303 %     [Y_m+1_theta1,Y_m+1_theta2,Y_m+1_theta3,Y_m+1_theta4]
304
305 function Y_m = ImpedanceJW(Y_m_1,N_m,u_m,l_m)
306     Y_m =
307         N_m.*(Y_m_1+N_m.*tanh(u_m.*l_m))./(N_m+Y_m_1.*tanh(u_m.*l_m));
307 end
308
309 %% Transmission Line
310 function Z = ImpedanceCalculatorTLin(Zval,gamma,l,numLayer)
311     Z = [];
312     Zval_M = Zval(1,,:);
313     Z_M = Zval_M.*ones(1,size(gamma,2),size(gamma,3));
314     Z = Z_M;
315     for currentlayer = 2:numLayer-1

```

```

316     gamma_m = gamma(currentlayer, :, :);
317     l_m = l(currentlayer, :, :);
318     Zval_m = Zval(currentlayer, :, :); %organized so top is last
        slab
319     Z_m = ImpedanceJW(Z(end, :, :), Zval_m, gamma_m, l_m);
320     Z(end+1, :, :) = Z_m;
321 end
322
323 end
324
325
326 function Z_in = ImpedanceTLin(Z_m_1, Z_m, gamma_m, l_m)
327     Z_in = Z_m.*(Z_m_1+Z_m.*tanh(gamma_m.*l_m))./(Z_m+Z_m_1...
328     .*tanh(gamma_m.*l_m));
329 end
330
331
332 %% Rutgers Impedance
333 function etaT_in = ImpedanceCalculatorRut(etaTval, del, numLayer)
334     etaT_in = [];
335     etaTval_M = etaTval(1, :, :);
336     etaT_M = etaTval_M.*ones(1, size(del, 2), size(del, 3));
337     etaT_in = etaT_M;
338     for currentlayer = 2:numLayer-1
339         del_m = del(currentlayer, :, :);
340         etaTval_m = etaTval(currentlayer, :, :); %organized so top is
            last slab
341         etaT_m = ImpedanceRut(etaT_in(end, :, :), etaTval_m, del_m);
342         etaT_in(end+1, :, :) = etaT_m;
343     end
344
345 end
346 %Y = [Y_M_theta1, Y_M_theta2, Y_M_theta3, Y_M_theta4]
347 %     [Y_m+1_theta1, Y_m+1_theta2, Y_m+1_theta3, Y_m+1_theta4]
348
349 function etaT = ImpedanceRut(etaT_m_1, etaT_m, del_m)
350     etaT = etaT_m.*(etaT_m_1+etaT_m.*tanh(del_m.*1i))...
351     ./((etaT_m+etaT_m_1.*tanh(del_m.*1i)));
352 end
353
354 %% Declaring Constants
355
356 function [freq, w, thetAf, etaTf, nTf, Zf, lf, smallgammaf, smallgamma2f...
357     , delf, uf, Nf] = InitializeVariables(numlayers, numangles, ...
358     numfrequencypoints, ZGlasses, gammaGlasses, lspacing, windowtype)
359     %% Declaring Constants
360     % All variables with an f have multiple frequencies
361     thetAf = zeros(numlayers, numangles, numfrequencypoints);
362     etaTf = zeros(numlayers, numangles, numfrequencypoints);
363     nTf = zeros(numlayers, numangles, numfrequencypoints);
364     Zf = zeros(numlayers, numangles, numfrequencypoints);
365     lf = zeros(numlayers, 1, numfrequencypoints);
366     smallgammaf = zeros(numlayers, numangles, numfrequencypoints);

```



```

367     smallgamma2f = zeros(numlayers,1,numfrequencypoints);
368     delf = zeros(numlayers,numangles,numfrequencypoints);
369     uf = zeros(numlayers,numangles,numfrequencypoints);
370     Nf = zeros(numlayers,numangles,numfrequencypoints);
371
372     w = zeros(numfrequencypoints,1);
373     freq = zeros(numfrequencypoints,1);
374
375     frequencies=linspace(125,4000,numfrequencypoints);
376
377     i = 1;
378     for f = 1:length(frequencies)
379
380         w(i,:) = 2.*pi.*frequencies(i);
381
382         c = 343; %In Air m/s
383         cglass = 4540;
384         cargon = 319; %In Argon at 20c
385         rho0 = 1.293;
386         rhoArgon = 1.603; %Engineering Toolbox
387
388         lambdaAir = c./frequencies(i);
389         lambdaGlass = cglass./frequencies(i);
390
391         %% Transmission Line Calculation
392         ZAir = rho0.*c;
393         ZGlass = ZGlasses(i);
394         ZAir2 = rho0.*c; %rho0.*c;
395         ZArgon = rhoArgon.*cargon;
396
397         %k = Beta-i*alpha
398         %ik = gamma = alpha+iBeta
399         gammaAir = 1i.*w(i,:)./c;
400         gammaGlass = gammaGlasses(i);
401         gammaAir2 = 1i.*w(i,:)./c;
402         gammaArgon = 1i.*w(i,:)./cargon;
403
404         %% Width of the glass pane
405         lglass = 0.003;
406     %     lglass = 0.09;
407
408         %%Length of tranmsission line
409         la = 0;
410         l1 = lglass;
411         lb = lspacing;
412         l2 = lglass;
413         lc = 0;
414
415
416         %%Propagation Constant
417         smallgammaGlass = gammaGlass;
418         smallgammaAir = gammaAir;
419         smallgammaArgon = gammaArgon;

```

```

420
421 %Phase difference
422 delAir = (gammaAir./1i).*lc;
423 delGlass = (gammaGlass./1i).*l2;
424 delAir2 = (gammaAir./1i).*lb;
425 delArgon = (gammaArgon./1i).*lb;
426 delGlass2 = (gammaGlass./1i).*l1;
427 delAir3 = (gammaAir./1i).*la;
428
429 switch windowtype
430     case 0
431         etaT = [ZAir;ZGlass;ZAir;ZGlass;ZAir;ZGlass;ZAir];
432         Z = etaT;
433         l = [lc;l2;lb;l1;lb;l1;la];
434         smallgamma =
435             [smallgammaAir;smallgammaGlass;smallgammaAir...
436              ;smallgammaGlass;smallgammaAir;smallgammaGlass...
437              ;smallgammaAir];
438         del =
439             [delAir;delGlass;delAir2;delGlass2;delAir2;delGlass2;delAir3];
440     case 1
441         etaT = [ZAir;ZGlass;ZAir;ZGlass;ZAir]; %Double Pane
442             Air Gap
443         Z = etaT;
444         l = [lc;l2;lb;l1;la]; %Double Pane Air Gap
445         smallgamma =
446             [smallgammaAir;smallgammaGlass;smallgammaAir...
447              ;smallgammaGlass;smallgammaAir]; %Double Pane
448             Air Gap
449         del = [delAir;delGlass;delAir2;delGlass2;delAir3];
450     case 2
451         etaT = [ZAir;ZGlass;ZAir]; %Single Pane
452         Z = etaT;
453         l = [lc;l2;lb]; %Single Pane
454         smallgamma = [smallgammaAir;smallgammaGlass...
455                       ;smallgammaAir]; %Single Pane
456         del = [delAir;delGlass;delAir2];
457     case 3
458         etaT = [ZAir;ZGlass;ZArgon;ZGlass;ZArgon;ZGlass...
459                ;ZAir]; %Triple Pane Argon
460         Z = etaT;
461         l = [lc;l2;lb;l1;lb;l1;la]; %Triple Pane Argon
462         smallgamma = [smallgammaAir;smallgammaGlass...
463                       ;smallgammaArgon;smallgammaGlass;smallgammaArgon...
464                       ;smallgammaGlass;smallgammaAir]; %Triple Pane
465             Argon
466         del = [delAir;delGlass;delArgon;delGlass2...
467                ;delArgon;delGlass2;delAir3];
468     case 4
469         etaT = [ZAir;ZGlass;ZArgon;ZGlass;ZAir]; %Double
470             Pane Argon
471         Z = etaT;
472         l = [lc;l2;lb;l1;la]; %Double Pane Argon

```

```
466         smallgamma = [smallgammaAir;smallgammaGlass...
467             ;smallgammaArgon;smallgammaGlass;smallgammaAir];
468         del = [delAir;delGlass;delArgon;delGlass2;delAir3];
469     end
470
471     etaTf(:, :, i) = etaT;
472     Zf(:, :, i) = Z;
473     lf(:, :, i) = l;
474     smallgammaf(:, :, i) = smallgamma;
475     delf(:, :, i) = del;
476
477     freq(i, :) = frequencies(i);
478     i = i+1;
479
480 end
481 end
```